

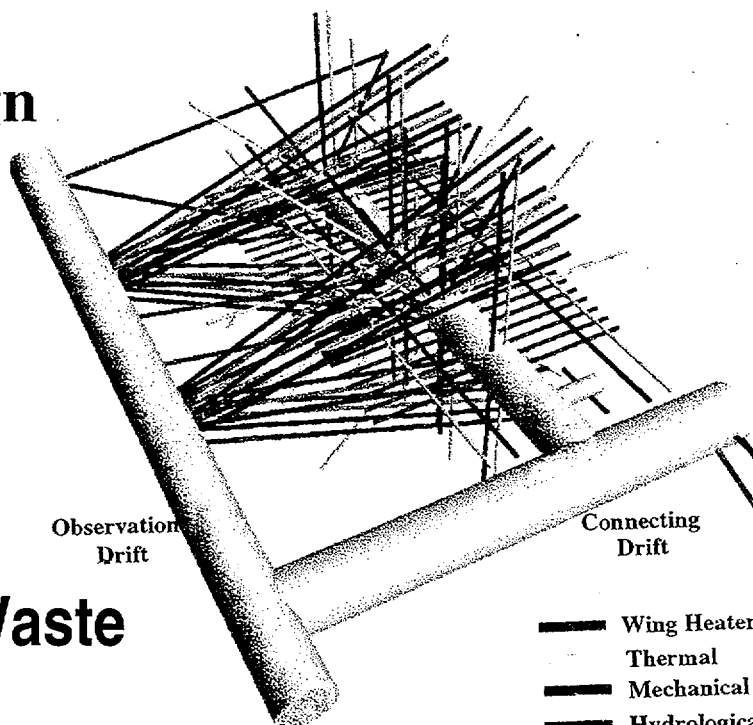
12/11/97



TRW Environmental
Safety Systems Inc.

Drift Scale Test Design and Forecast Results

December 11, 1997



Civilian Radioactive Waste Management System

Management & Operating Contractor

B&W Federal Services
Duke Engineering & Services, Inc.
Fluor Daniel, Inc.
Framatome Cogema Fuels
Integrated Resources Group
INTERA, Inc.
JAI Corporation

JK Research Associates, Inc.
Lawrence Berkeley National Laboratory
Lawrence Livermore National Laboratory
Los Alamos National Laboratory
Morrison-Knudsen Corporation
Sandia National Laboratories

Science Applications International Corporation
TRW Environmental Safety Systems Inc.
Winston & Strawn
Woodward-Clyde Federal Services
Cooperating Federal Agency:
U.S. Geological Survey

Prepared by:
TRW Environmental Safety
Systems Inc.

Prepared for:
U.S. Department of Energy
Office of Civilian Radioactive Waste
Management
1000 Independence Avenue, S.W.
Washington, D.C. 20565

**Civilian Radioactive Waste Management System
Management & Operating Contractor**

Drift Scale Test Design and Forecast Results

BAB000000-01717-4600-00007 REV 01

December 11, 1997

Prepared for:

U.S. Department of Energy
Yucca Mountain Site Characterization Office
P.O. Box 30307
North Las Vegas, NV 89036-0307

Prepared by:

TRW Environmental Safety Systems Inc.
1180 Town Center Drive
Las Vegas, Nevada 89134

Under Contract Number
DE-AC01-91RW00134

2/2/97

DISCLAIMER

This report was prepared as an account of work sponsored by an agency of the United States Government. Neither the United States nor any agency thereof, nor any of their employees, makes any warranty, express or implied, or assumes any legal liability or responsibility for the accuracy, completeness, or usefulness of any information, apparatus, product, or process disclosed, or represents that its use would not infringe privately owned rights. Reference herein to any specific commercial product, process, or service by trade name, trademark, manufacturer, or otherwise, does not necessarily constitute or imply its endorsement, recommendation, or favoring by the United States Government or any agency thereof. The views and opinions of authors expressed herein do not necessarily state or reflect those of the United States Government or any agency thereof.

Civilian Radioactive Waste Management System
Management & Operating Contractor

Drift Scale Test Design and Forecast Results

BAB000000-01717-4600-00007 REV 01

December 11, 1997

Prepared by:

Ralph A. Wagner
R. A. Wagner - ESF Thermal Test Team

Date: 12-12-97

Reviewed by*:

R. J. Henning
R. J. Henning - Scientific Program Operations

Date: 12/12/97

Approved by:

R. N. Datta
R. N. Datta - Technical Lead, ESF Thermal Test Team

Date: 12/12/97

For N. Z. Elkins
N. Z. Elkins - Manager, Thermal Testing &
Engineering Support

Date: 12/18/97

L. R. Hayes
L. R. Hayes - Manager, Scientific Program Operations

Date: 12/15/97

* Signature indicates document was reviewed in accordance with QAP-3-1/Rev. 7.

Civilian Radioactive Waste Management System
Management & Operating Contractor

Drift Scale Test Design and Forecast Results

BAB000000-01717-4600-00007 REV 00

July 16, 1997

Prepared by:

Ralph A. Wagner
R. A. Wagner - ESF Thermal Test Team

Date: July 15, 1997

Reviewed by*:

Terry R. Crump
T. Crump - Licensing

Date: 7/15/97

R. J. Henning
R. J. Henning - Scientific Program Operations

Date: 7/16/97

B. R. Justice
B. R. Justice - Engineering Assurance

Date: 7/16/97

G. N. Kimura
G. N. Kimura - Design

Date: 7/15/97

D. Sevougian
D. Sevougian - Performance Assessment

Date: 7/15/97

Approved by:

R. N. Datta
R. N. Datta - Technical Lead, ESF Thermal Test Team

Date: 7/16/97

N. Z. Elkins
N. Z. Elkins - Manager, Thermal Testing & Engineering Support

Date: 7/15/97

L. R. Hayes
L. R. Hayes - Manager, Scientific Program Operations

Date: 7/16/97

* Signature indicates document was reviewed in accordance with QAP-3-1/Rev. 7

PREFACE

The thermal test in the Exploratory Studies Facility (ESF) is an integral part of Yucca Mountain Site Characterization Project site investigations conducted for the U.S. Department of Energy (DOE). The Civilian Radioactive Waste Management System (CRWMS) Management and Operating Contractor (M&O) manages site characterization activities for the DOE and performs them along with the U.S. Geological Survey. The purpose of the site investigations program is to characterize Yucca Mountain in Nye County, Nevada for the evaluation of its suitability as a potential site for permanent geologic disposal of spent nuclear fuel and high-level nuclear waste.

The ESF Thermal Test has two main components: the single heater test (SHT) and the drift scale test (DST). The intent of the SHT and the DST is to measure/monitor the observable effects of the thermal, mechanical, hydrological, and chemical processes in the near-field rock. The SHT was started on August 26, 1996, and will be followed by the DST, scheduled to start December 8, 1997. The SHT is considered a simplified version of the DST, and generally consists of heating and instrumenting a comparatively smaller rock mass in the ESF. The DST has several elements: the main heated drift test, the plate loading test, and the sequential drift mining test. Both the SHT and the DST are conducted by the ESF Thermal Test Team of the Scientific Programs Operations Department of the CRWMS M&O.

Since the SHT has started and was discussed in detail in a previous report (CRWMS M&O 1996a), this report is primarily a conceptual plan and overview, as of July 1997, of the DST. As such, this plan is one of the primary vehicles by which the ESF Thermal Test Team conceptually describes the technical content and requirements of the DST to interested readers and to the ESF Test Coordination Office (TCO), the entity responsible for preparing the Field Work Package (FWP - Reference FWP-ESF-96-003, Rev 3).¹ The FWP is the controlling document governing the implementation of field activities and test facility design and construction associated with the thermal test. The FWP ensures requirements contained in such documents as the *Exploratory Studies Facility Design Requirements* (YMP 1996a) are addressed and captured for effective flow-down. As a conceptual planning and overview document, information or inputs in this report cannot be used in any other document that is subject to *Quality Assurance Requirements and Description* (DOE 1997) requirements unless the information is identified as TBV and controlled in accordance with appropriate procedures. The vehicle for formal transmission of technical content and requirements to the ESF TCO is the Design and Test Related Information memo.

The sequence of activities associated with field implementation of the DST is:

- Preparation and ongoing updates of design and test-related information by the ESF Thermal Test Team and formal transmittal of that information to the ESF TCO
- Preparation of the FWP by the ESF TCO
- Design of the test facility by the ESF designer

¹ Formerly referred to as the Test Planning Package and the Job Package.

- Construction of the facility by the constructor
- Installation of instruments/equipment and conduct of the test by the tester.

The controlled process of performing these activities under quality assurance procedure begins with the preparation of the FWP by the TCO.

The process, described in the previous paragraph, in which the FWP plays a central role in the control of activities associated with the field implementation of the test, is intended to provide the ability to respond to changing conditions and proceed with test activities in an expeditious manner. Changes may be necessitated because of a variety of reasons, such as a decision to increase or reduce the scope of the test or encountering geologic conditions different from those anticipated.

Interfaces associated with the field implementation of the DST are ESF Thermal Test Team/ESF TCO, ESF TCO/ESF Designer, and ESF TCO/ESF Constructor-Operator. The FWP is the document for the formal control of these interfaces.

There are two ESF Thermal Test related Study Plans under the *Site Characterization Plan* (SCP, DOE 1988). These are Study Plan 8.3.1.15.1.6, In Situ Thermomechanical Properties; and Study Plan 8.3.4.2.4.4, Engineered Barrier System Field Tests. The plan presented in this document complies with these two study plans and hence with those SCP (DOE 1988) issues germane to thermal testing. Also, the three Site Characterization Analysis open items related to thermal testing (comments 4 and 11; question 59) have been addressed both in this report and a complementary report released last year (CRWMS M&O 1996a).

This planning document provides much detail on the pertinent technical issues that encompass the DST. The inclusion of this detail was intentional because of the need to describe the complexities of the DST in a single document. Since this conceptual plan represents a snapshot-in-time of the status of the DST, it does not include a section dedicated to conclusions or recommendations.

CONTENTS

| | Page |
|---|------|
| 1. INTRODUCTION | 1-1 |
| 1.1 BASELINE REPORT | 1-1 |
| 1.1.1 Background | 1-1 |
| 1.1.2 Linkage of the ESF Thermal Test to the SCP and Subsequent Program Directives | 1-7 |
| 1.1.3 Information Needs | 1-8 |
| 1.1.4 Relevant Processes | 1-8 |
| 1.1.5 Scales for Thermal Testing | 1-9 |
| 1.2 UPDATED OVERVIEW OF THE SINGLE HEATER TEST | 1-9 |
| 1.3 REPORT ORGANIZATION | 1-15 |
| 2. OBJECTIVES | 2-1 |
| 2.1 DRIFT SCALE TEST | 2-1 |
| 2.2 OTHER TESTS | 2-2 |
| 2.2.1 Sequential Drift Mining Test | 2-2 |
| 2.2.2 Plate Loading Test | 2-2 |
| 2.2.3 Ground Support Test | 2-3 |
| 2.2.4 Backfill Test | 2-3 |
| 3. DRIFT SCALE TEST FACILITY | 3-1 |
| 3.1 LOCATION | 3-1 |
| 3.2 CONFIGURATION | 3-2 |
| 3.3 MISCELLANEOUS REQUIREMENTS | 3-6 |
| 3.4 SCOPE COMPARISON | 3-6 |
| 4. CHARACTERIZATION | 4-1 |
| 4.1 PRE-TEST | 4-1 |
| 4.1.1 Laboratory | 4-1 |
| 4.1.1.1 Sampling | 4-1 |
| 4.1.1.2 Thermal | 4-2 |
| 4.1.1.3 Mechanical | 4-2 |
| 4.1.1.4 Hydrological | 4-2 |
| 4.1.1.5 Chemical | 4-3 |
| 4.1.2 Field | 4-3 |
| 4.1.2.1 Thermal | 4-3 |
| 4.1.2.2 Mechanical | 4-3 |
| 4.1.2.3 Hydrological | 4-4 |
| 4.1.2.4 Chemical | 4-4 |
| 4.2 POST-TEST | 4-4 |
| 4.2.1 Laboratory | 4-4 |
| 4.2.2 Field | 4-5 |

CONTENTS (Continued)

| | Page |
|--|------|
| 5. ANALYSES | 5-1 |
| 5.1 THREE-PHASE APPROACH | 5-1 |
| 5.2 TEST SCOPING ANALYSES | 5-4 |
| 5.2.1 Thermal-Hydrological Analyses | 5-4 |
| 5.2.2 Thermal-Mechanical Analyses | 5-5 |
| 5.3 PRE-TEST ANALYSES | 5-6 |
| 5.3.1 Summation of the Pre-test, TH Analyses Part 1 | 5-7 |
| 5.3.1.1 Introduction | 5-7 |
| 5.3.1.2 Results | 5-8 |
| 5.3.2 Summation of the Pre-test, TH Analyses - Part 2 | 5-9 |
| 5.3.2.1 Introduction | 5-9 |
| 5.3.2.2 Results | 5-12 |
| 5.3.3 Summation of the Pre-test, Thermal-Mechanical-Hydrological Analyses | 5-14 |
| 5.3.3.1 Introduction | 5-14 |
| 5.3.3.2 Results | 5-15 |
| 5.3.4 Summation of the Pre-test, Thermal-Chemical Analyses | 5-17 |
| 5.3.4.1 Introduction | 5-17 |
| 5.3.4.2 Results | 5-18 |
| 5.4 POST-TEST ANALYSES | 5-19 |
| 6. MEASURING SYSTEMS | 6-1 |
| 6.1 BASES FOR DEVELOPMENT | 6-1 |
| 6.1.1 Background for Scientific Rationale/Engineering Judgement | 6-1 |
| 6.1.2 Background for Thermal Tests | 6-2 |
| 6.1.3 Sensor Reliability | 6-3 |
| 6.1.4 Temperature Measurements | 6-3 |
| 6.1.5 Mechanical Measurements | 6-5 |
| 6.1.6 Hydrological Measurements | 6-6 |
| 6.1.7 Chemical Measurements | 6-7 |
| 6.2 THERMAL | 6-7 |
| 6.2.1 Temperatures | 6-7 |
| 6.2.2 Thermal Conductivity and Thermal Diffusivity | 6-9 |
| 6.3 MECHANICAL | 6-9 |
| 6.3.1 Displacement Measurement | 6-11 |
| 6.3.2 Coupled Thermal-Mechanical Measurement | 6-11 |
| 6.3.3 Modulus Measurement | 6-11 |
| 6.3.4 Acoustic Emissions/Seismic Imaging Measurements | 6-12 |
| 6.4 HYDROLOGICAL | 6-12 |
| 6.4.1 Gas/Air Pressure | 6-12 |
| 6.4.2 Humidity | 6-14 |
| 6.4.3 Liquid Water Saturation | 6-15 |

CONTENTS (Continued)

| | Page |
|--|------|
| 6.5 CHEMICAL | 6-17 |
| 6.5.1 Rock-Water Interaction | 6-18 |
| 6.5.2 Waste Package Materials | 6-18 |
| 6.5.3 Introduced Materials | 6-20 |
| 6.6 MISCELLANEOUS | 6-20 |
| 6.6.1 Moisture Introduced/Extracted During Drilling | 6-20 |
| 6.6.2 Ventilation | 6-20 |
| 6.6.3 Visual (Video Camera) and Remote Observations | 6-20 |
| 6.6.4 Vapor/Air Flow in the Heated Drift | 6-22 |
| 6.6.5 Video Logs of Boreholes | 6-22 |
| 7. CONSTRUCTION | 7-1 |
| 7.1 OBSERVATION DRIFTS | 7-1 |
| 7.2 DRIFT SCALE TEST | 7-2 |
| 7.3 ANCILLARY ESF THERMAL TEST ACTIVITIES | 7-3 |
| 8. HEATING SYSTEMS | 8-1 |
| 8.1 INTRODUCTION | 8-1 |
| 8.2 HEATER DESCRIPTION | 8-1 |
| 8.2.1 Floor Canister Heaters | 8-1 |
| 8.2.2 Wing Heaters | 8-4 |
| 8.2.3 Heater Monitor Panels and Controllers | 8-4 |
| 8.3 HEATING/COOLING PLAN | 8-6 |
| 9. DATA COLLECTION AND SERVICE SYSTEMS | 9-1 |
| 9.1 DATA COLLECTION SYSTEM (INTEGRATED) | 9-1 |
| 9.1.1 General Description | 9-1 |
| 9.1.2 Location and Layout | 9-1 |
| 9.1.3 Drift Scale Test Instrumentation Data Collection Channel Requirements - 5620 Channels | 9-3 |
| 9.1.4 Hardware Description | 9-3 |
| 9.1.5 Data Management | 9-6 |
| 9.1.6 Data Distribution | 9-8 |
| 9.2 DATA COLLECTION SYSTEMS (NON-INTEGRATED) | 9-9 |
| 9.3 DATA SERVICE SYSTEM | 9-9 |
| 9.3.1 Background | 9-9 |
| 9.3.2 Objectives | 9-9 |
| 9.3.3 Features | 9-10 |

CONTENTS (Continued)

| | Page |
|---|------|
| 10. CONTINGENCY PLANNING | 10-1 |
| 10.1 RESERVE HEATING CAPACITY | 10-1 |
| 10.2 POWER OUTAGES | 10-1 |
| 10.2.1 Short-Term | 10-2 |
| 10.2.2 Long-Term | 10-2 |
| 10.3 ROCKFALLS | 10-3 |
| 10.4 REPAIR AND MAINTENANCE STRATEGY | 10-4 |
| 10.5 ADDITIONAL HEATING PERIOD | 10-5 |
| 10.6 WAREHOUSE SPARE PARTS | 10-5 |
| 10.7 INADEQUATE SENSOR PERFORMANCE | 10-5 |
| 11. SCHEDULE | 11-1 |
| 11.1 PURPOSE AND SCOPE | 11-1 |
| 11.2 PLANNING | 11-1 |
| 11.3 FACILITY CONSTRUCTION | 11-3 |
| 11.4 DRIFT SCALE TEST | 11-3 |
| 12. QUALITY ASSURANCE | 12-1 |
| 12.1 PURPOSE AND SCOPE | 12-1 |
| 12.2 PLANNING | 12-1 |
| 12.2.1 Analyses and Software | 12-3 |
| 12.2.2 Preparedness Assessment | 12-4 |
| 12.3 TEST IMPLEMENTATION AND DOCUMENTATION | 12-4 |
| 12.4 ORGANIZATIONAL STRUCTURE OF THE ESF THERMAL TEST TEAM | 12-6 |
| 13. REFERENCES | 13-1 |

FIGURES

| | Page |
|------|--|
| 1-1 | Plan View of ESF Thermal Test Facility 1-2 |
| 1-2 | Schematic of the Single Heater Test 1-3 |
| 1-3 | Schematic of the Drift Scale Test 1-4 |
| 1-4 | Interrelationships Between Processes, ESF Thermal Tests, Process Models, and End Users 1-6 |
| 1-5 | Layout of Single Heater Test 1-10 |
| 1-6 | Summary Schedule for the Single Heater Test 1-14 |
| | |
| 3-1 | Layout of Drift Scale Test 3-3 |
| 3-2 | Drift Scale Test (Cross Section A-A) 3-4 |
| 3-3 | Drift Scale Test (Cross Section B-B) 3-5 |
| | |
| 5-1 | Anticipated One-to-One Coupling of the TMHC Processes Evaluated in the DST . . . 5-2 |
| 5-2 | Temporal Relationship between Data Evolutions, Numerical Analyses, and Computer Programs for the Drift Scale Test 5-3 |
| | |
| 6-1 | Temperature Sensors in Plain and Thin Walled Tubes 6-8 |
| 6-2 | Sketch of REKA Probe 6-10 |
| 6-3 | Schematic of a Packer System with Humidity Sensors and Pressure Transducers . . . 6-13 |
| 6-4 | Neutron Measurement Boreholes 6-15 |
| 6-5 | Schematic Diagram Showing Data Collection Approach for ERT Measurements . . . 6-16 |
| 6-6 | SEAMIST System for Chemical Sensors and Sampling 6-19 |
| 6-7 | Remote Controlled Camera Designed for the Heated Drift 6-21 |
| | |
| 8-1 | Plan View Showing Locations of Floor and Wing Heaters 8-2 |
| 8-2 | Floor Heater Design 8-3 |
| 8-3 | Wing Heater Design 8-5 |
| | |
| 9-1 | Drift Scale Test Data Collection System (Block Diagram) 9-2 |
| 9-2 | Data Collection System Hardware Block Diagram 9-4 |
| 9-3 | Data Collection System Organization Chart 9-7 |
| 9-4 | Data Flowchart for the ESF Thermal Test 9-11 |
| | |
| 11-1 | Summary Schedule (Calendar Years) for Drift Scale Test 11-2 |
| | |
| 12-1 | Test Planning Process and Controls 12-2 |
| 12-2 | Drift Scale Test Implementation 12-5 |
| 12-3 | Organizational Structure of the ESF Thermal Test Team 12-7 |

INTENTIONALLY LEFT BLANK

TABLES

| | | Page |
|-----|---|-------------|
| 1-1 | Thermal Testing Scales | 1-9 |
| 1-2 | Borehole and Sensor Information for the Single Heater Test | 1-11 |
| 3-1 | Borehole Information for the Drift Scale Test | 3-7 |
| 3-2 | Scope Comparison of the Drift Scale Test and 16 Other Thermal Tests | 3-13 |
| | | |
| 6-1 | Sensor Performance of Other In Situ Heater Tests | 6-4 |
| | | |
| 9-1 | Geotechnical Instrumentation Data Collection Channel Requirements | 9-3 |

INTENTIONALLY LEFT BLANK

ACRONYMS

| | |
|---------|--|
| AC | Alternating Current |
| A/D | Analog to Digital |
| CRWMS | Civilian Radioactive Waste Management System |
| D/A | Digital to Analog |
| DCS | Data Collection System |
| DKM | Dual Permeability Model |
| DOE | U.S. Department of Energy |
| DSS | Data Service System |
| DST | Drift Scale Test |
| ECM | Effective Continuum Model |
| ERT | Electrical Resistivity Tomography |
| FWP | Field Work Package |
| GPR | Ground Penetrating Radar |
| HD | Heated Drift |
| LAN | Local Area Network |
| M&O | Management and Operating Contractor |
| MPBX | Multi-point Borehole Extensometers |
| PI | Principal Investigator |
| REKA | Rapid Estimation of Thermal Conductivity (k) and Thermal Expansion (alpha-α) |
| RTD | Resistance Temperature Detector |
| SCP | Site Characterization Plan |
| SDMT | Sequential Drift Mining Test |
| SEAMIST | Science Engineering Associates Membrane In Situ Sampling Technique |
| SHT | Single Heater Test |
| TCO | Test Coordination Office |
| TC | Thermal-Chemical |
| TH | Thermal-Hydrological |
| TM | Thermal-Mechanical |

ACRONYMS (Continued)

| | |
|--------|--|
| TMHC | Thermal-Mechanical-Hydrological-Chemical |
| Tptpmn | T ertiary Miocene (Age), P aintbrush (Group), T opopah Spring Tuff (Formation), C ystal- P oor (Member), M iddle Non Lithophysal (Zone) |
| UPS | Uninterruptible Power Supply |
| WWF | Welded Wire Fabric |

1. INTRODUCTION

The Exploratory Studies Facility (ESF) Thermal Test Facility (see Figure 1-1) is the location of two heater tests, the single heater test (SHT) and the drift scale test (DST). Schematics of these two heater tests are shown in Figures 1-2 and 1-3. The layout and details of the SHT were presented in a previous document [Civilian Radioactive Waste Management System (CRWMS) Management and Operating Contractor (M&O) 1996a]. Since the discussion of the DST was limited in the previous report, the following discussion will mostly be related to the DST; however, an updated overview of the SHT is provided in Section 1.2.

1.1 BASELINE REPORT

The *Test Design, Plans and Layout Report for the ESF Thermal Test* (CRWMS M&O 1996a) is a baseline planning report that was published last year and presented much information about the ESF Thermal Test. Specifically, the discussion of the SHT and DST in this baseline report included the following scope:

- Background Information
- Objectives
- ESF Thermal Test Facility
- Characterization of the Rock Mass
- Analyses
- Construction
- Heating
- Data Collection
- Contingencies
- Schedule and Operations
- Quality Assurance.

This report introduces refinements and additions to the baseline report mentioned above. Significant refinements and additions have occurred in the analyses section from those reported previously (CRWMS M&O 1996a), whereas changes in the other scope components are considered minor.

1.1.1 Background

The ESF Thermal Test is an integral part of the site investigations program to characterize Yucca Mountain in Nye County, Nevada for the permanent disposal of spent nuclear fuel and high-level nuclear waste. The purpose of the ESF Thermal Test is to acquire a more in-depth understanding of the coupled thermal, mechanical, hydrological, and chemical (TMHC) processes likely to exist in the rock mass surrounding the potential geologic repository at Yucca Mountain. Plans for a suite of in situ thermal tests to be conducted in the ESF began with the *Site Characterization Plan* (SCP) (U.S. Department of Energy [DOE] 1988). The planning basis documented in the SCP has evolved over the past several years to meet the changing needs and updated knowledge base of the project. The most recent iteration, in which the SCP thermal testing program was re-evaluated and consolidated, is discussed in *In Situ Thermal Testing Program Strategy* (DOE 1995). An update

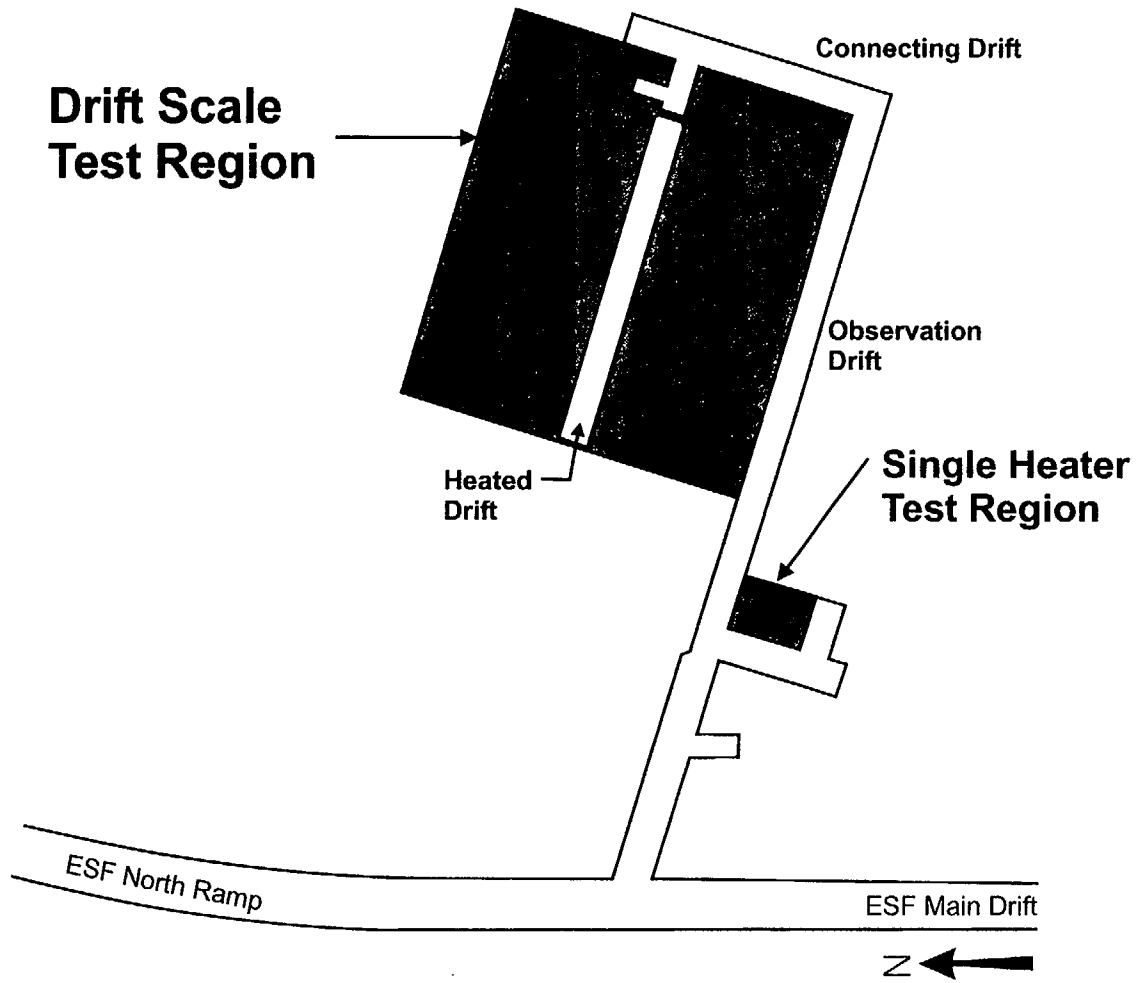


Figure 1-1. Plan View of ESF Thermal Test Facility

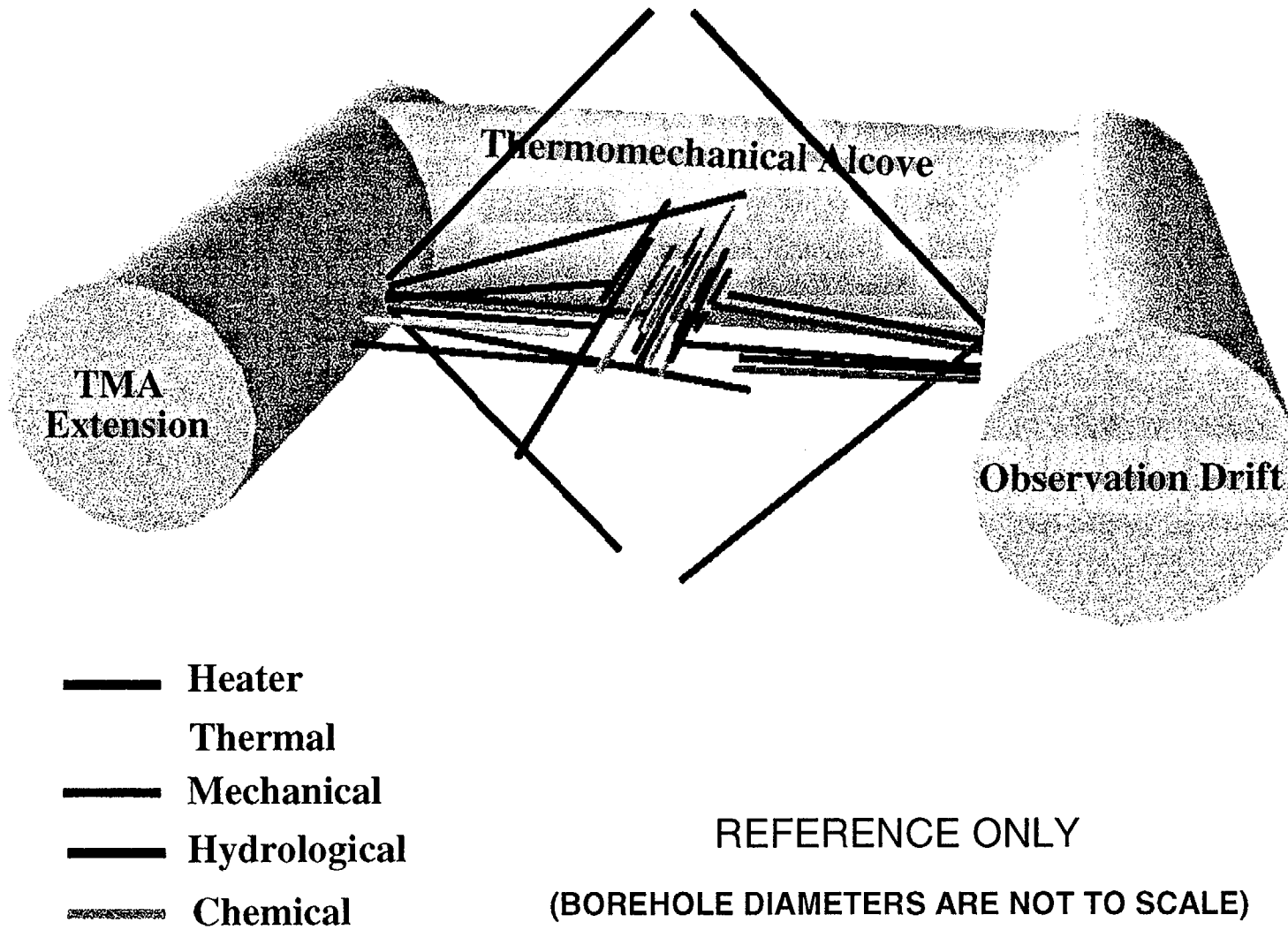


Figure 1-2. Schematic of the Single Heater Test

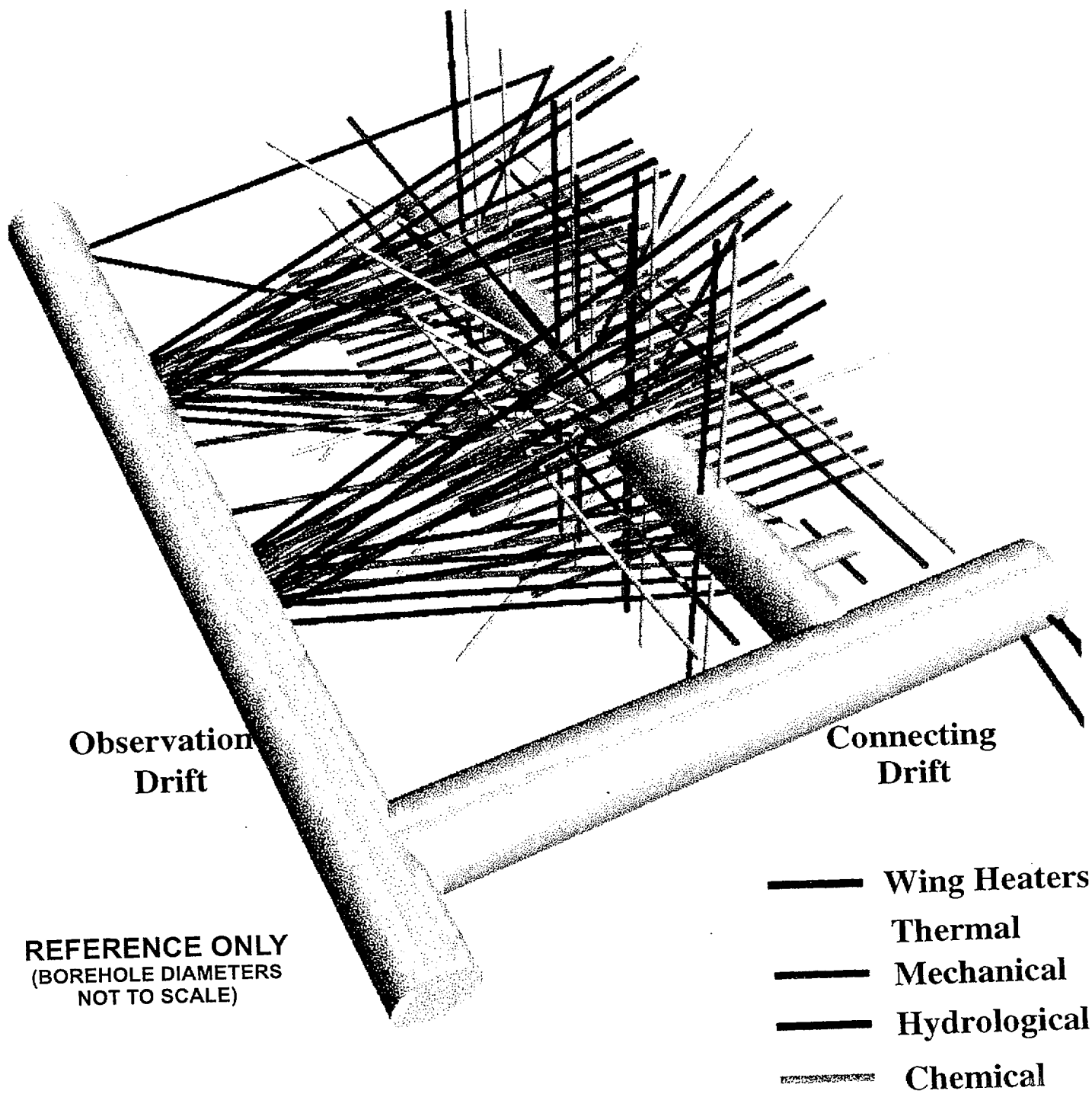


Figure 1-3. Schematic of the Drift Scale Test

to that report has been prepared by the ESF Thermal Test Team and was submitted to DOE for review in March 1997. The ESF Thermal Test is being conducted in a facility specifically constructed for this purpose in the Tptpmn [Tertiary Miocene (Age), Paintbrush (Group), Topopah Spring Tuff (Formation), Crystal-Poor (Member), Middle Non Lithophysal (Zone)] lithologic unit of the proposed repository horizon.

The ESF Thermal Test is based on the interrelationships among four process types and three end-users as shown in Figure 1-4. The relationship represents the manner in which field tests play an integral role in supplying data, information, and model refinement to support a robust license application. Therefore, it is important that these interrelationships be well established and properly maintained to ensure the ESF Thermal Test is designed in a responsive manner. To this extent, numerous meetings, conversations, and correspondence have occurred between the ESF Thermal Test Team and representatives of the waste package, repository, and ESF design teams, and the performance assessment group.

Interfacing between the ESF Thermal Test Team and the end-users was conducted to develop a well-planned thermal test and to resolve any problems. Problems or issues have been resolved informally with meetings and phone conversations, formally with technical memorandums, or through the M&O review process (QAP-3-1, *Document Review*) in which the end-users were formal reviewers. To ensure changes made to accommodate an end-user are acceptable to the other end-users, workshops and formal meetings have been held to discuss those refinements or adjustments in which representatives from all the end-users were invited.

With the adoption of the *Civilian Radioactive Waste Management Program Plan (Program Plan)* (DOE 1994), a re-evaluation program for in situ thermal testing in the ESF, as described in the SCP (DOE 1988), was initiated. The first phase of this re-evaluation, documented in *In Situ Thermal Testing Program Strategy* (DOE 1995), resulted in a consolidated list of five types of in situ thermal tests:

- Large Block Test
- Single element heater tests (vertical and horizontal)
- Plate source test
- Emplacement drift test.

The first phase re-evaluation addressed the needs of the *Program Plan* (DOE 1994) milestone for a Technical Site Suitability determination in 1998 and a license application to construct the repository in 2001.

In addressing the needs of the *Program Plan* milestone for the license amendment to receive and process high-level waste in 2008, a second phase re-evaluation considered the following:

- A larger suite of tests/studies
- Time and resources needed to conduct them
- Relative contribution toward the needs of various program milestones.

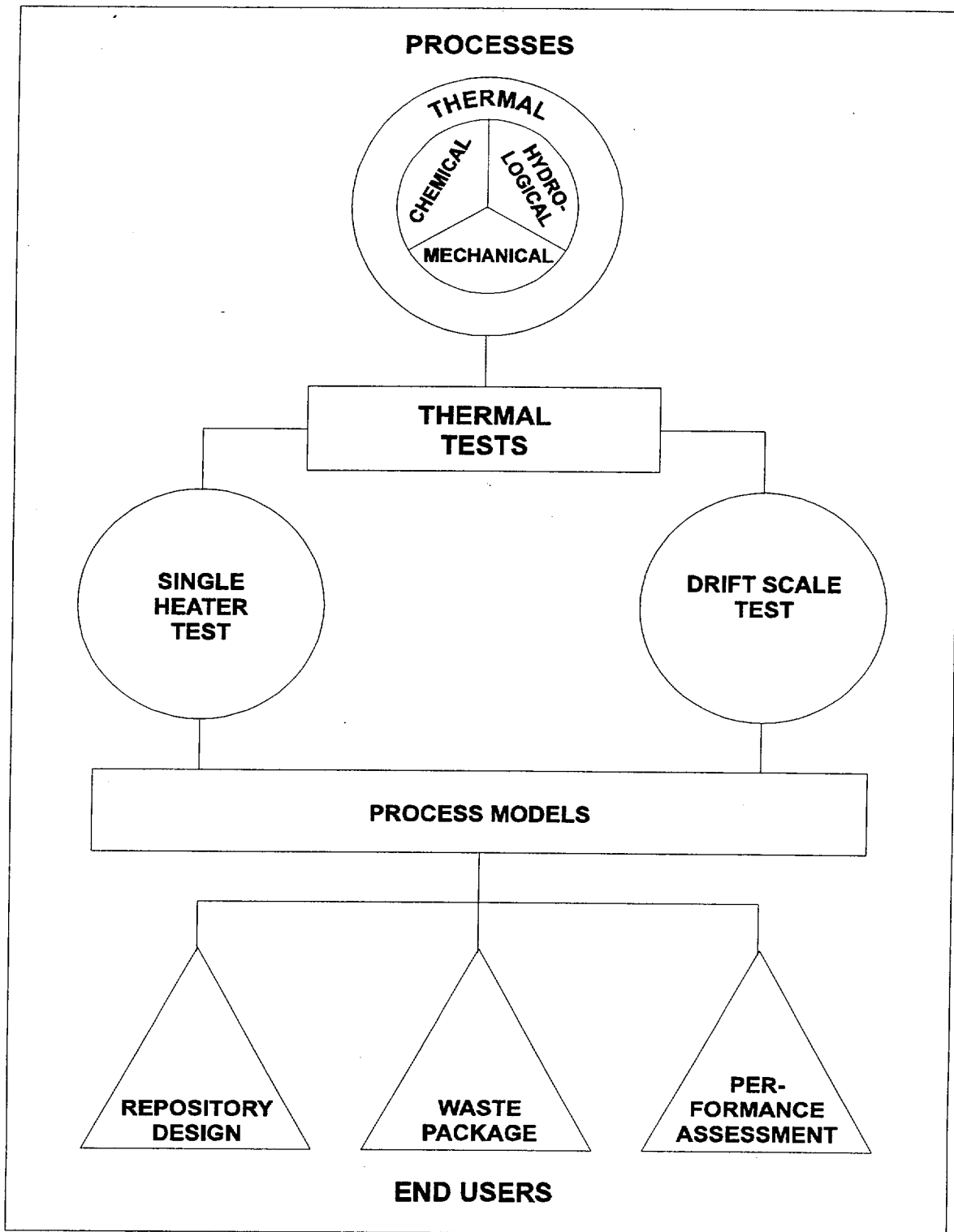


Figure 1-4. Interrelationships Between Processes, ESF Thermal Tests, Process Models, and End Users

The outcome of the second phase re-evaluation, to be documented in a DOE Yucca Mountain Site Characterization Office report, was a further consolidated thermal testing program comprised of four types of in situ tests: the Large Block Test, the single element heater test (horizontal), the DST, and the large-scale, long-duration test. Of these, the single element heater test can be conducted at multiple locations in the ESF to address data needs associated with representativeness and spatial variability.

Subsequently, the significant budget reductions for FY 1996 and projections of similar budgets for future years, led to the decision to delay the Large Block Test at Fran Ridge and to proceed with the implementation of a single in situ thermal test in the ESF. The ESF Thermal Test is comprised of an SHT and a DST. The DST consists of a sequential drift mining test (SDMT), a plate loading test, and a heated drift test. In the DST, the local rock mass will be heated by 50 electrical heaters placed in horizontal boreholes drilled at the springline and 9 floor heaters located in the heated drift (HD). Ultimately, TMHC behavior in the local (near field) rock mass and the performance of a prototype ground support system will be measured in the main DST. Additional thermal and/or mechanical responses will be measured in the SDMT and the plate loading test of the DST.

1.1.2 Linkage of the ESF Thermal Test to the SCP and Subsequent Program Directives

The linkage of the ESF Thermal Test to the SCP (DOE 1988) and subsequent program directives has been well chronicled over the past eight years. The following citations represent current Yucca Mountain Site Characterization Project documents that describe scientific plans for the ESF Thermal Test. These documents, together with related study plans, include:

- SCP Studies:
 - Section 8.3.1.15.1.5 Excavation Investigations
 - Section 8.3.1.15.1.6 In Situ Thermal-Mechanical Properties
 - Section 8.3.1.15.1.7 In Situ Mechanical Properties
 - Section 8.3.4.2.4.4 Engineered Barrier System Field Tests
- *FY 1996 Annual Project Implementation Plan* (CRWMS M&O 1995b)
- *In Situ Thermal Testing Program Strategy* (DOE 1995)

The SCP (DOE 1988) is the basis for the site characterization testing program. With subsequent major changes described in the *Program Plan* (DOE 1994), the testing basis was adjusted to reflect the new strategy. The needed changes were mostly changes in timing and degree, but additional technical and budget constraints also dictated changes in the testing basis. In this section, a brief review of the SCP (DOE 1988) basis for thermal testing is presented and followed by a more detailed examination of the requirements basis for the thermal test program under the *Program Plan*. This revised requirements basis was developed using a user-supplier model. Major users for thermal test data include waste package and repository design, preclosure and postclosure performance assessment, and the licensing and site suitability organizations. As the supplier, the test community has worked with the users to reach agreement on the basic data that the test program should provide. These requirements must fit within the basic licensing framework outlined in the SCP (DOE 1988) (i.e., the issue resolution strategy) and must also meet the evolving needs of the project.

In Section 8.3 of the SCP (DOE 1988), a number of in situ thermal tests were proposed to investigate various aspects of thermal performance. These tests included measurement of thermal properties, investigations of TM effects on drift stability, and study of coupled TMHC processes that may affect the near field and waste package performance or the far field natural system performance. The objective of this suite of tests was to provide data for use in determining site suitability, for direct input into repository and waste package design, for model development and validation, and for performance assessments of preclosure safety and postclosure performance. In the SCP (DOE 1988), the conceptual nature of the testing program was discussed along with the explicit ties to the data needs. Each test was expected to provide primary or confirmatory information for resolving specific performance and design issues within the SCP issues hierarchy. The tests were divided into two main categories: tests focused principally on the resolution of preclosure and postclosure repository design issues (SCP Section 8.3.1.15.1), and tests focused on resolving postclosure waste package design and near field performance issues (SCP Section 8.3.4.2.4). In summary, not all aspects of the SCP will be discussed in the ESF Thermal Test. Rather, the test will focus primarily on obtaining a better understanding of the TMHC behavior in the local rock mass.

1.1.3 Information Needs

The data needs for the thermal testing program are identified in the SCP (DOE 1988) and further refined in the *In Situ Thermal Testing Program Strategy* (DOE 1995). These needs are described in three basic terms (bounded, conservative, and substantially finished) and provide the anticipated status of information and data following the completion of the ESF Thermal Test.

1.1.4 Relevant Processes

Four processes are identified that are evaluated in the ESF Thermal Test: thermal, mechanical, hydrological, and chemical. Each process consists of at least four subprocesses that are considered either primary or secondary in importance.

Discussion of the matrix of processes alludes to the appropriateness of the temporal and spatial scales in the ESF Thermal Tests. On a comparative basis, the temporal and spatial scales planned for the ESF Thermal Test are approximately equivalent or substantially longer and larger than other thermal tests associated with geologic disposal of nuclear waste (DOE 1995). This comparison with other thermal tests, combined with the ESF Thermal Test objective to better understand the coupled TMHC processes, ensures, to a large degree, that the planned temporal and spatial scales are appropriate. By linking the objective to the TMHC processes, investigators can properly address scaling issues because emphasis is placed on heating and cooling a substantial volume of rock such that observable dryout and rewetting zones are created. Conversely, a definitive measure of time and space would have been unnecessarily restrictive.

In summary, the temporal and spatial scales are suitable for the ESF Thermal Test such that emphasis can be placed on better understanding the TMHC coupled processes that influence postclosure behavior. Characterizing other postclosure behavior is outside the scope of the ESF Thermal Test.

1.1.5 Scales for Thermal Testing

Thermal testing needed to better understand the coupled TMHC processes surrounding a nuclear waste repository includes a wide range of scales. Specifically, Table 1-1 lists six scales of thermal testing that range from laboratory testing of small rock specimens to performance confirmation of the rock mass surrounding a nuclear waste repository. These six different types of thermal tests are compared in terms of total measurements, volume of perturbed rock, and test duration. These estimates of the volume of perturbed rock are based mostly on scoping and pre-test analyses (see Section 5).

Table 1-1. Thermal Testing Scales

| Test Scale | Total Measurements (No. - Estimated) | Volume of Perturbed Rock (m ³ - Estimated) | Test Duration (Years - Estimated) |
|--|---|--|--------------------------------------|
| Laboratory | $< 1 \times 10^3$ | $< 1 \times 10^{-1}$ | < 0.5 |
| Large Block | 1×10^6 | 4×10^{-1} | 0.9 |
| Single Heater | 5×10^6 | 1×10^3 | 1.5 |
| Drift Scale | 3×10^8 | 1×10^5 | 8 |
| Large Scale, Long-Duration (Plan Pending) | 1×10^9 | 2×10^5 | 10 |
| Performance Confirmation | 1×10^{10} | 5×10^7 | 100 |

Ranges of values for total measurements and test volume are approximately eight orders of magnitude, whereas the ranges of values for test duration are approximately four orders of magnitude. These substantial ranges provide a cross-section of measured data that can be compared to a complementary suite of predicted data to ensure a robust evaluation of coupled TMHC processes in the rock mass surrounding a nuclear waste repository.

1.2 UPDATED OVERVIEW OF THE SINGLE HEATER TEST

Although the SHT was discussed thoroughly in the baseline planning report (CRWMS M&O 1996a), additional detail has been provided in this report for continuity purposes. A detailed description, which reflects the as-built conditions of the SHT, is provided in Figure 1-5 and Table 1-2. Table 1-2 also provides a breakdown of sensor number and type for the SHT. The SHT consists of a nominal 4 kW heater emplaced in one of 41 boreholes that have a cumulative length of approximately 230 m. The remaining boreholes house 530 sensors that measure the thermal (333 sensors— thermocouples, resistance temperature detectors [RTDs], and thermistors), mechanical (45 sensors— load cells and extensometers), hydrological (52 sensors—humidity, pressure transducers, and electrical resistivity tomography [ERT]), and/or chemical (100 sensors—absorbent pads) responses from heat generated by the emplaced heater. Most of these measurements are recorded by a data collection system (DCS) on at least an hourly basis. Sensors located on the heater are scanned every 15 minutes. The DCS is a Geomation Model 2380 meter control unit in NEMA-12 enclosures that is the central component of a system that consists of approximately 15 km (10 miles) of wiring, 1600 connections, and 640 channels. The non-DCS measurements are made by independent systems such as ERT, neutron logging, ground penetrating radar (GPR), Goodman jack, and air-permeability. These non-DCS measurements are taken much less frequently than the DCS measurements because of logistical and

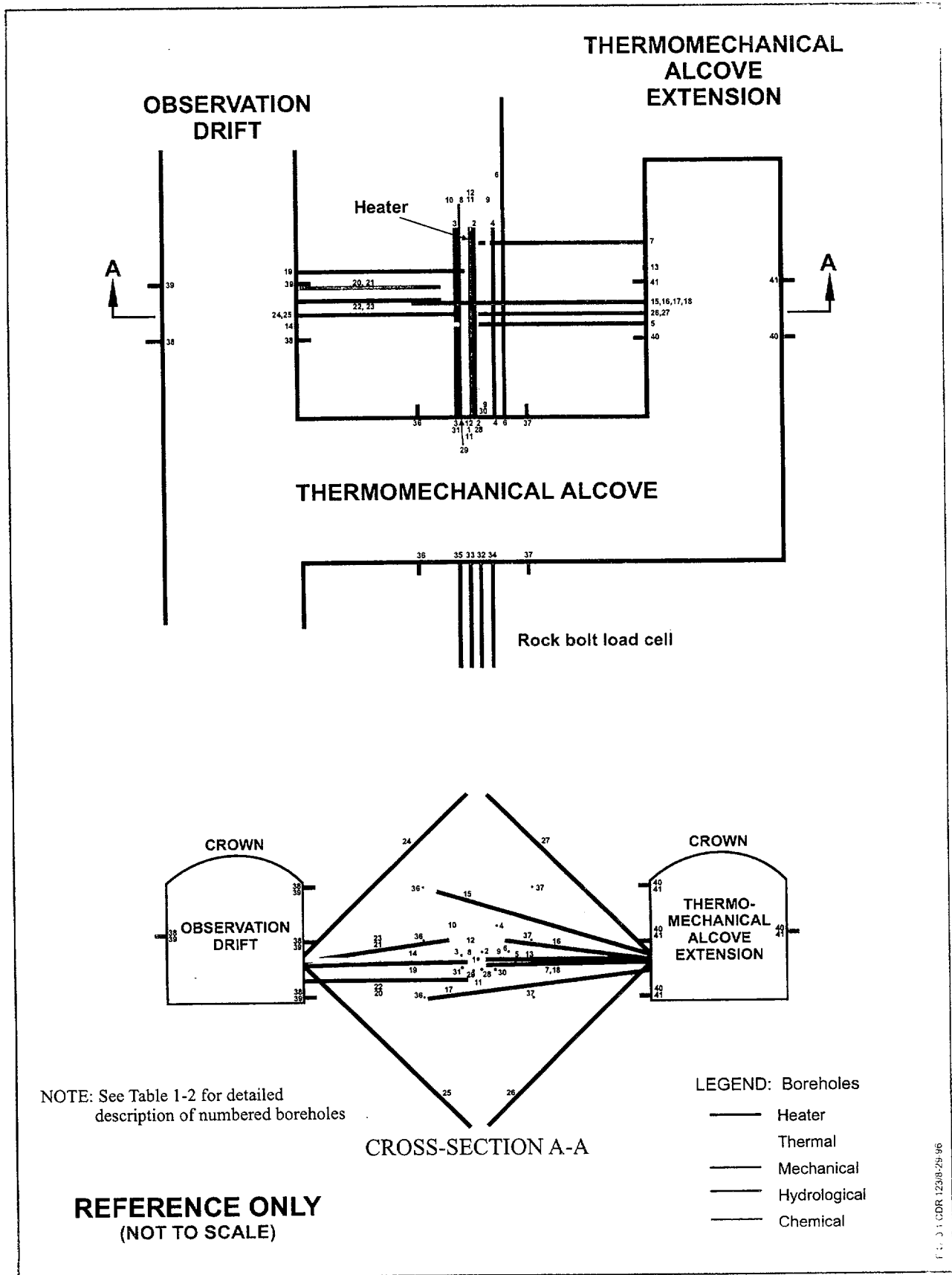


Figure 1-5. Layout of Single Heater Test

INTENTIONALLY LEFT BLANK

INTENTIONALLY LEFT BLANK

technical reasons. In general, these measurements are taken every 100 days or less. This reduced frequency is considered technically acceptable because of the nature of the measured responses and its gradual change in the local rock mass.

The SHT was initiated on August 26, 1996 with the activation of the heater. The SHT continued heating for nine months until the heater was turned off on May 28, 1997. The cooling phase is anticipated to last approximately nine months until the end of February 1998. The summary schedule for the SHT is provided in Figure 1-6.

Measured and predicted data have been compared, evaluated, and documented on a quarterly basis, and compilation of these evaluations have been documented in the *Single Heater Test Interim Report* (CRWMS M&O 1997a). The following conclusions provide a summation of findings presented in the SHT interim report.

The comparison of predicted and measured temperatures indicates good overall agreement despite some temporal and spatial disparities. The ability to predict the measured temperature is important since the thermal behavior drives the MHC processes. Also, it appears that conduction is the dominant mode of heat transfer in the SHT block.

Comparison of predicted and measured data has led to the following observations of the TM responses. First, the agreement between predicted and measured displacements appears satisfactory for the initial several months of heating. Second, the anticipated one-way coupling of TM processes has been confirmed. One-way coupling implies one process (thermal) influences the other process (mechanical) much more than the converse. Also, the measured data indicate that the presence of fractures substantially influences the TM behavior during the early stages of heating. In general, the rock mass stiffens as temperature increases.

Measurements by ERT, neutron logging, and GPR indicate the development of a dryout region surrounding the heater. Subsequent condensation of moisture at some distance away from the heater has also been observed indirectly, using air-permeability testing. Predictions using the NUFT code do not closely compare with observations in this regard. Nonetheless, strong one-way TH coupling appears to exist in the SHT. Also, lowering of measured bulk air-permeability because of increased saturation from moisture condensation has been observed.

The TC comparison of predicted and measured data is largely limited to the evaluation of the water extracted from the inner portion of borehole 16. Chemical analyses confirmed that this water is condensate of evaporate pore water and appears to have been exposed to fracture filling minerals. The chemical sensors installed in the SHT block failed in the harsh thermal environment. Absorbent pads emplaced in boreholes have yielded samples for ongoing laboratory analyses of water chemistry.

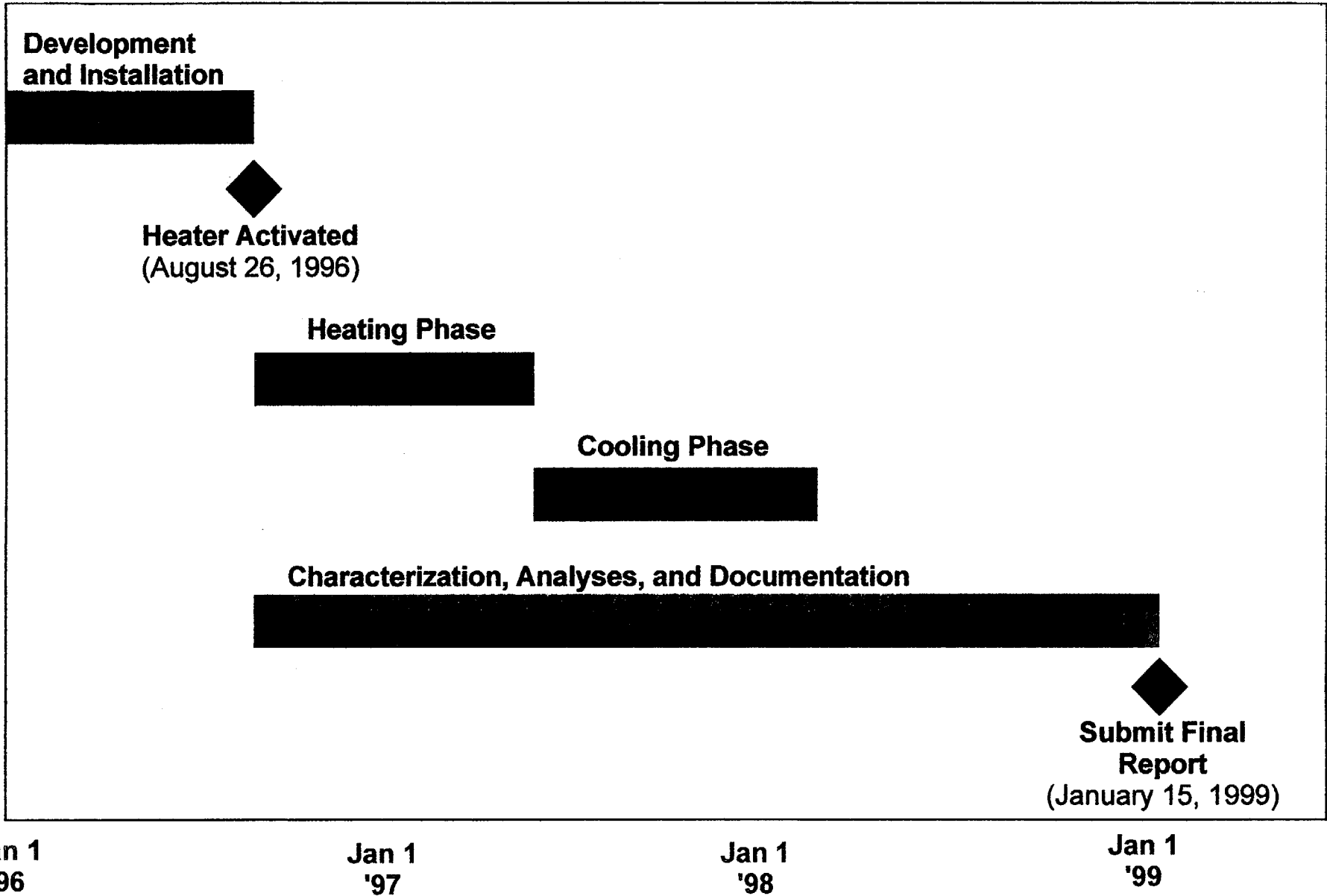


Figure 1-6. Summary Schedule for the Single Heater Test

1.3 REPORT ORGANIZATION

This report is organized such that refinements and additions to the DST, as reported previously (CRWMS M&O 1996a), are emphasized.

Section 2 Restates the DST objectives in terms of primary and complementary components.

Section 3 Updates the description of the DST.

Section 4 Presents characterization methodology for the DST block.

Section 5 Presents scoping analyses and extensive pre-test analyses of the DST which provides a basis for future calculations.

Section 6 Introduces refinements in measuring systems in which many components are similar to those used in the SHT.

Section 7 Discusses construction activities and issues including the rationale for implementing drill-and-blast mining and the design of the bulkhead.

Section 8 Contains a description of the wing and floor (canister) heaters and the corresponding heating/cooling plan.

Section 9 The DCS for the DST is highlighted along with the introduction of a complementary component referred to as the data service system.

Section 10 Presents an update of contingency planning.

Section 11 Presents DST summary schedule.

Section 12 Provides discussion of quality assurance.

Section 13 Provides a list of the references cited in this report.

INTENTIONALLY LEFT BLANK

2. OBJECTIVES

Although the following objectives have been discussed previously in the *Test Design, Plans and Layout Report for the ESF Thermal Test* (CRWMS M&O 1996a), they are refined here for clarification. Objectives are presented for the DST and other related, but smaller, tests.

2.1 DRIFT SCALE TEST

The primary objective of the DST is to develop a more in-depth understanding of the in situ coupled TMHC processes anticipated in the local rock mass surrounding the proposed repository. This objective implies that the understanding of the coupled TMHC processes is more important than fielding an experiment that replicates the actual repository environment. Development of actual repository conditions, geometries, and heating rates is neither practical nor necessary to satisfy this DST objective.

The primary objective is augmented by a series of complementary objectives that are mostly divided among the four processes. Many of these objectives stem from those established for the Plate-Source Thermal Test and the Emplacement Drift Thermal Test described in the *In Situ Thermal Testing Program Strategy* (DOE 1995).

- **Thermal**

- Measure the temporal and spatial distributions of temperature.
- Evaluate influence of heat transfer modes.
- Investigate possible formation of heat pipes.
- Determine rock mass thermal properties.

- **Mechanical**

- Measure rock-mass TM properties at ambient and elevated temperatures.
- Evaluate ground support response under controlled conditions.
- Measure drift convergence at elevated temperatures.
- Observe effects of thermal loading on prototypical ground support systems and overall room stability.

- **Hydrological**

- Measure changes in rock saturation particularly in the drying zone.
- Monitor the propagation of drying and subsequent re-wetting regions, if any, including potential condensate cap and drainage.

- Measure changes in bulk permeability (pneumatic).
- Measure drift-air humidity, temperature, and pressure.
- **Chemical**
 - Observe corrosion products on typical waste package materials emplaced in the HD and boreholes.
 - Observe changes in water chemistry, mineralogy, and rock chemistry during heating and cooling.
 - Observe impacts of introduced materials (ground support, etc.) on water and rock chemistry.
 - Observe thermal effects on ground support materials.
- **Overall**
 - Evaluate conceptual models that calculate the coupled TMHC behavior such that realistic bounds can be developed for the expected near-field environment.

Although the objectives of the DST are clearly delineated, it is important to note that much emphasis of the DST is on the measurement and prediction of the TH behavior. Developing a better understanding of the TH behavior on a comparatively large scale is considered important because of the TH complexity and ramifications on performance of the natural barrier system to provide postclosure containment of radionuclides.

2.2 OTHER TESTS

2.2.1 Sequential Drift Mining Test

The objective of the SDMT is to evaluate the mechanical response, from the excavation, of representative rock mass surrounding a repository-scale drift. Specifically, the SDMT provided baseline information on the mechanical response of the HD portion of the ESF Thermal Test. Because this small, rapid deformation occurs as the drift is excavated, it is important that the measurements were designed to capture, to the extent practical, this initial response. The instrumentation for the SDMT will become part of the DST now that the baseline (excavation) response has been measured.

2.2.2 Plate Loading Test

The objective of the Plate Loading Test is to characterize the rock mass deformation modulus in the Tptpmn under both ambient and elevated temperatures. The rock mass deformation modulus is an important parameter in the TM and TH modeling of the rock mass and ground support interactions for the ESF and the repository design.

2.2.3 Ground Support Test

The objective of the ground support test is to evaluate the interactions between the heated rock mass and the ground support systems under consideration. Also, changes in ground support components will be evaluated at elevated temperatures.

2.2.4 Backfill Test

The backfill testing is pending a systems study regarding its feasibility based, in part, on technical and regulatory considerations.

INTENTIONALLY LEFT BLANK

3. DRIFT SCALE TEST FACILITY

This section discusses the test facility for the DST in terms of location and configuration. Preliminary analyses, previous testing experience, and preliminary interactions with facility construction and design personnel were used to develop the DST. This configuration of the DST represents an update to the previously reported configuration (CRWMS M&O 1996a). The overall changes are not considered substantial since the geometry, boreholes, heating, and measuring systems have remained somewhat similar. Also, it is anticipated that the following description will be close to the as-built conditions since construction of the drifts and several boreholes are complete.

3.1 LOCATION

The general location of the ESF Thermal Test Facility and the DST are shown in Figure 1-1. As was described in Section 2, the DST is required to satisfy numerous technical objectives as well as support key program milestones. Other constraints and requirements that influenced the selection of the DST's location are cited below:

- The DST will be conducted in the Tptpmn lithologic unit, the primary unit of the proposed repository horizon, to ensure that rock mass characteristics are representative.
- The DST will not adversely impact the available area for waste storage should the site be selected for the repository. Therefore, the ESF Thermal Test location is in a nearby area currently not considered for primary waste emplacement. This area is directly south of the north ramp and east of the north-south main drift of the ESF.
- The DST will be sufficiently removed from the main drift of the ESF such that the ESF will not interfere with the measurement of the TMHC response. Formal design criteria (Letter from R. Datta to D. J. Weaver: *Design and Test Related Information for the First ESF Thermal Test (Test Planning Package 95-12 and Job Package 95-29)*. SCPS: 8.3.1.15.1.6 and 8.3.4.2.4.4. LV.SI.RND.10/95-557.) dictate that a standoff distance of 50 m will be maintained between the north-south main drift of the ESF and the DST HD. Similarly, a standoff of about 25 m is needed between the north-south main drift of the ESF and the SHT.
- The DST will include a sufficient thickness of Tptpmn above the HD to minimize potential edge effects from stratigraphic changes. Preliminary analyses (Buscheck and Nitao 1995) indicate that a minimum of about 10 m of nonlithophysal tuff (Tptpmn) is required above the top of the DST to minimize TH and TM edge effects associated with stratigraphic changes. Likewise, a minimum overburden of 5 m is required for the SHT.
- Sufficient distance between the SHT and the DST will exist to prevent test-to-test interference. Based on past experiences and engineering judgement, it is estimated that this distance be a minimum of 25 m. This standoff will minimize potential deleterious effects of ventilation and excavation on either the ambient saturation or bulk permeability of the local rock mass.

3.2 CONFIGURATION

The configuration for the DST, which is shown in Figure 1-1, includes a declining observation drift driven mostly east and downward from near the intersection of the north ramp and main drift. Specifically, the breakout of the observation drift from the main drift of the ESF is at station 2,827 m which is referenced to the north ramp portal. The downward slope of the observation drift, which ranges from 11.5 to 14.0 percent, ensures the minimum 10 m overburden for the DST (see Section 3.1). The length of the observation drift is approximately 140 m.

At the elevation of the DST, nominally 10 m below the upper extent of the Tptpmn, the connecting drift will break out to the north from the observation drift currently at 136 m from the main drift of the ESF (see Figure 1-1). The actual distance of the breakout from the main drift was determined by the requisite overburden (at least 10 m) and, to a lesser extent, by rock quality and rock mass permeability testing determined by ambient site characterization activities (see Section 4). The length of the connecting drift is approximately 40 m.

The plan view and representative cross-sections of the DST are shown in Figures 3-1, 3-2, and 3-3, respectively. The DST consists of a nearly 50-m long, 5-m diameter HD. The HD is complemented with both a connecting and observation drift of similar diameter. Other components include plate loading and DCS niches. Heat is generated from 50 wing heaters and 9 floor (canister) heaters. These two types of electrical heaters will have an initial, combined power output of approximately 200 kW. Both the wing heaters and boreholes are perpendicular to the longitudinal axis of the HD. Wing heaters are evenly distributed on 1.83 m spacings in horizontal boreholes located on both walls of the HD. Each wing heater has 10 m of heated length evenly divided between inner and outer heating elements. The TMHC responses are measured with approximately 3500 sensors housed in 147 boreholes. These sensors will be connected to a DCS with an estimated 125 miles of wire. The cumulative length of these boreholes is 3300 m (2 miles). The sensors are divided into the following categories:

- 3000 thermal (thermocouples, RTDs, and thermistors)
- 110 mechanical (extensometers)
- 412 hydrological (humidity, pressure transducer, and ERT)
- 30 chemical.

Numerous variables, including temperature, heat flux, heater power, thermal expansion, thermal conductivity, moisture, water flux, water chemistry, displacements, and ground support behavior will be measured from sensors installed from within the DST drift and from the connecting and observation drifts. Table 3-1 provides a tabulation of DST borehole information including location, geometry, sensor types, and sensor spacings. Planned durations for the heating and cooling phases are four years each. The heating phase should elevate temperatures of the rock above 100°C in more than 10,000 cubic meters of rock while allowing the temperature along the drift wall to reach 200°C.

Instrumentation for measurement of numerous variables including temperature, heat flux, heater power, thermal expansion, thermal conductivity, moisture, water flux, water chemistry, stress, displacements, and ground support behavior will be installed from within the DST drift and from the connecting and observation drifts.

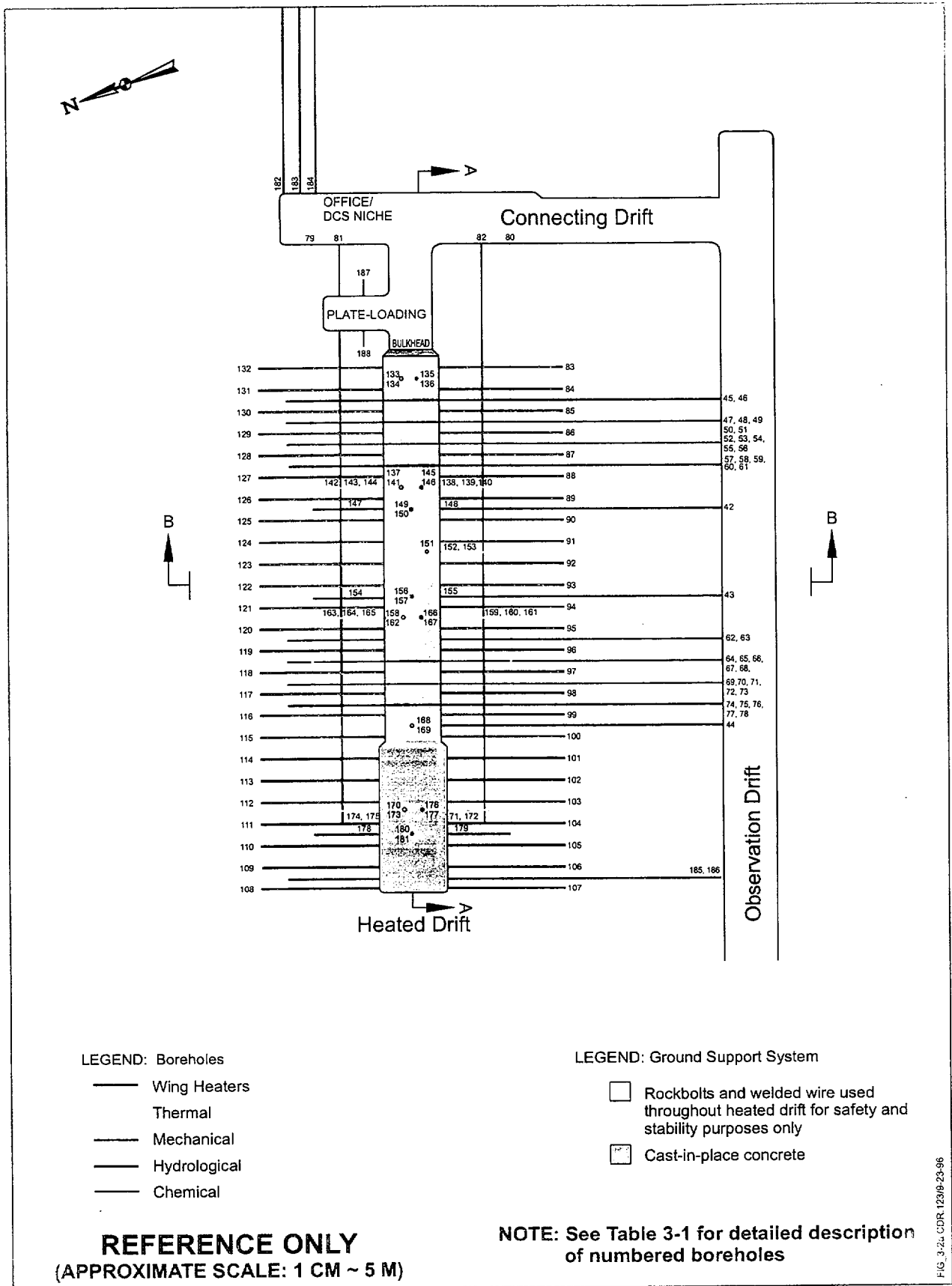
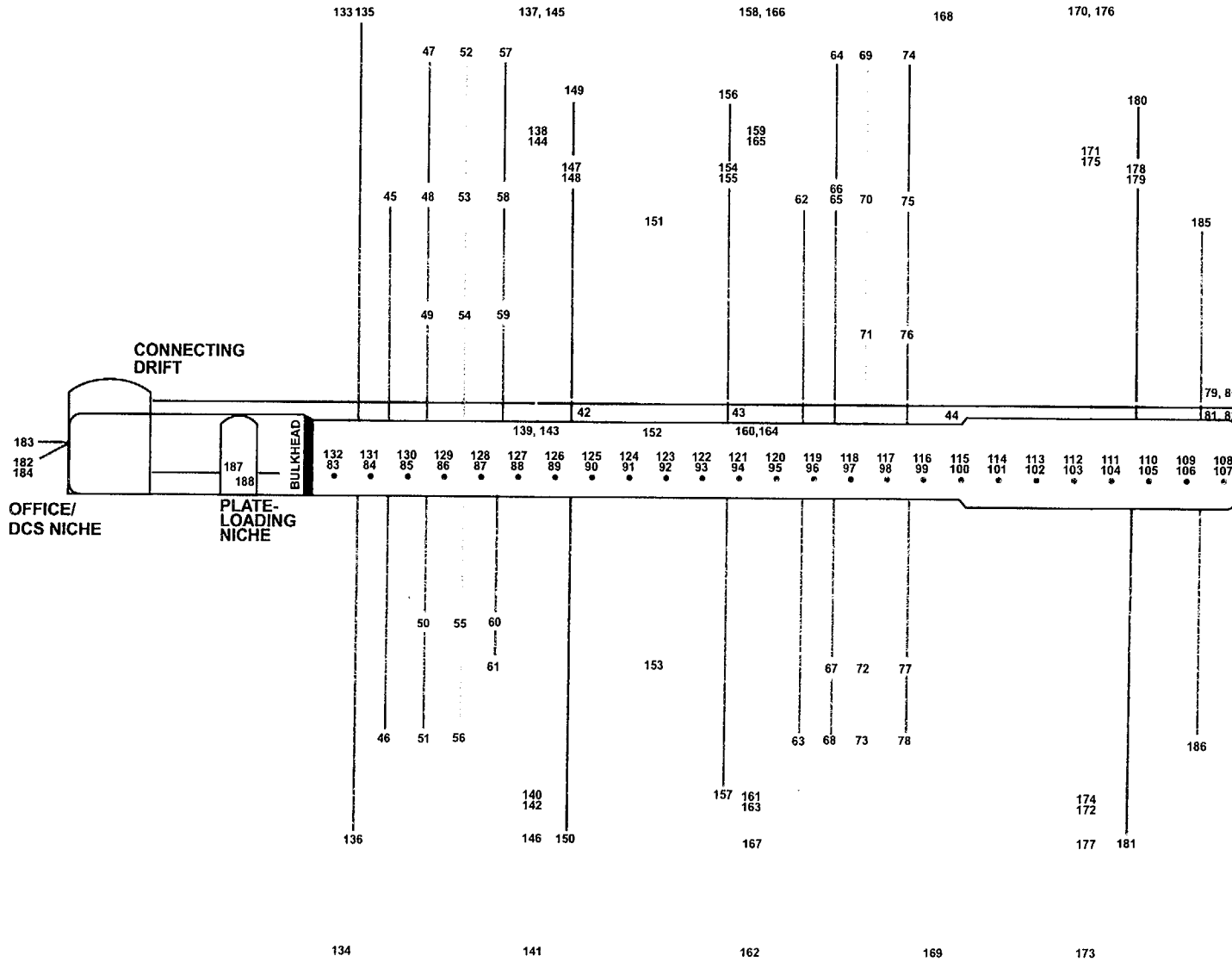


Figure 3-1. Layout of Drift Scale Test



REFERENCE ONLY
 (APPROXIMATE SCALE: 1 CM ~ 3 M)

Figure 3-2. Drift Scale Test (Cross Section A-A)

LEGEND: Boreholes

- Wing Heaters
- - - Thermal
- · · Mechanical
- · - Hydrological
- - - Chemical

The DST also includes a rock mass deformation modulus or plate loading alcove near the entrance to the HD. This alcove, located on the unheated side of a thermal bulkhead (see Figure 1-1), will be approximately 6-m long and 2-m wide. The comparatively small width is necessary to minimize the size of the plate loading reaction frame needed to induce a desired stress level in the rock to measure rock mass deformation modulus. The DST is configured to include an ambient temperature mine-by (SDMT) which will provide baseline data on the mechanical response from excavation of the HD. Mechanical data will continue to be collected during and after heating to evaluate the TM response of the drift and ground support as well as the TM influence on the hydrology. The HD will be constructed parallel to the observation drift at an approximately 26-m separation. A ground support system located along the length of the HD will be evaluated. Specifically, a cast-in-place concrete liner has been installed in the last 12 m of the HD. The performance of the cast-in-place concrete liner will be measured with borehole extensometers located in the local rock mass and with strain gauges and wire extensometers attached to the concrete liner. Also, a video camera will be used for periodic visual inspections. Rockbolts and welded wire mesh have been initially installed throughout the HD but only to ensure safety and stability of the DST facility.

3.3 MISCELLANEOUS REQUIREMENTS

Miscellaneous requirements include the need for application of thermal insulation on the thermally perturbed rock surfaces around the DST block including the observation drift, connecting drift, and HD bulkhead. This insulation will be installed after instrumentation has been installed. A thermal bulkhead, required to control boundary conditions, is needed at the entry to the DST HD. This bulkhead need be only a thermal barrier, but it will be constructed to withstand or accept minor rock movement. Also, the bulkhead will be designed to allow visual inspection, emergency access, and relief of excessive pressure buildup from internally generated gases or water vapor. Geotechnical mapping of the test excavations, based on the Q and Rock Mass Rating systems, has been required throughout drift construction. The results of this mapping will be used to refine the locations of key elements of the DST including the drifts, alcoves, niches and boreholes. Mapping follows directly behind the excavation. Precautions have been taken to protect all borehole collars and instrumentation heads from mining operation and day-to-day traffic in the DST.

3.4 SCOPE COMPARISON

The DST is considered unprecedented based on a comparison to other thermal tests conducted nationally and internationally. Table 3-2 provides a tabulation of 16 other thermal tests in terms of power, duration, and processes. When these components are compared, either individually or collectively, to the DST's 200 kW heater power output, eight-year duration, and four processes (TMHC), it is clear that the DST is a comparatively extensive and comprehensive thermal test. This comparative increase in size, duration, and complexity is intended to provide much more in-depth understanding of the performance of the proposed repository at Yucca Mountain. The knowledge and benefits gained from the DST are anticipated to play an integral role in the licensing process for Yucca Mountain especially with regard to the licensing amendments needed to operate and to close the repository.

Table 3-1. Borehole Information for the Drift Scale Test

| Borehole Number | Borehole Identification | Primary Purpose | Collar Coordinates (meter) 1 | | | Bottom Coordinates (meter) 1 | | | Orientation Degree | Diameter cm | Length meters | Volume m ³ | Types and No. of Sensors | | | | | | | | Comments | | | | |
|-----------------|-------------------------|-----------------------------------|------------------------------|----------|----------|------------------------------|----------|----------|--------------------|-------------|---------------|-----------------------|--------------------------|-----|-------------|------|----------------|-----------------|---------------------|------------------------|----------|----------|--|--|--|
| | | | x meters | y meters | z meters | x meters | y meters | z meters | | | | | Thermo-Couples | RTD | Thermistors | REKA | Anchor in MPBX | Humidity Sensor | Pressure Transducer | Electrode Sensor (ERT) | | Chemical | | | |
| 42 | ESF-SDM-MPBX-1 | MPBX - Rock Mass Displacement | -29.50 | 13.72 | 4.69 | -3.48 | 13.72 | 0.10 | -10.0 | 7.57 | 26.42 | 0.12 | 16 | | | | | 6 | | | | | Thermocouple Sensors between and at Anchors in MPBX | | |
| 43 | ESF-SDM-MPBX-2 | MPBX - Rock Mass Displacement | -29.50 | 21.03 | 5.10 | -3.49 | 21.03 | 0.04 | -11.0 | 7.57 | 26.50 | 0.12 | 16 | | | | | 6 | | | | | Thermocouple Sensors between and at Anchors in MPBX | | |
| 44 | ESF-SDM-MPBX-3 | MPBX - Rock Mass Displacement | -29.50 | 32.00 | 5.10 | -3.49 | 32.00 | 0.04 | -11.0 | 7.57 | 26.50 | 0.12 | 16 | | | | | 6 | | | | | Thermocouple Sensors between and at Anchors in MPBX | | |
| 45 | ESF-HD-ERT-1 | Electrical Resistivity Tomography | -29.50 | 4.57 | 3.95 | 9.31 | 4.57 | 13.63 | 14.0 | 7.57 | 40.00 | 0.18 | | | | | | | | | | 41 | Electrical Resistivity Tomography Arrays, Electrode Sensor on 1m Intervals | | |
| 46 | ESF-HD-ERT-2 | Electrical Resistivity Tomography | -29.50 | 4.57 | 2.45 | 7.59 | 4.57 | -12.53 | -22.0 | 7.57 | 40.00 | 0.18 | | | | | | | | | | 41 | Electrical Resistivity Tomography Arrays, Electrode Sensor on 1m Intervals | | |
| 47 | ESF-HD-NEU-1 | Neutron Probe | -29.50 | 6.40 | 4.45 | 7.04 | 6.40 | 20.72 | 24.0 | 7.57 | 40.00 | 0.18 | | | | | | | | | | | Open Holes for Neutron Probe Runs | | |
| 48 | ESF-HD-NEU-2 | Neutron Probe | -29.50 | 6.40 | 3.95 | 9.31 | 6.40 | 13.63 | 14.0 | 7.57 | 40.00 | 0.18 | | | | | | | | | | | Open Holes for Neutron Probe Runs | | |
| 49 | ESF-HD-NEU-3 | Neutron Probe | -29.50 | 6.40 | 3.45 | 10.28 | 6.40 | 7.63 | 6.0 | 7.57 | 40.00 | 0.18 | | | | | | | | | | | Open Holes for Neutron Probe Runs | | |
| 50 | ESF-HD-NEU-4 | Neutron Probe | -29.50 | 6.40 | 2.95 | 9.14 | 6.40 | -7.40 | -15.0 | 7.57 | 40.00 | 0.18 | | | | | | | | | | | Open Holes for Neutron Probe Runs | | |
| 51 | ESF-HD-NEU-5 | Neutron Probe | -29.50 | 6.40 | 2.45 | 7.59 | 6.40 | -12.53 | -22.0 | 7.57 | 40.00 | 0.18 | | | | | | | | | | | Open Holes for Neutron Probe Runs | | |
| 52 | ESF-HD-CHE-1 | Chemistry - SEAMIST | -29.50 | 8.23 | 4.45 | 7.04 | 8.23 | 20.72 | 24.0 | 9.60 | 40.00 | 0.29 | | | | | | | | | | | 13 | 3 Gas Sampling Ports in SEAMIST System at Depths of 5, 20 and 35 m and 10 Absorbent Pads | |
| 53 | ESF-HD-CHE-2 | Chemistry - SEAMIST | -29.50 | 8.23 | 3.95 | 9.31 | 8.23 | 13.63 | 14.0 | 9.60 | 40.00 | 0.29 | | | | | | | | | | | 13 | as above | |
| 54 | ESF-HD-CHE-3 | Chemistry - SEAMIST | -29.50 | 8.23 | 3.45 | 10.28 | 8.23 | 7.63 | 6.0 | 9.60 | 40.00 | 0.29 | | | | | | | | | | | 13 | as above | |
| 55 | ESF-HD-CHE-4 | Chemistry - SEAMIST | -29.50 | 8.23 | 2.95 | 9.14 | 8.23 | -7.40 | -15.0 | 9.60 | 40.00 | 0.29 | | | | | | | | | | | 13 | as above | |
| 56 | ESF-HD-CHE-5 | Chemistry - SEAMIST | -29.50 | 8.23 | 2.45 | 7.59 | 8.23 | -12.53 | -22.0 | 9.60 | 40.00 | 0.29 | | | | | | | | | | | 13 | as above | |
| 57 | ESF-HD-HYD-1 | Hydrology | -29.50 | 10.06 | 4.45 | 7.04 | 10.06 | 20.72 | 24.0 | 7.57 | 40.00 | 0.18 | | 4 | | | | | 4 | 4 | | | | Pressure, RTD & Humidity Sensors in Packer at Depth of 23, 28, 33, and 38 m | |
| 58 | ESF-HD-HYD-2 | Hydrology | -29.50 | 10.06 | 3.95 | 9.31 | 10.06 | 13.63 | 14.0 | 7.57 | 40.00 | 0.18 | | 4 | | | | | 4 | 4 | | | | Pressure, RTD & Humidity Sensors in Packer at Depth of 23, 28, 33, and 38 m | |
| 59 | ESF-HD-HYD-3 | Hydrology | -29.50 | 10.06 | 3.45 | 10.28 | 10.06 | 7.63 | 6.0 | 7.57 | 40.00 | 0.18 | | 4 | | | | | 4 | 4 | | | | Pressure, RTD & Humidity Sensors in Packer at Depth of 23, 28, 33, and 38 m | |
| 60 | ESF-HD-HYD-4 | Hydrology | -29.50 | 10.06 | 2.95 | 9.14 | 10.06 | -7.40 | -15.0 | 7.57 | 40.00 | 0.18 | | 4 | | | | | 4 | 4 | | | | Pressure, RTD & Humidity Sensors in Packer at Depth of 23, 28, 33, and 38 m | |
| 61 | ESF-HD-HYD-5 | Hydrology | -29.50 | 10.06 | 2.45 | 7.59 | 10.06 | -12.53 | -22.0 | 7.57 | 40.00 | 0.18 | | 4 | | | | | 4 | 4 | | | | Pressure, RTD & Humidity Sensors in Packer at Depth of 23, 28, 33, and 38 m | |
| 62 | ESF-HD-ERT-3 | Electrical Resistivity Tomography | -29.50 | 24.69 | 6.27 | 9.89 | 24.69 | 13.22 | 10.0 | 7.57 | 40.00 | 0.18 | | | | | | | | | | | 41 | Electrical Resistivity Tomography Arrays, Electrode Sensor on 1m Intervals | |
| 63 | ESF-HD-ERT-4 | Electrical Resistivity Tomography | -29.50 | 24.69 | 4.77 | 6.45 | 24.69 | -12.76 | -26.0 | 7.57 | 40.00 | 0.18 | | | | | | | | | | | 41 | Electrical Resistivity Tomography Arrays, Electrode Sensor on 1m Intervals | |
| 64 | ESF-HD-NEU-6 | Neutron Probe | -29.50 | 26.52 | 6.77 | 8.09 | 26.52 | 20.45 | 20.0 | 7.57 | 40.00 | 0.18 | | | | | | | | | | | | Open Holes for Neutron Probe Runs | |
| 65 | ESF-HD-NEU-7 | Neutron Probe | -29.50 | 26.52 | 6.27 | 9.89 | 26.52 | 13.22 | 10.0 | 7.57 | 40.00 | 0.18 | | | | | | | | | | | | Open Holes for Neutron Probe Runs | |
| 66 | ESF-HD-NEU-8 | Neutron Probe | -29.50 | 26.52 | 5.77 | 9.77 | 26.52 | 13.40 | 11.0 | 7.57 | 40.00 | 0.18 | | | | | | | | | | | | Open Holes for Neutron Probe Runs | |
| 67 | ESF-HD-NEU-9 | Neutron Probe | -29.50 | 26.52 | 5.27 | 8.09 | 26.52 | -8.41 | -20.0 | 7.57 | 40.00 | 0.18 | | | | | | | | | | | | Open Holes for Neutron Probe Runs | |
| 68 | ESF-HD-NEU-10 | Neutron Probe | -29.50 | 26.52 | 4.77 | 6.45 | 26.52 | -12.76 | -26.0 | 7.57 | 40.00 | 0.18 | | | | | | | | | | | | Open Holes for Neutron Probe Runs | |
| 69 | ESF-HD-CHE-6 | Chemistry - SEAMIST | -29.50 | 28.35 | 6.77 | 8.09 | 28.35 | 20.45 | 20.0 | 7.57 | 40.00 | 0.18 | | | | | | | | | | | | 13 | 3 Gas Sampling Ports in SEAMIST System at Depths of 5, 20 and 35 m and 10 Absorbent Pads |
| 70 | ESF-HD-CHE-7 | Chemistry - SEAMIST | -29.50 | 28.35 | 6.27 | 9.89 | 28.35 | 13.22 | 10.0 | 7.57 | 40.00 | 0.18 | | | | | | | | | | | | 13 | as above |
| 71 | ESF-HD-CHE-8 | Chemistry - SEAMIST | -29.50 | 28.35 | 5.77 | 10.49 | 28.35 | 6.47 | 1.0 | 9.60 | 40.00 | 0.29 | | | | | | | | | | | | 13 | as above |
| 72 | ESF-HD-CHE-9 | Chemistry - SEAMIST | -29.50 | 28.35 | 5.27 | 8.09 | 28.35 | -8.41 | -20.0 | 9.60 | 40.00 | 0.29 | | | | | | | | | | | | 13 | as above |
| 73 | ESF-HD-CHE-10 | Chemistry - SEAMIST | -29.50 | 28.35 | 4.77 | 6.45 | 28.35 | -12.76 | -26.0 | 7.57 | 40.00 | 0.18 | | | | | | | | | | | | 13 | as above |
| 74 | ESF-HD-HYD-6 | Hydrology | -29.50 | 30.18 | 6.77 | 8.09 | 30.18 | 20.45 | 20.0 | 7.57 | 40.00 | 0.18 | | 4 | | | | | 4 | 4 | | | | | Pressure, RTD & Humidity Sensors in Packer at Depth of 23, 28, 33, and 38 m |
| 75 | ESF-HD-HYD-7 | Hydrology | -29.50 | 30.18 | 6.27 | 9.89 | 30.18 | 13.22 | 10.0 | 7.57 | 40.00 | 0.18 | | 4 | | | | | 4 | 4 | | | | | Pressure, RTD & Humidity Sensors in Packer at Depth of 23, 28, 33, and 38 m |
| 76 | ESF-HD-HYD-8 | Hydrology | -29.50 | 30.18 | 5.77 | 10.49 | 30.18 | 6.47 | 1.0 | 7.57 | 40.00 | 0.18 | | 4 | | | | | 4 | 4 | | | | | Pressure, RTD & Humidity Sensors in Packer at Depth of 23, 28, 33, and 38 m |
| 77 | ESF-HD-HYD-9 | Hydrology | -29.50 | 30.18 | 5.27 | 8.09 | 30.18 | -8.41 | -20.0 | 7.57 | 40.00 | 0.18 | | 4 | | | | | 4 | 4 | | | | | Pressure, RTD & Humidity Sensors in Packer at Depth of 23, 28, 33, and 38 m |
| 78 | ESF-HD-HYD-10 | Hydrology | -29.50 | 30.18 | 4.77 | 6.45 | 30.18 | -12.76 | -26.0 | 7.57 | 40.00 | 0.18 | | 4 | | | | | 4 | 4 | | | | | Pressure, RTD & Humidity Sensors in Packer at Depth of 23, 28, 33, and 38 m |
| 79 | ESF-HD-TEMP-1 | Temperature | 9.50 | -11.00 | 3.50 | 9.50 | 48.50 | 3.50 | 0.0 | 9.60 | 59.50 | 0.43 | | 60 | | | | | | | | | | | RTDs on 1 m Intervals |
| 80 | ESF-HD-TEMP-2 | Temperature | -9.50 | -11.00 | 3.50 | -9.50 | 48.50 | 3.50 | 0.0 | 9.60 | 59.50 | 0.43 | | 60 | | | | | | | | | | | RTDs on 1 m Intervals |
| 81 | ESF-HD-MPBX-1 | MPBX - Rock Mass Displacement | 7.00 | -11.00 | 3.50 | 7.00 | 35.00 | 3.50 | 0.0 | 7.57 | 46.00 | 0.21 | 16 | | | | | | 6 | | | | | | Thermocouple Sensors between and at Anchors in MPBX |
| 82 | ESF-HD-MPBX-2 | MPBX - Rock Mass Displacement | -7.00 | -11.00 | 3.50 | -7.00 | 35.00 | 3.50 | 0.0 | 7.57 | 46.00 | 0.21 | 16 | | | | | | 6 | | | | | | Thermocouple Sensors between and at Anchors in MPBX |
| 83 | ESF-HD-WH-1 | Wing Heater | -2.50 | 1.83 | -0.25 | -14.00 | 1.83 | -0.25 | 0.0 | 9.60 | 11.50 | 0.08 | 5 | | | | | | | | | | | | Temperature Sensors on 2.5 m Intervals in 2 Heater Assemblies |
| 84 | ESF-HD-WH-2 | Wing Heater | -2.50 | 3.66 | -0.25 | -14.00 | 3.66 | -0.25 | 0.0 | 9.60 | 11.50 | 0.08 | 5 | | | | | | | | | | | | Temperature Sensors on 2.5 m Intervals in 2 Heater Assemblies |
| 85 | ESF-HD-WH-3 | Wing Heater | -2.50 | 5.49 | -0.25 | -14.00 | 5.49 | -0.25 | 0.0 | 9.60 | 11.50 | 0.08 | 5 | | | | | | | | | | | | Temperature Sensors on 2.5 m Intervals in 2 Heater Assemblies |
| 86 | ESF-HD-WH-4 | Wing Heater | -2.50 | 7.32 | -0.25 | -14.00 | 7.32 | -0.25 | 0.0 | 9.60 | 11.50 | 0.08 | 5 | | | | | | | | | | | | Temperature Sensors on 2.5 m Intervals in 2 Heater Assemblies |
| 87 | ESF-HD-WH-5 | Wing Heater | -2.50 | 9.14 | -0.25 | -14.00 | 9.14 | -0.25 | 0.0 | 9.60 | 11.50 | 0.08 | 5 | | | | | | | | | | | | Temperature Sensors on 2.5 m Intervals in 2 Heater Assemblies |
| 88 | ESF-HD-WH-6 | Wing Heater | -2.50 | 10.97 | -0.25 | -14.00 | 10.97 | -0.25 | 0.0 | 9.60 | 11.50 | 0.08 | 5 | | | | | | | | | | | | Temperature Sensors on 2.5 m Intervals in 2 Heater Assemblies |
| 89 | ESF-HD-WH-7 | Wing Heater | -2.50 | 12.80 | -0.25 | -14.00 | 12.80 | -0.25 | 0.0 | 9.60 | 11.50 | 0.08 | 5 | | | | | | | | | | | | Temperature Sensors on 2.5 m Intervals in 2 Heater Assemblies |
| 90 | ESF-HD-WH-8 | Wing Heater | -2.50 | 14.63 | -0.25 | -14.00 | 14.63 | -0.25 | 0.0 | 9.60 | 11.50 | 0.08 | 5 | | | | | | | | | | | | Temperature Sensors on 2.5 m Intervals in 2 Heater Assemblies |
| 91 | ESF-HD-WH-9 | Wing Heater | -2.50 | 16.46 | -0.25 | -14.00 | 16.46 | -0.25 | 0.0 | 9.60 | 11.50 | 0.08 | 5 | | | | | | | | | | | | Temperature Sensors on 2.5 m Intervals in 2 Heater Assemblies |
| 92 | ESF-HD-WH-10 | Wing Heater | -2.50 | 18.29 | -0.25 | -14.00 | 18.29 | -0.25 | 0.0 | 9.60 | 11.50 | 0.08 | 5 | | | | | | | | | | | | Temperature Sensors on 2.5 m Intervals in 2 Heater Assemblies |
| 93 | ESF-HD-WH-11 | Wing Heater | -2.50 | 20.12 | -0.25 | -14.00 | 20.12 | -0.25 | 0.0 | 9.60 | 11.50 | 0.08 | 5 | | | | | | | | | | | | Temperature Sensors on 2.5 m Intervals in 2 Heater Assemblies |
| 94 | ESF-HD-WH-12 | Wing Heater | -2.50 | 21.95 | -0.25 | -14.00 | 21.95 | -0.25 | 0.0 | 9.60 | 11.50 | 0.08 | 5 | | | | | | | | | | | | Temperature Sensors on 2.5 m Intervals in 2 Heater Assemblies |

APERTURE CARD

INTENTIONALLY LEFT BLANK

Table 3-1. Borehole Information for the Drift Scale Test
(Continued)

| Borehole Number | Borehole Identification | Primary Purpose | Collar Coordinates (meter) 1 | | | Bottom Coordinates (meter) 1 | | | Orientation Degree | Diameter cm | Length meters | Volume m ³ | Types and No. of Sensors | | | | | | | Comments | | |
|-----------------|-------------------------|--------------------------------------|------------------------------|-------------|-------------|------------------------------|-------------|-------------|-----------------------|----------------|------------------|--------------------------|--------------------------|-----|-------------|------|-------------------|--------------------|------------------------|----------|---------------------------|--|
| | | | X meters | Y meters | Z meters | X meters | Y meters | Z meters | | | | | Thermo- Couples | RTD | Thermistors | REKA | Anchor in MPBX | Humidity Sensor | Pressure Transducer | | Electrode Sensor (ERT) | Chemical |
| 95 | ESF-HD-WH-13 | Wing Heater | -2.50 | 23.77 | -0.25 | -14.00 | 23.77 | -0.25 | 0.0 | 9.60 | 11.50 | 0.08 | 5 | | | | | | | | | Temperature Sensors on 2.5 m Intervals in 2 Heater Assemblies |
| 96 | ESF-HD-WH-14 | Wing Heater | -2.50 | 25.60 | -0.25 | -14.00 | 25.60 | -0.25 | 0.0 | 9.60 | 11.50 | 0.08 | 5 | | | | | | | | | Temperature Sensors on 2.5 m Intervals in 2 Heater Assemblies |
| 97 | ESF-HD-WH-15 | Wing Heater | -2.50 | 27.43 | -0.25 | -14.00 | 27.43 | -0.25 | 0.0 | 9.60 | 11.50 | 0.08 | 5 | | | | | | | | | Temperature Sensors on 2.5 m Intervals in 2 Heater Assemblies |
| 98 | ESF-HD-WH-16 | Wing Heater | -2.50 | 29.26 | -0.25 | -14.00 | 29.26 | -0.25 | 0.0 | 9.60 | 11.50 | 0.08 | 5 | | | | | | | | | Temperature Sensors on 2.5 m Intervals in 2 Heater Assemblies |
| 99 | ESF-HD-WH-17 | Wing Heater | -2.50 | 31.09 | -0.25 | -14.00 | 31.09 | -0.25 | 0.0 | 9.60 | 11.50 | 0.08 | 5 | | | | | | | | | Temperature Sensors on 2.5 m Intervals in 2 Heater Assemblies |
| 100 | ESF-HD-WH-18 | Wing Heater | -2.50 | 32.92 | -0.25 | -14.00 | 32.92 | -0.25 | 0.0 | 9.60 | 11.50 | 0.08 | 5 | | | | | | | | | Temperature Sensors on 2.5 m Intervals in 2 Heater Assemblies |
| 101 | ESF-HD-WH-19 | Wing Heater | -2.50 | 34.75 | -0.25 | -14.00 | 34.75 | -0.25 | 0.0 | 9.60 | 11.50 | 0.08 | 5 | | | | | | | | | Temperature Sensors on 2.5 m Intervals in 2 Heater Assemblies |
| 102 | ESF-HD-WH-20 | Wing Heater | -2.50 | 36.58 | -0.25 | -14.00 | 36.58 | -0.25 | 0.0 | 9.60 | 11.50 | 0.08 | 5 | | | | | | | | | Temperature Sensors on 2.5 m Intervals in 2 Heater Assemblies |
| 103 | ESF-HD-WH-21 | Wing Heater | -2.50 | 38.40 | -0.25 | -14.00 | 38.40 | -0.25 | 0.0 | 9.60 | 11.50 | 0.08 | 5 | | | | | | | | | Temperature Sensors on 2.5 m Intervals in 2 Heater Assemblies |
| 104 | ESF-HD-WH-22 | Wing Heater | -2.50 | 40.23 | -0.25 | -14.00 | 40.23 | -0.25 | 0.0 | 9.60 | 11.50 | 0.08 | 5 | | | | | | | | | Temperature Sensors on 2.5 m Intervals in 2 Heater Assemblies |
| 105 | ESF-HD-WH-23 | Wing Heater | -2.50 | 42.06 | -0.25 | -14.00 | 42.06 | -0.25 | 0.0 | 9.60 | 11.50 | 0.08 | 5 | | | | | | | | | Temperature Sensors on 2.5 m Intervals in 2 Heater Assemblies |
| 106 | ESF-HD-WH-24 | Wing Heater | -2.50 | 43.89 | -0.25 | -14.00 | 43.89 | -0.25 | 0.0 | 9.60 | 11.50 | 0.08 | 5 | | | | | | | | | Temperature Sensors on 2.5 m Intervals in 2 Heater Assemblies |
| 107 | ESF-HD-WH-25 | Wing Heater | -2.50 | 45.72 | -0.25 | -14.00 | 45.72 | -0.25 | 0.0 | 9.60 | 11.50 | 0.08 | 5 | | | | | | | | | Temperature Sensors on 2.5 m Intervals in 2 Heater Assemblies |
| 108 | ESF-HD-WH-26 | Wing Heater | 2.50 | 45.72 | -0.25 | 14.00 | 45.72 | -0.25 | 0.0 | 9.60 | 11.50 | 0.08 | 5 | | | | | | | | | Temperature Sensors on 2.5 m Intervals in 2 Heater Assemblies |
| 109 | ESF-HD-WH-27 | Wing Heater | 2.50 | 43.89 | -0.25 | 14.00 | 43.89 | -0.25 | 0.0 | 9.60 | 11.50 | 0.08 | 5 | | | | | | | | | Temperature Sensors on 2.5 m Intervals in 2 Heater Assemblies |
| 110 | ESF-HD-WH-28 | Wing Heater | 2.50 | 42.06 | -0.25 | 14.00 | 42.06 | -0.25 | 0.0 | 9.60 | 11.50 | 0.08 | 5 | | | | | | | | | Temperature Sensors on 2.5 m Intervals in 2 Heater Assemblies |
| 111 | ESF-HD-WH-29 | Wing Heater | 2.50 | 40.23 | -0.25 | 14.00 | 40.23 | -0.25 | 0.0 | 9.60 | 11.50 | 0.08 | 5 | | | | | | | | | Temperature Sensors on 2.5 m Intervals in 2 Heater Assemblies |
| 112 | ESF-HD-WH-30 | Wing Heater | 2.50 | 38.40 | -0.25 | 14.00 | 38.40 | -0.25 | 0.0 | 9.60 | 11.50 | 0.08 | 5 | | | | | | | | | Temperature Sensors on 2.5 m Intervals in 2 Heater Assemblies |
| 113 | ESF-HD-WH-31 | Wing Heater | 2.50 | 36.58 | -0.25 | 14.00 | 36.58 | -0.25 | 0.0 | 9.60 | 11.50 | 0.08 | 5 | | | | | | | | | Temperature Sensors on 2.5 m Intervals in 2 Heater Assemblies |
| 114 | ESF-HD-WH-32 | Wing Heater | 2.50 | 34.75 | -0.25 | 14.00 | 34.75 | -0.25 | 0.0 | 9.60 | 11.50 | 0.08 | 5 | | | | | | | | | Temperature Sensors on 2.5 m Intervals in 2 Heater Assemblies |
| 115 | ESF-HD-WH-33 | Wing Heater | 2.50 | 32.92 | -0.25 | 14.00 | 32.92 | -0.25 | 0.0 | 9.60 | 11.50 | 0.08 | 5 | | | | | | | | | Temperature Sensors on 2.5 m Intervals in 2 Heater Assemblies |
| 116 | ESF-HD-WH-34 | Wing Heater | 2.50 | 31.09 | -0.25 | 14.00 | 31.09 | -0.25 | 0.0 | 9.60 | 11.50 | 0.08 | 5 | | | | | | | | | Temperature Sensors on 2.5 m Intervals in 2 Heater Assemblies |
| 117 | ESF-HD-WH-35 | Wing Heater | 2.50 | 29.26 | -0.25 | 14.00 | 29.26 | -0.25 | 0.0 | 9.60 | 11.50 | 0.08 | 5 | | | | | | | | | Temperature Sensors on 2.5 m Intervals in 2 Heater Assemblies |
| 118 | ESF-HD-WH-36 | Wing Heater | 2.50 | 27.43 | -0.25 | 14.00 | 27.43 | -0.25 | 0.0 | 9.60 | 11.50 | 0.08 | 5 | | | | | | | | | Temperature Sensors on 2.5 m Intervals in 2 Heater Assemblies |
| 119 | ESF-HD-WH-37 | Wing Heater | 2.50 | 25.60 | -0.25 | 14.00 | 25.60 | -0.25 | 0.0 | 9.60 | 11.50 | 0.08 | 5 | | | | | | | | | Temperature Sensors on 2.5 m Intervals in 2 Heater Assemblies |
| 120 | ESF-HD-WH-38 | Wing Heater | 2.50 | 23.77 | -0.25 | 14.00 | 23.77 | -0.25 | 0.0 | 9.60 | 11.50 | 0.08 | 5 | | | | | | | | | Temperature Sensors on 2.5 m Intervals in 2 Heater Assemblies |
| 121 | ESF-HD-WH-39 | Wing Heater | 2.50 | 21.95 | -0.25 | 14.00 | 21.95 | -0.25 | 0.0 | 9.60 | 11.50 | 0.08 | 5 | | | | | | | | | Temperature Sensors on 2.5 m Intervals in 2 Heater Assemblies |
| 122 | ESF-HD-WH-40 | Wing Heater | 2.50 | 20.12 | -0.25 | 14.00 | 20.12 | -0.25 | 0.0 | 9.60 | 11.50 | 0.08 | 5 | | | | | | | | | Temperature Sensors on 2.5 m Intervals in 2 Heater Assemblies |
| 123 | ESF-HD-WH-41 | Wing Heater | 2.50 | 18.29 | -0.25 | 14.00 | 18.29 | -0.25 | 0.0 | 9.60 | 11.50 | 0.08 | 5 | | | | | | | | | Temperature Sensors on 2.5 m Intervals in 2 Heater Assemblies |
| 124 | ESF-HD-WH-42 | Wing Heater | 2.50 | 16.46 | -0.25 | 14.00 | 16.46 | -0.25 | 0.0 | 9.60 | 11.50 | 0.08 | 5 | | | | | | | | | Temperature Sensors on 2.5 m Intervals in 2 Heater Assemblies |
| 125 | ESF-HD-WH-43 | Wing Heater | 2.50 | 14.63 | -0.25 | 14.00 | 14.63 | -0.25 | 0.0 | 9.60 | 11.50 | 0.08 | 5 | | | | | | | | | Temperature Sensors on 2.5 m Intervals in 2 Heater Assemblies |
| 126 | ESF-HD-WH-44 | Wing Heater | 2.50 | 12.80 | -0.25 | 14.00 | 12.80 | -0.25 | 0.0 | 9.60 | 11.50 | 0.08 | 5 | | | | | | | | | Temperature Sensors on 2.5 m Intervals in 2 Heater Assemblies |
| 127 | ESF-HD-WH-45 | Wing Heater | 2.50 | 10.97 | -0.25 | 14.00 | 10.97 | -0.25 | 0.0 | 9.60 | 11.50 | 0.08 | 5 | | | | | | | | | Temperature Sensors on 2.5 m Intervals in 2 Heater Assemblies |
| 128 | ESF-HD-WH-46 | Wing Heater | 2.50 | 9.14 | -0.25 | 14.00 | 9.14 | -0.25 | 0.0 | 9.60 | 11.50 | 0.08 | 5 | | | | | | | | | Temperature Sensors on 2.5 m Intervals in 2 Heater Assemblies |
| 129 | ESF-HD-WH-47 | Wing Heater | 2.50 | 7.32 | -0.25 | 14.00 | 7.32 | -0.25 | 0.0 | 9.60 | 11.50 | 0.08 | 5 | | | | | | | | | Temperature Sensors on 2.5 m Intervals in 2 Heater Assemblies |
| 130 | ESF-HD-WH-48 | Wing Heater | 2.50 | 5.49 | -0.25 | 14.00 | 5.49 | -0.25 | 0.0 | 9.60 | 11.50 | 0.08 | 5 | | | | | | | | | Temperature Sensors on 2.5 m Intervals in 2 Heater Assemblies |
| 131 | ESF-HD-WH-49 | Wing Heater | 2.50 | 3.66 | -0.25 | 14.00 | 3.66 | -0.25 | 0.0 | 9.60 | 11.50 | 0.08 | 5 | | | | | | | | | Temperature Sensors on 2.5 m Intervals in 2 Heater Assemblies |
| 132 | ESF-HD-WH-50 | Wing Heater | 2.50 | 1.83 | -0.25 | 14.00 | 1.83 | -0.25 | 0.0 | 9.60 | 11.50 | 0.08 | 5 | | | | | | | | | Temperature Sensors on 2.5 m Intervals in 2 Heater Assemblies |
| 133 | ESF-HD-TEMP-3 | Temperature | 0.75 | 2.74 | 2.40 | 0.75 | 2.74 | 22.40 | 0.0 | 7.57 | 20.00 | 0.09 | | 67 | | | | | | | | RTDs on 30 cm Intervals |
| 134 | ESF-HD-TEMP-4 | Temperature | 0.75 | 2.74 | -1.30 | 0.75 | 2.74 | -22.50 | 0.0 | 7.57 | 21.20 | 0.10 | | 71 | | | | | | | | RTDs on 30 cm Intervals |
| 135 | ESF-HD-ERT-5 | Electrical Resistivity Tomography | -0.75 | 2.74 | 2.40 | -0.75 | 2.74 | 22.40 | 0.0 | 7.57 | 20.00 | 0.09 | | | | | | | 21 | | | Electrical Resistivity Tomography Arrays, Electrode Sensor on 1m Intervals |
| 136 | ESF-HD-ERT-6 | Electrical Resistivity Tomography | -0.75 | 2.74 | -1.30 | -0.75 | 2.74 | -17.50 | 0.0 | 7.57 | 16.20 | 0.07 | | | | | | | 17 | | | Electrical Resistivity Tomography Arrays, Electrode Sensor on 1m Intervals |
| 137 | ESF-HD-TEMP-5 | Temperature | 0.75 | 11.89 | 2.40 | 0.75 | 11.89 | 22.40 | 0.0 | 7.57 | 20.00 | 0.09 | | 67 | | | | | | | | RTDs on 30 cm Intervals |
| 138 | ESF-HD-TEMP-6 | Temperature | -1.80 | 11.89 | 1.80 | -15.94 | 11.89 | 15.94 | 45.0 | 7.57 | 20.00 | 0.09 | | 67 | | | | | | | | RTDs on 30 cm Intervals |
| 139 | ESF-HD-TEMP-7 | Temperature | -2.50 | 11.89 | 0.00 | -22.50 | 11.89 | 0.00 | 0.0 | 7.57 | 20.00 | 0.09 | | 67 | | | | | | | | RTDs on 30 cm Intervals |
| 140 | ESF-HD-TEMP-8 | Temperature | -1.30 | 11.89 | -1.30 | -15.65 | 11.89 | -15.65 | -45.0 | 7.57 | 20.30 | 0.09 | | 68 | | | | | | | | RTDs on 30 cm Intervals |
| 141 | ESF-HD-TEMP-9 | Temperature | 0.75 | 11.89 | -1.30 | 0.75 | 11.89 | -22.50 | 0.0 | 7.57 | 21.20 | 0.10 | | 71 | | | | | | | | RTDs on 30 cm Intervals |
| 142 | ESF-HD-TEMP-10 | Temperature | 1.30 | 11.89 | -1.30 | 15.65 | 11.89 | -15.65 | -45.0 | 7.57 | 20.30 | 0.09 | | 68 | | | | | | | | RTDs on 30 cm Intervals |
| 143 | ESF-HD-TEMP-11 | Temperature | 2.50 | 11.89 | 0.00 | 22.50 | 11.89 | 0.00 | 0.0 | 7.57 | 20.00 | 0.09 | | 67 | | | | | | | | RTDs on 30 cm Intervals |
| 144 | ESF-HD-TEMP-12 | Temperature | 1.80 | 11.89 | 1.80 | 15.94 | 11.89 | 15.94 | 45.0 | 7.57 | 20.00 | 0.09 | | 67 | | | | | | | | RTDs on 30 cm Intervals |
| 145 | ESF-HD-ERT-7 | Electrical Resistivity Tomography | -0.75 | 11.89 | 2.40 | -0.75 | 11.89 | 22.40 | 0.0 | 7.57 | 20.00 | 0.09 | | | | | | | 21 | | | Electrical Resistivity Tomography Arrays, Electrode Sensor on 1m Intervals |
| 146 | ESF-HD-ERT-8 | Electrical Resistivity Tomography | -0.75 | 11.89 | -1.30 | -0.75 | 11.89 | -17.50 | 0.0 | 7.57 | 16.20 | 0.07 | | | | | | | 17 | | | Electrical Resistivity Tomography Arrays, Electrode Sensor on 1m Intervals |
| 147 | ESF-HD-MPBX-3 | MPBX - Rock Mass Displacement | 1.30 | 13.72 | 2.10 | 8.80 | 13.72 | 15.09 | 60.0 | 7.57 | 15.00 | 0.07 | 16 | | | | | | 6 | | | Thermocouple Sensors between and at Anchors in MPBX |
| 148 | ESF-HD-MPBX-4 | MPBX - Rock Mass Displacement | -1.30 | 13.72 | 2.10 | -8.80 | 13.72 | 15.09 | 60.0 | 7.57 | 15.00 | 0.07 | 16 | | | | | | 6 | | | Thermocouple Sensors between and at Anchors in MPBX |
| 149 | ESF-HD-MPBX-5 | MPBX - Rock Mass Displacement | 0.00 | 13.72 | 2.50 | 0.00 | 13.72 | 17.50 | 0.0 | 7.57 | 15.00 | 0.07 | 16 | | | | | | 6 | | | Thermocouple Sensors between and at Anchors in MPBX |
| 150 | ESF-HD-MPBX-6 | MPBX - Rock Mass Displacement | 0.00 | 13.72 | -1.30 | 0.00 | 13.72 | -17.50 | 0.0 | 7.57 | 16.20 | 0.07 | 16 | | | | | | 6 | | | Thermocouple Sensors between and at Anchors in MPBX |
| 151 | ESF-HD-REKA-1 | Thermal Conductivity and Diffusivity | -0.75 | 17.37 | 2.40 | -0.75 | 17.37 | 12.40 | 0.0 | 4.80 | 10.00 | 0.02 | 10 | | | | | | | | | A Total of 10 Temperature Sensors (Both Directions) on 25 cm Intervals in REKA Probe Beginning at Depth of 7 m |
| 152 | ESF-HD-REKA-2 | Thermal Conductivity and Diffusivity | -2.50 | 17.37 | 0.00 | -12.50 | 17.37 | 0.00 | 0.0 | 4.80 | 10.00 | 0.02 | 10 | | | | | | | | | as above |
| 153 | ESF-HD-REKA-3 | Thermal Conductivity and Diffusivity | -1.20 | 17.37 | -1.30 | -8.80 | 17.37 | -8.90 | -45.0 | 4.80 | 10.75 | 0.02 | 10 | | | | | | | | | as above |
| 154 | ESF-HD-MPBX-7 | MPBX - Rock Mass Displacement | 1.30 | 21.03 | 2.10 | 8.80 | 21.03 | 15.09 | 60.0 | 7.57 | 15.00 | 0.07 | 16 | | | | | | 6 | | | Thermocouple Sensors between and at Anchors in MPBX |

INTENTIONALLY LEFT BLANK

Table 3-1. Borehole Information for the Drift Scale Test
(Continued)

| Borehole Number | Borehole Identification | Primary Purpose | Collar Coordinates (meter) 1 | | | Bottom Coordinates (meter) 1 | | | Orientation Degree | Diameter cm | Length meters | Volume m ³ | Types and No. of Sensors | | | | | | | Comments | | | | | | |
|-----------------|-------------------------|-----------------------------------|------------------------------|----------|----------|------------------------------|----------|----------|--------------------|-------------|---------------|-----------------------|--------------------------|------------|-------------|------------|----------------|-----------------|---------------------|-----------|------------------------|---|--|--|-------------|--|
| | | | x meters | y meters | z meters | x meters | y meters | z meters | | | | | Thermo-Couples | RTD | Thermistors | REKA | Anchor in MPBX | Humidity Sensor | Pressure Transducer | | Electrode Sensor (ERT) | Chemical | | | | |
| 155 | ESF-HD-MPBX-8 | MPBX - Rock Mass Displacement | -1.30 | 21.03 | 2.10 | -8.80 | 21.03 | 15.09 | 60.0 | 7.57 | 15.00 | 0.07 | 16 | | | | 6 | | | | | Thermocouple Sensors between and at Anchors in MPBX | | | | |
| 156 | ESF-HD-MPBX-9 | MPBX - Rock Mass Displacement | 0.00 | 21.03 | 2.50 | 0.00 | 21.03 | 17.50 | 0.0 | 7.57 | 15.00 | 0.07 | 16 | | | | 6 | | | | | Thermocouple Sensors between and at Anchors in MPBX | | | | |
| 157 | ESF-HD-MPBX-10 | MPBX - Rock Mass Displacement | 0.00 | 21.03 | -1.30 | 0.00 | 21.03 | -17.50 | 0.0 | 7.57 | 16.20 | 0.07 | 16 | | | | 6 | | | | | Thermocouple Sensors between and at Anchors in MPBX | | | | |
| 158 | ESF-HD-TEMP-13 | Temperature | 0.75 | 22.86 | 2.40 | 0.75 | 22.86 | 22.40 | 0.0 | 7.57 | 20.00 | 0.09 | | 67 | | | | | | | | RTDs on 30 cm Intervals | | | | |
| 159 | ESF-HD-TEMP-14 | Temperature | -1.80 | 22.86 | 1.80 | -15.94 | 22.86 | 15.94 | 45.0 | 7.57 | 20.00 | 0.09 | | 67 | | | | | | | | RTDs on 30 cm Intervals | | | | |
| 160 | ESF-HD-TEMP-15 | Temperature | -2.50 | 22.86 | 0.00 | -22.50 | 22.86 | 0.00 | 0.0 | 7.57 | 20.00 | 0.09 | | 67 | | | | | | | | RTDs on 30 cm Intervals | | | | |
| 161 | ESF-HD-TEMP-16 | Temperature | -1.30 | 22.86 | -1.30 | -15.65 | 22.86 | -15.65 | -45.0 | 7.57 | 20.30 | 0.09 | | 68 | | | | | | | | RTDs on 30 cm Intervals | | | | |
| 162 | ESF-HD-TEMP-17 | Temperature | 0.75 | 22.86 | -1.30 | 0.75 | 22.86 | -22.50 | 0.0 | 7.57 | 21.20 | 0.10 | | 71 | | | | | | | | RTDs on 30 cm Intervals | | | | |
| 163 | ESF-HD-TEMP-18 | Temperature | 1.30 | 22.86 | -1.30 | 15.65 | 22.86 | -15.65 | -45.0 | 7.57 | 20.30 | 0.09 | | 68 | | | | | | | | RTDs on 30 cm Intervals | | | | |
| 164 | ESF-HD-TEMP-19 | Temperature | 2.50 | 22.86 | 0.00 | 22.50 | 22.86 | 0.00 | 0.0 | 7.57 | 20.00 | 0.09 | | 67 | | | | | | | | RTDs on 30 cm Intervals | | | | |
| 165 | ESF-HD-TEMP-20 | Temperature | 1.80 | 22.86 | 1.80 | 15.94 | 22.86 | 15.94 | 45.0 | 7.57 | 20.00 | 0.09 | | 67 | | | | | | | | RTDs on 30 cm Intervals | | | | |
| 166 | ESF-HD-ERT-9 | Electrical Resistivity Tomography | -0.75 | 22.86 | 2.40 | -0.75 | 22.86 | 22.40 | 0.0 | 7.57 | 20.00 | 0.09 | | | | | | | | 21 | | Electrical Resistivity Tomography Arrays, Electrode Sensor on 1m Intervals | | | | |
| 167 | ESF-HD-ERT-10 | Electrical Resistivity Tomography | -0.75 | 22.86 | -1.30 | -0.75 | 22.86 | -17.50 | 0.0 | 7.57 | 16.20 | 0.07 | | | | | | | | 17 | | Electrical Resistivity Tomography Arrays, Electrode Sensor on 1m Intervals | | | | |
| 168 | ESF-HD-TEMP-21 | Temperature | 0.00 | 32.00 | 2.40 | 0.00 | 32.00 | 22.40 | 0.0 | 7.57 | 20.00 | 0.09 | | 67 | | | | | | | | RTDs on 30 cm Intervals | | | | |
| 169 | ESF-HD-TEMP-22 | Temperature | 0.00 | 32.00 | -1.30 | 0.00 | 32.00 | -22.50 | 0.0 | 7.57 | 21.20 | 0.10 | | 71 | | | | | | | | RTDs on 30 cm Intervals | | | | |
| 170 | ESF-HD-TEMP-23 | Temperature | 0.75 | 39.32 | 2.40 | 0.75 | 39.32 | 22.40 | 0.0 | 7.57 | 20.00 | 0.09 | | 67 | | | | | | | | RTDs on 30 cm Intervals | | | | |
| 171 | ESF-HD-TEMP-24 | Temperature | -1.80 | 39.32 | 1.80 | -15.94 | 39.32 | 15.94 | 45.0 | 7.57 | 20.00 | 0.09 | | 67 | | | | | | | | RTDs on 30 cm Intervals | | | | |
| 172 | ESF-HD-TEMP-25 | Temperature | -1.30 | 39.32 | -1.30 | -15.65 | 39.32 | -15.65 | -45.0 | 7.57 | 20.30 | 0.09 | | 68 | | | | | | | | RTDs on 30 cm Intervals | | | | |
| 173 | ESF-HD-TEMP-26 | Temperature | 0.75 | 39.32 | -1.30 | 0.75 | 39.32 | -22.50 | 0.0 | 7.57 | 21.20 | 0.10 | | 71 | | | | | | | | RTDs on 30 cm Intervals | | | | |
| 174 | ESF-HD-TEMP-27 | Temperature | 1.30 | 39.32 | -1.30 | 15.65 | 39.32 | -15.65 | -45.0 | 7.57 | 20.30 | 0.09 | | 68 | | | | | | | | RTDs on 30 cm Intervals | | | | |
| 175 | ESF-HD-TEMP-28 | Temperature | 1.80 | 39.32 | 1.80 | 15.94 | 39.32 | 15.94 | 45.0 | 7.57 | 20.00 | 0.09 | | 67 | | | | | | | | RTDs on 30 cm Intervals | | | | |
| 176 | ESF-HD-ERT-11 | Electrical Resistivity Tomography | -0.75 | 39.32 | 2.40 | -0.75 | 39.32 | 22.40 | 0.0 | 7.57 | 20.00 | 0.09 | | | | | | | | 21 | | Electrical Resistivity Tomography Arrays, Electrode Sensor on 1m Intervals | | | | |
| 177 | ESF-HD-ERT-12 | Electrical Resistivity Tomography | -0.75 | 39.32 | -1.30 | -0.75 | 39.32 | -17.50 | 0.0 | 7.57 | 16.20 | 0.07 | | | | | | | | 17 | | Electrical Resistivity Tomography Arrays, Electrode Sensor on 1m Intervals | | | | |
| 178 | ESF-HD-MPBX-11 | MPBX - Rock Mass Displacement | 1.30 | 41.15 | 2.10 | 8.80 | 41.15 | 15.09 | 60.0 | 7.57 | 15.00 | 0.37 | 16 | | | 6 | | | | | | Thermocouple Sensors between and at Anchors in MPBX | | | | |
| 179 | ESF-HD-MPBX-12 | MPBX - Rock Mass Displacement | -1.30 | 41.15 | 2.10 | -8.80 | 41.15 | 15.09 | 60.0 | 7.57 | 15.00 | 0.37 | 16 | | | 6 | | | | | | Thermocouple Sensors between and at Anchors in MPBX | | | | |
| 180 | ESF-HD-MPBX-13 | MPBX - Rock Mass Displacement | 0.00 | 41.15 | 2.50 | 0.00 | 41.15 | 17.50 | 0.0 | 7.57 | 15.00 | 0.37 | 16 | | | 6 | | | | | | Thermocouple Sensors between and at Anchors in MPBX | | | | |
| 181 | ESF-HD-MPBX-14 | MPBX - Rock Mass Displacement | 0.00 | 41.15 | -1.30 | 0.00 | 41.15 | -17.50 | 0.0 | 7.57 | 16.20 | 0.37 | 16 | | | 6 | | | | | | Thermocouple Sensors between and at Anchors in MPBX | | | | |
| 182 | ESF-HD-PERM-1 | Ambient Characterization | 11.91 | -17.75 | 2.20 | 11.91 | -36.54 | -4.64 | -20.0 | 7.57 | 20.00 | 0.09 | | | | | | | | | | Air-K Testing with Packer Systems | | | | |
| 183 | ESF-HD-PERM-2 | Ambient Characterization | 10.98 | -17.75 | 2.96 | 10.98 | -37.75 | 2.96 | 0.0 | 7.57 | 20.00 | 0.09 | | | | | | | | | | Air-K Testing with Packer Systems | | | | |
| 184 | ESF-HD-PERM-3 | Ambient Characterization | 9.15 | -17.75 | 2.20 | 9.15 | -36.54 | -4.64 | -20.0 | 7.57 | 20.00 | 0.09 | | | | | | | | | | Air-K Testing with Packer Systems | | | | |
| 185 | ESF-HD-HYD-11 | Hydrology | -29.50 | 44.80 | 8.00 | 10.22 | 44.80 | 12.74 | 6.8 | 7.57 | 40.00 | 0.18 | | 4 | | | 4 | 4 | | | | Pressure, RTD & Humidity Sensors in Packer at Depth of 23, 28, 33, and 38 m | | | | |
| 186 | ESF-HD-HYD-12 | Hydrology | -29.50 | 44.80 | 7.00 | 5.35 | 44.80 | -12.64 | -29.4 | 7.57 | 40.00 | 0.18 | | 4 | | | 4 | 4 | | | | Pressure, RTD & Humidity Sensors in Packer at Depth of 23, 28, 33, and 38 m | | | | |
| 187 | ESF-PL-MPBX-1 | MPBX - Rock Mass Displacement | 5.50 | -5.00 | -0.27 | 5.50 | -7.50 | -0.27 | 0.0 | 7.57 | 2.50 | 0.1 | 8 | | | 4 | | | | | | Thermocouple Sensors between and at Anchors in MPBX | | | | |
| 188 | ESF-PL-MPBX-2 | MPBX - Rock Mass Displacement | 5.50 | -3.00 | -0.27 | 5.50 | -0.50 | -0.27 | 0.0 | 7.57 | 2.50 | 0.1 | 8 | | | 4 | | | | | | Thermocouple Sensors between and at Anchors in MPBX | | | | |
| | ESF-HD-FH-1 | Floor Heater | 0 | 0.6 | -0.25 | | | | | | | | 24 | | | | | | | | | 8 Thermocouple Sensors on Each Ring & 3 Rings in Floor Canister Heater | | | | |
| | ESF-HD-FH-2 | Floor Heater | 0 | 5.88 | -0.25 | | | | | | | | 24 | | | | | | | | | 8 Thermocouple Sensors on Each Ring & 3 Rings in Floor Canister Heater | | | | |
| | ESF-HD-FH-3 | Floor Heater | 0 | 11.16 | -0.25 | | | | | | | | 24 | | | | | | | | | 8 Thermocouple Sensors on Each Ring & 3 Rings in Floor Canister Heater | | | | |
| | ESF-HD-FH-4 | Floor Heater | 0 | 16.44 | -0.25 | | | | | | | | 24 | | | | | | | | | 8 Thermocouple Sensors on Each Ring & 3 Rings in Floor Canister Heater | | | | |
| | ESF-HD-FH-5 | Floor Heater | 0 | 21.72 | -0.25 | | | | | | | | 24 | | | | | | | | | 8 Thermocouple Sensors on Each Ring & 3 Rings in Floor Canister Heater | | | | |
| | ESF-HD-FH-6 | Floor Heater | 0 | 27 | -0.25 | | | | | | | | 24 | | | | | | | | | 8 Thermocouple Sensors on Each Ring & 3 Rings in Floor Canister Heater | | | | |
| | ESF-HD-FH-7 | Floor Heater | 0 | 32.28 | -0.25 | | | | | | | | 24 | | | | | | | | | 8 Thermocouple Sensors on Each Ring & 3 Rings in Floor Canister Heater | | | | |
| | ESF-HD-FH-8 | Floor Heater | 0 | 37.56 | -0.25 | | | | | | | | 24 | | | | | | | | | 8 Thermocouple Sensors on Each Ring & 3 Rings in Floor Canister Heater | | | | |
| | ESF-HD-FH-9 | Floor Heater | 0 | 42.84 | -0.25 | | | | | | | | 24 | | | | | | | | | 8 Thermocouple Sensors on Each Ring & 3 Rings in Floor Canister Heater | | | | |
| | ESF-CD-TS-1 thru 57 | Connecting Drift | | | | | | | | | | | | | | | | | | 57 | | Thermistors on Every 4 m ² in Observation Drift Wall | | | | |
| | ESF-OD-TS-1 thru 13 | Observation Drift | | | | | | | | | | | | | | | | | | 138 | | Thermistors on Every 4 m ² in Observation Drift Wall | | | | |
| Total | | | | | | | | | | | | 3257.37 | 17.34 | 784 | 1936 | 195 | 3 | 110 | 48 | 48 | 316 | 130 | Total Number of Sensors (All Types) : | | 3570 | |

Notes:

- Borehole Coordinates are Referenced to a 0,0,0 Coordinate Located at the Center of the Bulkhead in the Heated Drift.
- Borehole Length is Based on the Designed 27 Meter Width from the Observation Drift to the Heated Drift and Current Design Dimensions.

9903020197-04

APERTURE CARD

INTENTIONALLY LEFT BLANK

Table 3-2. Scope Comparison of the Drift Scale Test and 16 Other Thermal Tests

| Location | Power (kW) | Total Test Duration (Years) | Processes |
|--|------------|-----------------------------|-------------|
| Yucca Mountain (Drift Scale Test)* | 200 | 8.0 | TMHC |
| Yucca Mountain (Single Heater Test) | 4.0 | 1.5 | TMHC |
| Yucca Mountain (Large Block Test) | 2.3 | 0.8 | TMHC |
| G-Tunnel (Small Diameter Experiment) | 2.1 | 0.3 | TMH |
| G-Tunnel (Heated Block Experiment) | 0.8 | 1.0 | TM |
| G-Tunnel (TH Experiment) | 3.3 | 1.0 | TH |
| Climax (Spent Fuel Test) | 19.5 | 3.0 | TM |
| Waste Isolation Pilot Plant (Room A) | 57.3 | 4.0 | TM |
| Waste Isolation Pilot Plant (Room B) | 58.6 | 4.0 | TM |
| Waste Isolation Pilot Plant (Room H) | 81.6 | 9.0 | TM |
| Underground Research Laboratory-Canada (Buffer Container Experiment) | 1.2 | 2.5 | TMH |
| Underground Research Laboratory-Canada (Heated Failure Tests) | 1.2 | 2.5 | TMH |
| Underground Research Laboratory (Thermal Hydraulic Experiment) | 1.0 | 1.0 | TMH |
| Basalt Waste Isolation Plant (Test-1 No. 1) | 5.0 | 2.0 | TM |
| Basalt Waste Isolation Plant (Test-2 No. 2) | 5.0 | 4.5 | TM |
| Stripa - Sweden (3 Experiments) | 6.1 | 4.5 | TM |
| Avery Island - (Site A) | 6.0 | 1.5 | TM |

*Basis for DST heating schedule/duration provided in Section 8.3

INTENTIONALLY LEFT BLANK

4. CHARACTERIZATION

Discussion of characterization of the DST block is divided temporally into pre-test and post-test phases. Measurement of the rock response during the DST is not considered in this discussion of characterization. These measurements are discussed in Section 6. Furthermore, it is not the intent of this report to present measured data from characterization activities since this information is documented in the *Ambient Characterization of the Drift Scale Test Block* (CRWMS M&O 1997b) (Deliverable Identifier: SP3308M3). The following discussion presents an overview of the different types of characterization activities planned and being conducted for the DST in terms of their respective objectives.

4.1 PRE-TEST

The objective of pre-test ambient characterization is to define the initial conditions of the local rock mass to assist in the interpretation and analyses of the coupled TMHC processes associated with the DST. Site characterization of the DST block commenced soon after mining of the observation drift was completed. The following discussion of pre-test characterization has been divided into laboratory and field for each of the four processes (TMHC) considered in the DST.

4.1.1 Laboratory

4.1.1.1 Sampling

Because of inherent spatial variability of the rock mass, rock characteristics such as fracture density, fracture connectivity, and fracture surface chemistry are expected to span over a range of parameter values. Therefore, samples have been collected systematically from cored boreholes located throughout the ESF Thermal Test facility including the SHT block, the observation drift, the connecting drift, and the HD. This systematic and comprehensive sampling ensures representative characterization of the Tptpmn lithologic unit. Because special features, such as discontinuities, will be sought and sampled, geologic reconnaissance of the structural features of the drifts and niches will also be conducted.

The cores taken from the DST block to characterize the local rock mass are considered sufficient in terms of the volume of rock tested. Specifically, the cores taken for testing are the group of allocated cores that receive special handling; they come from the:

- Ten chemistry boreholes (boreholes 52 through 56, 69 through 73)
- Two hydrology boreholes (185, 186)
- Eight multi-point borehole extensometers (MPBX) boreholes.

Of the latter, some originate from the observation drift (boreholes 42, 43), some from the HD (boreholes 149, 150, 156, 157), and two longitudinal boreholes that are parallel to the HD and which originate from the connecting drift. In addition to the above wet-drilled boreholes, cores from three dry-drilled ambient characterization boreholes (182, 183, 184) will be tested.

4.1.1.2 Thermal

Laboratory testing of thermal properties has a two-fold objective, to characterize the thermal properties of the DST block and to determine if significant spatial variation of these properties exists within the region. Thermal conductivity is a measure of the ability of a material to transmit heat, and so relates to the ability of the host rock to conduct heat away from waste containers. Thus, thermal conductivity is an important parameter for predicting the transient temperature field from heat generated by emplaced nuclear waste.

Thermal expansion is the material property that describes changes in volume or length that result from changes in temperature. The coefficient is usually recorded as strain (linear dimension per unit original length) per °C.

4.1.1.3 Mechanical

Laboratory testing of mechanical properties characterizes the intact rock properties in the DST block, including elastic constants and strength parameters and their spatial distribution and variability. These data are necessary as input to numerical models used to predict the mechanical response of the local rock mass surrounding the repository.

Unconfined compression experiments were performed on specimens of Tptpmn welded tuff recovered from boreholes in the DST block. These laboratory-determined properties of intact rock samples represent upper limit values of the strength and deformability of the in situ rock mass since rock mass factors such as discontinuities (e.g., joints and fractures) and other defects are not reflected in the intact rock. The reduction of strength and stiffness typically observed in the field is a function of the frequency and nature of existing discontinuities.

4.1.1.4 Hydrological

Laboratory testing of hydrological properties determines density, matrix porosity, and saturation values for Tptpmn samples taken from the DST block. These measurements are significant because matrix properties determine the amount of pore water available for evaporation and boiling during the heating phase, and the initial laboratory-determined saturations can be compared with the results of neutron logging monitoring changes in water content during thermal testing. Laboratory process testing, such as imbibition experiments, that probe the hydrologic interaction between fractures and matrix will be conducted. Additional and more complex laboratory testing may address the following:

- Redistribution of moisture because of thermal load
- Development of fast flow paths
- Waste canister environment with regard to water saturation and temperature
- Development of heat pipes
- Thermally driven buoyant gas flow enhancement of vapor diffusion
- Enhancement of vapor diffusion
- Thermal alteration of rock-matrix hydrologic properties.

4.1.1.5 Chemical

Laboratory testing using quantitative x-ray diffraction characterizes the relative mineral abundances in core taken from the DST block. Because other sub-samples from this core were used for thermal testing, the abundance of minerals that could affect thermal behavior was of particular interest. These minerals include cristobalite, which undergoes a phase transition and volume change at elevated temperatures, and smectite and clinoptilolite that can dehydrate at elevated temperatures with accompanying volume reduction.

The method of quantification involves the addition of a standard (corundum) to the sample in known proportion, and diffraction intensities from sample components are referenced to a diffraction line from the corundum. A proportionality constant, the reference intensity ratio, relates the intensity of the corundum reference line to the diffraction line(s) of sample components. Reference intensity ratios are determined from separate measurements of the x-ray line intensities of 1:1 mixtures of corundum with standard minerals that are proxies for the mineral components in the sample.

Chemical and isotopic data will be collected on water from hydrology and chemistry boreholes. Field pH and temperature data will be taken immediately after sampling. Laboratory analytical techniques will include inductively-coupled plasma spectrometry, gas-source mass spectrometry, and solid-source mass spectrometry.

4.1.2 Field

4.1.2.1 Thermal

The objective of the field measurements of thermal properties is to characterize both thermal conductivity and thermal diffusivity. A rapid estimation of thermal conductivity (**k**) and thermal diffusivity (α) device, referred to as the REKA probe, has been developed and will provide direct field measurements of these two thermal properties (see Section 6.2).

4.1.2.2 Mechanical

Field testing of the ambient mechanical condition consists of mapping, rock mass classification, and stress measurements. Geologic mapping in the DST block area determines the vertical and horizontal variability of fracture networks, characterizes faults and fault zones, maps the lithostratigraphic features of geologic subunits and the abundance and character of lithophysal zones, and assists in selection of test locations. Two data collection techniques were used, full-periphery mapping and detailed line surveys.

Rock mass quality determinations in the DST assess the stability of the local rock mass, assist in the location for heater and instrument placement, and provide estimates of the representativeness of test data. Rock mass quality assessments were performed in all of the thermal testing excavations using line mapping surveys. Determination of rock mass quality was based on both the Q system (Barton et al. 1974) and the Rock Mass Rating system (Bieniawski 1974).

In situ stress measurements establish the ambient state of stress prior to heating the DST block. Hydraulic fracturing was selected as the preferred method to measure in situ stress for various reasons including that it measures the in situ stress state over a much greater area than another popular technique, overcoring. Also, overcoring can produce greater variability than obtained from hydraulic fracturing.

4.1.2.3 Hydrological

Hydrological field measurements characterize the DST block by implementing several techniques including air-permeability, GPR, neutron logging, ERT, infrared imaging, and video borehole logging.

The air permeability structure in the DST block describes the gas phase movement in the DST block, which is important during heating since the fluid movement and its redistribution principally occur in the gas phase once the rock mass heats up and water vaporizes. Furthermore, rock surfaces on the drift walls surrounding the DST block are characterized by infrared imaging. This is intended to establish the initial conditions on the drift walls, specifically, the temperature distributions at the outlets of potential pathways for fluids and gases. During the heating period, thermally induced flow can change the temperature at and near the exits and hot spots can be detected.

Pre-test moisture content in the rock mass will be determined in situ by neutron logging, ERT, and GPR tomography. Boreholes dedicated to ERT and neutron logging are planned for the DST. GPR surveys will be carried out in the neutron logging boreholes. Video logging will be conducted on an estimated 137 of the total 147 boreholes within the DST block. These video logs augment the understanding of hydrological behavior from their record of fracture sizes and locations.

4.1.2.4 Chemical

Chemical characterization identifies fracture zones and minerals for sampling (using scraping or a side-hole sampler) in the manner documented by Steefel and Yabusali (1995) with the use of borehole video logs. Therefore, measurements of fractures and minerals have been conducted for samples taken before the DST and are planned for samples to be taken after the DST. Where core is available, visual and microscopic examinations will be conducted. The resulting mineral map will be used as input for modeling expected heat-induced changes. The mineral map will also be compared to samples and video logs taken after the DST is complete.

4.2 POST-TEST

As in the discussion of pre-test characterization activities, post-test characterization is divided into laboratory and field measurements.

4.2.1 Laboratory

Some overcoring and limited excavation is planned to study the thermally induced changes in the Tptpmn. While pre-test laboratory studies include both process and property testing, only properties will be measured after the completion of the DST. The mechanical properties measured from the

overcoring samples can help validate the measurements of the pre-test TM properties. The measured hydrological parameters correlated to their location in the field will help define the extent of the dryout and condensation processes. The post-test samples will also provide information on any chemical changes that may occur as a result of the hydrothermal processes in the DST.

4.2.2 Field

Since the primary objective of the DST is to acquire a better understanding of the coupled TMHC processes induced by electrical heaters, the spatial distribution of moisture and temperature are two parameters that will be closely monitored during the heating and the cooling phases of the DST. In particular, the vaporization and condensation of the liquid water in the heated rock can greatly affect the gas phase fluid flow during the heating and cooling period. Interference air injection tests in the packed hydrology boreholes are expected to provide hydrological tomography data. Post-test characterization after the cooling period will be similar to pre-test characterization discussed in Section 4.1.

INTENTIONALLY LEFT BLANK

5. ANALYSES

Figure 5-1 provides a schematic of anticipated one-to-one coupling of the TMHC processes evaluated in the DST. The coupling has been intuitively divided into primary and secondary relationships. This notion of the TMHC coupled processes represents a more complex relationship than considered thus far in which one-way coupling between thermal and the other three processes has been considered. Ultimately, the assessment of TMHC coupled processes will evolve into nearly instantaneous, four-way coupling after less complex coupling is sufficiently characterized and understood.

5.1 THREE-PHASE APPROACH

The temporal relationship inherent to the DST, between the development of data, application of the data in various models in terms of numerical analyses, and the implementation of corresponding computer programs (codes) is shown in Figure 5-2. The data, analyses, and codes are assembled for calculations at three distinct time intervals germane to the DST. This temporal relationship also pertains to the SHT. The DST analyses are divided into three phases: test scoping, pre-test, and mid/post-test. Post-test also includes analyses conducted during the DST. A distinction is made between test scoping and pre-test analyses in that the latter analyses (i.e., the forecast exercise) will benefit from site-specific characterization data generated in the laboratory and the field (see Section 4). Also, for the DST, more than one combination of conceptual models were evaluated in the pre-test (forecast) analyses (see Section 5.3). Consequently, the pre-test analyses provided more comprehensive and realistic simulations of the DST than was provided by the test-scoping analyses.

In the broadest sense, the DST is intended to generate site-specific observed data to build confidence in the conceptual models describing the heat-driven processes taking place in the rock adjacent to the repository openings (the near-field), both during the preclosure and postclosure periods of performance. Based on laboratory experiments, prior in situ thermal/radwaste tests conducted elsewhere, observations of natural geothermal processes, and additional knowledge of physical phenomena, a number of conceptual models of the TMHC processes in the near field have been developed or postulated.

The test scoping analyses are examples of models for each of the near field processes. The results of these test scoping analyses are largely relied upon as guidance to select such test features as the size and location of heaters, rate of application of heat, and spatial location of various measuring instruments. In contrast, the pre-test analyses provide baseline predictions of measured parameters such as temperature, displacement, and moisture content. Synergistic interpretive evaluation of the agreement between measured and predicted data will help to confirm and/or refine the models and thereby build confidence in them.

The test scoping analyses discussed in Subsection 5.2 do not use values for the various rock mass properties (such as thermal conductivity, thermal expansion coefficient, bulk permeability, moisture content, fracture frequency, and other fracture characteristics that are specific to the DST block) because such data were not available when the analyses were conducted. Such site-specific values for the input parameters would have made the test scoping results more likely to coincide with the

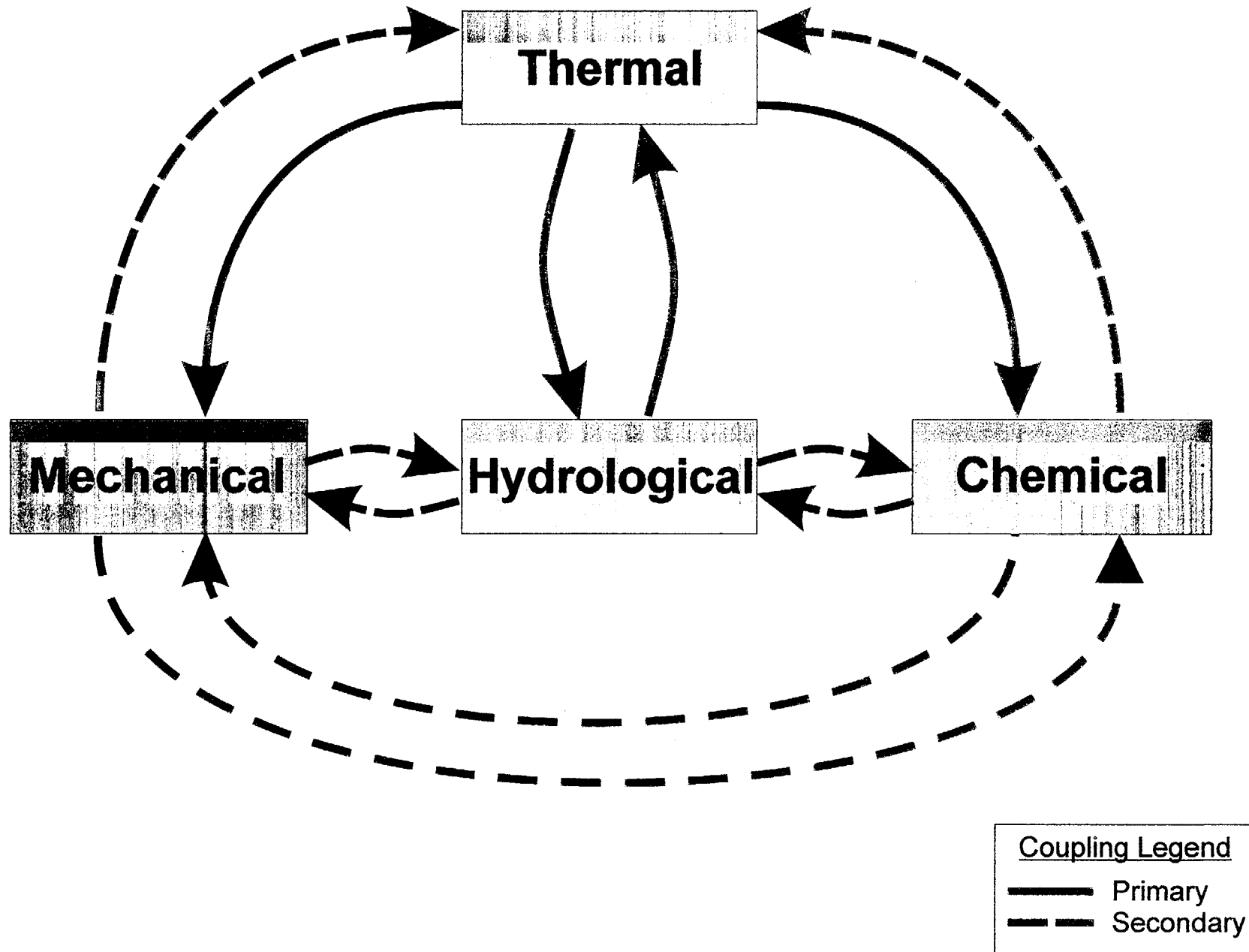


Figure 5-1. Anticipated One-to-One Coupling of the TMHC Processes Evaluated in the DST

| TIME → | | | |
|------------------------------|--------------------------------------|--|---|
| | <u>TEST PLANNING</u> | <u>PRE-TEST</u> | <u>DURING TEST/ POST-TEST</u> |
| <u>DATA</u> | Repository Block Characterization | → Site-Specific Characterization → | Measurements |
| <u>ANALYSES (MODELS)</u> | Test Scoping | Pre-test "Forecast" (Level 3 Deliverable) | During Test or Post-test or Model Refinement (6-Month Iteration) |
| <u>CODES</u> | Thermal | (e.g., V-TOUGH, NUFT, TOUGH2, COYOTE, FEHM, ANSYS) | |
| | Mechanical | (e.g., FLAC, UDEC, DDA, ANSYS, JAC) | |
| | Hydrological | (e.g., FEHM, NUFT, V-TOUGH, TOUGH2, FEMTRAN) | |
| | Chemical | (e.g., EQ 3/6, OS3D, GIMRT, FEHM, NUFT) | |

Figure 5-2. Temporal Relationship between Data Evolutions, Numerical Analyses, and Computer Programs for the Drift Scale Test

actual observed results. Ambient characterization of the DST, which is documented in CRWMS M&O 1997b, provides site-specific properties allowing conduct of pre-test analyses suitable for subsequent comparison with measured data.

There are conceptual models other than those used in the test scoping analyses that represent the heat-driven, near field processes. Some of the alternative models will be employed to predict the results of the SHT and DST. For example, in the test scoping analyses, an effective continuum model was used to simulate heat flow and fluid flow. Dual porosity, dual permeability, and discrete fracture-matrix interaction models are some of the alternative models that can be used to simulate these processes.

Additional predictions of test results have been made using the set of site-specific input parameters derived from the ambient characterization of the DST block with various combinations of conceptual models. The results of these predictive calculations and their agreement to the respective measured data have led to further refinement of the DST test features, such as heating rate and the spatial locations and density of measuring probes. In general, the pre-test analyses represent refined scoping and baseline post-test calculations.

Following the submittal of this report and the start of the DST, comparative analyses of the predicted and measured results will be performed approximately every six months to refine the conceptual models and to predict the measurements of the remaining test period. Criteria for evaluating the various conceptual models will be based on the closeness of agreement, in both trend and magnitude, between the calculated and measured data. Various types of TMHC responses will be evaluated including temperatures, displacements, liquid saturations, permeabilities, and water chemistry. It is expected that this predictive-corrective process will lead to the convergence of the results from near-field process models. Subsequently, this approach is expected to result in an acceptable level of confidence in the higher-level models used to assess the performance of the repository.

5.2 TEST SCOPING ANALYSES

As discussed in Section 2, the primary objective of the DST is to acquire a better understanding of the coupled TMHC processes in the local rock mass. Scoping calculations of the TH and TC processes assist in test design that targets the test objective. Since these calculations are intended to scope or size the tests, the input does not need to be as accurate as it would be for actual prediction of test behavior for comparison to measured data. The TH and TC calculations determine approximate values, preferred locations, and temporal and spatial variations of the measured parameters. The test design basis analyses are updated as sufficient new data on the local rock mass become available. After test design analyses are complete, these analyses will be repeated for the final configurations of the DST. Results from these pre-test and post-test analyses will be compared with measured data.

Given the wide range of values that may bound some parameters (e.g., rock mass permeability and moisture content), it is necessary to be cognizant of the potential for corresponding wide ranges of numerical predictions associated with simulating coupled TMHC processes. In many cases, mean parameter values are input in scoping, pre-test, and/or post-test analyses. Although the use of mean parameter values is acceptable, the response may not be average given the nonlinearity of the complex behavior corresponding to coupled TMHC processes.

5.2.1 Thermal-Hydrological Analyses

The V-TOUGH code (Nitao 1989) was used to conduct effective continuum model scoping calculations of the TH processes in the DST. The purpose of the analyses was to determine a range of heater sizes, heating rates, and heating duration for a range of plausible hydrological conditions. This approach helps to optimize the test, which is intended to evaluate the following processes:

- Dominant heat transfer mechanism
- Major TMHC processes that determine the magnitude and direction of vapor and condensate flow
- Influence of heterogeneous properties and conditions of the test region on the TMHC processes.

Buscheck and Nitao (1995) documented the calculations, results, and conclusions of their TH analyses. An important conclusion indicates that a heated area between 1,000 and 1,500 square meters is required to diagnose whether buoyant or nonbuoyant behavior dominates, and minimize the peak temperatures, within reasonable limits, for a given dryout volume. Also, it was determined that heating a single drift cannot perch enough condensate to generate a significant refluxing condition without pushing the peak rock temperature to greater than 235°C. A peak rock temperature greater than 235°C introduces complications from potential cristobalite transformations. The analyses indicated that an HD with wing heaters on both sides will satisfy the criteria for the heated area, dryout volume, and peak rock temperature.

The following wing and floor heater configuration was analyzed for the DST design: a row of drift heaters that generates 0.8 kW/m along the drift axis, flanked by wing heater arrays generating an areal power density of 125 W/m² averaged over the inner 5-m portion of the 11.5-m borehole, and 175 W/m² averaged over the outer 5-m portion of the 11.5-m borehole. A minimum of two years and possibly four years of full power heating will provide more in-depth information about the major TH regimes, the degree of vapor diffusion enhancement, and whether buoyant gas-phase convection of humid air will significantly increase the rate at which the dryout zone becomes rewetted. After three to four years of full power heating, the vertical thickness of the dryout zone is estimated to be about 10 to 15 m. The TH analysis also has given some indication of measurements that are the most important for determining the dominant TH regimes and dominant heat transfer mechanism. The dryout zone is basically defined as the region in which the moisture content is less than existed under ambient conditions. This implies that moisture may still be present in some areas of the dryout zone. The TH analysis also indicated the most diagnostic measurements for determining dominant regimes and heat transfer modes are:

- Vertical temperature distributions
- Vertical gas-phase pressure distributions
- Gas-phase pressure history in the drift during heating
- Relative humidity history in the drift during heating.

Vertical distributions for temperature and gas-phase pressure are considered important diagnostics since the vertical plane provides a description of the high gradients attributed to these two parameters.

The most important measurements for determining the influence of heterogeneity on the TH processes are:

- Horizontal temperature distributions
- Horizontal liquid saturation (or relative humidity) distributions
- Relative humidity history in the drift during heating.

5.2.2 Thermal-Mechanical Analyses

The FLAC code was used in the TM scoping calculations of the DST. FLAC calculated the changes in displacement and stresses from heating of an elastic continuum. A two-dimensional model, with x- and y- axes as the horizontal and vertical axes respectively, was used in the analyses of the vertical cross-section of the HD. This model assumes that the medium is homogeneous and that symmetry exists along the longitudinal axis of the HD.

The FLAC code was described by Blair et al. (1996). The calculations for the DST were described in detail by Berge (1996a). The major conclusions of his study are presented below:

- The region about 1 m from the HD wall reaches about 200°C in 200 days of heating.
- Compressive vertical stresses along the drift wall range from 30 MPa after 10 days of heating to 50 MPa after 200 days of heating.

- Shear stress concentrations near the roof-rib intersection of the HD are 30 MPa.
- Compressive vertical stress concentrations near the HD corner range from 60 MPa after 100 days of heating to 70 MPa after 200 days of heating.
- Temperature gradients between the HD wall and inner portion of the wing heaters are approximately 60°C over a 2 m distance.
- Stress gradients between the HD wall and the inner portion of the wing heaters are approximately 20 MPa after 100 days of heating.
- The horizontal displacement is the highest at the HD wall and near the far end of the wing heaters with ranges from 3 mm after 200 days of heating to 6 mm after 500 days.
- The vertical displacement is the highest in the regions from about 2 m to 10 m above and below the HD with ranges from 3 mm after 200 days to 5 mm after 500 days of heating.

5.3 PRE-TEST ANALYSES

Pre-test analyses for the DST can be divided into the following four, distinct studies:

- *Pretest Analysis of the Thermal-Hydrological Conditions of the ESF Drift Scale Test* (Birkholzer and Tsang 1997)
- *Pretest Thermal-Hydrological Analysis of the Drift Scale Thermal Test at Yucca Mountain* (Buscheck et al. 1997)
- *Pre-Experiment Thermal-Hydrological-Mechanical Analyses for the ESF Heated Drift Test* (Francis et al. 1997a)
- *Thermo-Chemical Analyses of the Drift Scale Heater Test: Mineralogical and Geochemical Characteristics* (Glassley 1997).

Each of these studies is discussed in detail within their respective reports. Therefore, only the highlights of the introduction and results are presented in the following discussions. Comparison of the different sets of calculations to measured data will be evaluated and documented in future planned reports. Criteria for future evaluation of predictions based on their agreement with measurements have been presented in Section 5.1

5.3.1 Summation of the Pre-test, TH Analyses Part 1

5.3.1.1 Introduction

The report, *Pretest Analysis of the Thermal-Hydrological Conditions of the ESF Drift Scale Test* (Birkholzer and Tsang 1997), presents the results of the modeling of both the heating and cooling phases of the DST. The temporal evolution and spatial variation of the TH conditions in the rock mass were analyzed and the impact of different input parameters (such as heating rates and schedules and different percolation fluxes at the test horizon) was evaluated. Furthermore, alternative conceptualization of the various physical processes is expected to play an equally important role in affecting the modeled TH responses of the rock mass. Therefore, the issue of conceptual model uncertainty is also addressed in this report. In particular, the processes examined are alternative conceptualization of the matrix-fracture interaction, such as the effective continuum model and the dual permeability formulation (DKM), and the effect of radiative heat exchange in the HD.

The most prominent TH response of the rock mass to the heater power output is the drying of the rock mass surrounding the heat source, the carrying away of moisture in the form of vapor from the heated area, and the subsequent condensation of the vapor in the cooler regions of the rock mass farther away from the heat source. After the heat source is removed and the rock mass starts to cool, rewetting occurs as water moves back to the vicinity of the heaters. To ensure that a large enough volume of water is heated to above boiling, and that the dominant drift scale TH processes expected in a repository can be monitored in the DST within a reasonable time frame, the DST has both canister heaters that will heat up the entire length (47.5 m) of the drift and wing heaters emplaced in 50 boreholes, orthogonal to and flanking the HD. The power of all canister and wing heaters can be varied within its full range. One objective for the pre-test analyses in this report is to provide input for arriving at an appropriate heating schedule for the DST. One main criterion governing the heating schedule is based on one of the thermal goals of the repository design, namely that the temperatures at the drift wall should not exceed 200°C.

To monitor the TH evolution in the DST test block, various measuring systems will be installed in boreholes drilled from the HD, as well as from the observation drift parallel to the HD. In particular, there are twelve hydrology boreholes, 40 m in length, and in three arrays of 5 (borehole nos. 57 to 61), 5 (borehole nos. 74 to 78), and 2 (borehole nos. 185 and 186) boreholes drilled from the observation drift. Each of these arrays of hydrology boreholes forms a fan in a plane orthogonal to the HD. Each hydrology borehole will be segregated by high-temperature inflatable packers into four zones, and each zone will be instrumented with sensors to monitor the temperature, relative humidity, and pressure. In addition to passive monitoring, active testing will be performed. This involves the injection of air in the individual zone isolated by packers, and the monitoring of the pressure response in all other packed zones in the hydrology boreholes at different stages of the DST. These air injection tests will help in understanding how the gas-phase permeability of the rock changes in time during heating and cooling, and in turn delineate the time evolution of the condensation zones. In this report's presentation of DST simulated results, particular attention will be paid to the predictions of the readings of the sensors in the 12 hydrology boreholes.

The numerical simulations presented in this report are performed in three dimensions with the multi-component, multi-phase flow simulator TOUGH2 (Pruess 1987 and 1991; Pruess et al. 1996; Wu et al. 1996). The configuration, parameters, and initial and boundary conditions of the numerical model developed in this study are designed to resemble the DST as closely as possible. Furthermore, all site-specific characterization data (such as laboratory measurements of TH properties of cores from the DST block, *in-situ* air permeability characterization, and borehole video logs) are incorporated into the conceptual model of the DST. Yet, because of the complexity of the multiple, coupled processes and uncertainty in key input parameters, such as fracture properties, deviations between measured and predicted data are anticipated. However, the presented model provides insight into DST performance and serves as a baseline that can later be refined and calibrated against measured data in subsequent analyses.

5.3.1.2 Results

The results of the modeling of both the heating and cooling phases of the DST are presented. The impact on the TH behavior from different input parameters, such as heating rates percolation fluxes, and alternative conceptualization of the matrix-fracture interaction were evaluated. In particular, the predictions provide the expected measurements transient of humidity, temperatures, and pressures in the DST block. These numerical simulations provide guidance to the location of the high-temperature packers and sensors to be installed in the hydrology boreholes. Furthermore, with regard to the active single hole air permeability tests to be conducted in the hydrology boreholes during the DST, discussion of when, where, and how the pressure response will occur was presented. The following results can be expected:

- The hydrology holes categorized as hot and wet or warm and wet are expected to show an increased single-hole pressure response to air injection, as the gas-phase permeability in the surrounding rock decreases after heat is activated. All these boreholes are partially located in the condensation zone, where matrix and fracture saturations build up because of condensation of vapor. Supposing that the packed-off injection zone is appropriately placed along the boreholes, injection tests will be able to detect this build-up. Once the saturation has increased, the hydrology holes further away from the heater, namely 57, 58, 74, 75, and 185, remain at this wet state throughout the heating and some part of the cooling period; i.e., they will probably show a similarly high pressure response throughout most of the testing. Other hydrology holes closer to the wing heaters or the HD, namely 59, 61, 76, 78, and 186, are expected to show a similar build-up of injection pressure throughout the first years of heating, but a reversed situation at the end of the heating period, as the local liquid saturation slowly decreases to or even below the pre-heat values.
- Sensors placed in hydrology holes categorized as hot and dry will reveal a significant decrease of liquid saturation along the near-heater borehole sections soon after heating starts. This decrease can be detected with the relative humidity readings. However, it is very unlikely that these saturation changes will be detectable in air injection tests, as the fractures start with low saturation values at ambient state, and the minor saturation decrease due to the dryout will not noticeably change the gas relative permeability.

- The simulation results reveal an extended zone of increased saturation below the heated areas, indicating that relatively fast gravity-driven flux is expected to occur in the fractures. According to the effective continuum mode analyses this zone may extend as much as 50 m in the vertical downward direction after four years of heating; according to the DKM analyses it may be even larger. However, with the present configuration of hydrology boreholes, there is no direct way of detecting potentially enhanced liquid flux in the fractures far below the heater area. Hydrology boreholes 61, 78, and 186, which bracket the heater area from the lower end, are only covering part of the condensation zone, with z-coordinates of about -12.5 m at the bottom of the boreholes. This limitation in test configuration is unfortunate since the two fracture-matrix interaction models applied in this study, effective continuum model and DKM, show considerable differences with respect to gravity-driven liquid flux.

The results indicate that the preferred heating scheme is near full heater power for a period of approximately one year at the beginning of the test to enforce a fast response in the DST, followed by a long period of reduced power output during which the temperatures are maintained at the desired level. The results also confirmed that the DST should have a heating period of four years because it allows for collecting more complete data on drying and rewetting phenomena.

The conclusions of this report are mainly based on qualified data and qualified software. The simulations presented were performed with a numerical model employing what is considered to be the best input parameters and the most reasonable conceptualization. The properties were based on the UZ site-scale model calibration of a surface-to-water-table column at well SD-9, and laboratory and field measurements that characterize the DST block. A complex three-dimensional grid design was developed to resemble the DST configuration as closely as possible. Where uncertainty due to parameter variability and conceptualization was anticipated, special care was taken to discuss their impact on the simulated results. Therefore, this pre-test analysis provides insight into how the DST is expected to perform and how to conduct the DST. It will serve as a baseline model upon which as-built data, further characterization data, and actual monitoring data may be used for refined analyses as discussed in Section 5.1.

5.3.2 Summation of the Pre-test, TH Analyses - Part 2

5.3.2.1 Introduction

The report, *Pretest Thermal-Hydrological Analysis of the Drift-Scale Thermal Test at Yucca Mountain* (Buscheck et al. 1997), describes the modeling and analysis that has been used to guide the refinements made during FY 1997 to the design and operational plans for the DST. The model calculations described in this report were conducted with the NUFT code (Nitao 1993, 1995). Most of the calculations are three-dimensional, accounting for the geometric details of the HD and nearby drifts, including the discrete representation of the floor and wing heaters, thermal radiation within the HD, and the thermal bulkhead. The primary purpose of these calculations is to provide input to help guide decisions about the following:

- The heat-generation rates and heating schedule for the heaters

- The design of the ventilation system
- The design of the thermal bulkhead that separates the heated and unheated portions of the HD
- The design of the heaters including the maximum power requirements as well as the temperatures that the heaters will be subjected to
- The temperature requirements for installed instrumentation and cabling
- The requirements for the spatial coverage of the monitoring network, such as the spatial extent of temperature increase and dryout.

For the TH models used in this study, it is assumed that the vertical layering of the hydrostratigraphic units in borehole SD-9 is applicable to the DST block. This assumption places the top of the Tptpmn 26 m above the heater horizon and places the bottom of the Tptpmn 10 m below the heater horizon. However, based on observations made in vertically upward boreholes in the observation drift, it is estimated that the Tptpmn extends 17 m to 21 m above the heater horizon from the bulkhead to the western end of the HD (personal communication between T. Buscheck, R. Wagner and D. Weaver on July 11, 1997). Accordingly, the distance between the bottom of the Tptpmn and the heater horizon ranges from approximately 19 m to 15 m over the same length of the HD. The differences between the actual and represented locations of the hydrostratigraphic contacts are expected to have a negligible effect on the TH behavior because:

- The boiling and dryout zones do not extend beyond these contact zones
- The thermal properties of the Tptpmn and the adjacent units above and below are virtually identical
- The hydrological properties of these units are similar.

Unlike earlier studies (Buscheck and Nitao 1995), this study did not investigate the sensitivity of TH behavior in the DST to a wide range of hydrological properties and conditions; however, the sensitivity of TH behavior to ambient percolation flux is examined. This study utilizes recent measurements of hydrological and thermal properties (Tsang et al. 1996) and focuses on examining the consequences of alternative heating schedules as well as alternative thermal property assumptions (thermal conductivity and emissivity) for the thermal bulkhead. Detailed descriptions of the temperature and liquid saturation distributions are provided for the major cases investigated in this study. Although not presented in this report, detailed descriptions of the heat flux distribution into the neighboring drifts have been provided to the project for several of the conduction-only cases that were investigated in this study.

A major consideration in establishing the heating configuration (and heating rates) of the DST is to provide information for resolving key issues in a timely manner (Buscheck and Nitao 1995). Based on these key issues, a minimum test area of 1000 to 1500 m² and a minimum full-power heating duration of two to four years were found to be necessary. Moreover, it was found that wing heaters

emplaced in arrays of horizontal boreholes on either side of the HD allow for the development of approximately tabular boiling and dryout zones. These dryout zones are overlain by substantial condensate buildup that increases the likelihood of the development of a significant heat-pipe zone.

There are at least four additional criteria in establishing the heating configuration and heating rates (and schedule):

- The sensitivity of TH behavior in the DST to percolation flux should be maximized. Measurements of temperature, liquid saturation, and relative humidity should be able to help discriminate the magnitude of percolation flux.
- The tendency for the development of a heat-pipe zone should be maximized.
- The tendency for post-boiling condensate drainage into the HD should be maximized.
- The volume of rock thermally perturbed must be sufficiently large compared to the scale of heterogeneity of the fracture networks.

The current thermal goal for the maximum drift wall temperature in repository drifts is 200°C. While the point-load design results in a peak drift-wall temperature range of 110–160°C, the line-load design, which is being considered as a design alternative, results in a peak drift-wall temperature range of 180 to 210°C for 83 MTU/acre which is comparable to the peak drift-wall temperature being considered for the DST. Because of the size of the DST, it is necessary to drive the peak drift-wall temperature to 200°C to dry out a large enough volume of rock to adequately assess fracture heterogeneity.

Model calculations (Buscheck and Nitao 1993) have indicated that the decay-heat-driven TH behavior of the repository can be divided into three sequential periods:

- Heat-up/drying period
- Quasi-steady period
- Cool-down/rewetting period.

The concept of these three periods is applicable over dynamically changing spatial regimes. Therefore, at a given time, certain locations in a repository (such as the edge of the repository) may already be in the rewetting regime while other locations (such as the center of the repository) may remain in the drying regime. The DST will definitely include a heat-up and cool-down period. A quasi-steady period can be added to the DST if the in-drift and wing-heater heat-generation rates are gradually ramped down after the initial full-power period. The heating rates can be increasingly throttled back so that the temperature at selected locations, such as the springline temperature at the center of the HD, is maintained at some target temperature (e.g., 200°C).

Depending on waste package spacing, spent nuclear fuel age and drift spacing, drift-scale TH behavior in the repository requires:

- 30 to 60 years to attain peak drift-wall temperatures
- 30 to 50 years to begin to coalesce the boiling zones between neighboring drifts
- 200 to 300 years to attain the maximum vertical length of the heat-pipe zone
- 500 to 700 years to attain the maximum spatial extent of boiling conditions.

Any *in situ* thermal test conducted within the license application time frame will have to be significantly accelerated relative to repository conditions. It is important that the DST result in TH behavior and coupled TMHC phenomena that are relevant to a much longer time frame. An important issue for the reference thermal load of 83 MTU/acre is the consequence of an extensive boiling zone that will eventually coalesce between drifts and extend as much as 300 m vertically. Therefore, it is important that the DST develop an extensive boiling zone relatively quickly and to maintain it for a sufficiently long duration to result in coupled TMHC effects that may significantly influence long-term performance of the repository. (Note: This type of technical rationale has been fed into the process for determining a preferred heating/cooling schedule as discussed in Section 8.3.)

5.3.2.2 Results

For many of the calculations, three different values of percolation flux were considered, along with four different heating schedules. All cases included a linear rampdown to zero power from four to five years.

From a modeling perspective, a key finding of this study concerns the importance of fully accounting for thermal radiation inside the emplacement drift. Calculations that neglected the contribution of thermal radiation on the distribution of temperatures within the HD predicted a large drift-wall temperature difference between the springline and crown as well as a large difference (in the axial direction) between the ends and center of the HD. Calculations that only accounted for thermal radiation between the in-drift heaters and drift surfaces predicted greater variability in drift-wall temperatures than calculations accounting for thermal radiation between all surfaces in the HD. This conclusion is applicable to analyses of drift scale behavior in the repository where large differences in heat output from waste package to waste package can result in large axial variability in temperatures along the drift. Accurately accounting for the contribution of thermal radiation to homogenizing this axial variability is extremely important to predictions of the near-field waste-package environment.

For most of the cases, the initial heating rate is 80 percent of full capacity for the floor heaters and 100 percent of full capacity for the wing-heater arrays. This 80 to 100 percent heating configuration causes tabular boiling and dryout zones (i.e., the upper and lower boiling and dryout fronts are nearly horizontal), which are expected to minimize the tendency for condensate shedding around the lateral edges of the heated area. A second set of cases, which used 80 percent of full capacity for both the floor heaters and wing-heater arrays, result in boiling and dryout zones that tend to slope more toward the lateral edges, thereby allowing more condensate shedding. The 80 to 80 percent heating configuration results in a slight reduction in peak temperature (22 to 24°C) at the springline of the

HD and a larger reduction (61°C) at the hottest wing-heater location. In general, reducing the heating rate in the wing-heater arrays is an ineffective way to reduce the peak temperature at the springline of the HD.

As mentioned previously, model calculations for repository thermal loading conditions show that TH behavior can be divided into three sequential periods: heat-up/dryout, quasi-steady, and cool-down/rewetting. A DST with a constant-power-heating period followed by a rapid rampdown to zero power will result in the heat-up and cool-down periods. If the constant-power-heating period is followed with a gradual rampdown of the heater power, it is possible to include a quasi-steady period during the DST. A sensitivity analysis was conducted to investigate how alternative heating rates and heating schedules can be used to create a period of quasi-steady peak temperatures in the vicinity of the HD. The springline at the center of the HD was chosen as the target temperature location because the maximum temperature occurs along the HD. Two cases were considered for target temperatures of 150 and 200°C , respectively, for ambient percolation fluxes of 0.36 and 3.6 mm/yr. For a 200°C target temperature, it is possible to maintain a constant 80 to 100 percent heating configuration for 1.5 and 2 years for the 0.36 - and 3.6 -mm/yr cases, respectively. Thereafter, the heating rate is linearly ramped down to 40 to 50 percent of full power at 4 years. For a 150°C target temperature, a constant 80 to 100 percent heating configuration can be maintained for 1 year. At 1 year, the power is stepped down to 56 to 70 percent and 64 to 80 percent of full capacity for the 0.36 - and 3.6 -mm/yr cases, respectively, and then for 1 to 4 years, it is linearly ramped down to 28 to 35 and 32 to 40 percent, respectively. For all cases it was possible to stay within 10°C of the target temperature during the quasi-steady period. While the 200°C target cases result in considerably lower springline temperatures, the reduction in the vertical extent of the dryout zone is relatively minor. This is in sharp contrast with the 150°C target cases, which result in a very large reduction in the dryout zone. In general, the 200°C target cases facilitate an effective tradeoff between perturbing a sufficiently large volume of rock and not driving peak temperatures excessively high.

Calculations were conducted for three values of ambient percolation flux (0.36 , 3.6 , and 6.2 mm/yr), each with a corresponding set of hydrological properties for the fracture and matrix continua in the effective continuum model. Temperatures appear to be quite sensitive to percolation flux; however, that sensitivity probably arises more from the manner in which percolation flux is accommodated in the fracture and matrix properties than from the actual value of percolation flux. The magnitude of percolation flux is small compared to the total liquid-phase flux (made up of condensate flux and percolation flux), which approaches 1000 mm/yr in the DST area. The hydrological property sets corresponding to the three values of percolation flux, each effectively allow a different partitioning between fracture and matrix flow. Moreover, the van Genuchten parameters (α and β) found in these property sets provide for different degrees of capillary-driven and gravity-driven flow in the fracture and matrix continua. Altogether, the hydrological properties of the fracture and matrix continua govern the mobility of liquid-phase flux that is returning to the boiling zone, which influences net dryout during the heat-up period and rewetting during the cool-down period. The important role that the DST plays is to maximize the tendency for condensate to build up above the boiling zone, which magnifies the sensitivity of dryout and rewetting to percolation flux and the hydrological properties governing liquid-phase mobility in the fracture and matrix continua.

Temperatures in the dryout zone (e.g., at the drift wall) are a direct indication of the balance between local heat flux and local incoming liquid flux, which is strongly influenced by the liquid-phase mobility in the fracture and matrix continua. The sensitivity of temperature to percolation flux (and the liquid-phase mobility of the fractures and matrix) occurs early during the heat-up/dryout period of the DST. At one year, the springline temperature at the central longitudinal location of the HD is 30°C hotter for the 0.36-mm/yr case than for the 6.2-mm/yr case. The rock temperature at the hottest wing-heater location is 43°C hotter for 0.36-mm/yr case than for the 6.2-mm/yr case. At two years, the springline and wing heater temperatures are 40 and 48°C higher, respectively, for the 0.36-mm/yr case than for the 6.2-mm/yr case. Relative humidity is also sensitive to the percolation flux particularly during the early heat-up/dryout period and during the cool-down/rewetting period. The vertical thickness of the dryout zone is moderately sensitive to percolation flux during the heat-up/dryout period; however, the extent of the dryout zone becomes more sensitive to percolation flux during the cool-down/rewetting period. Overall, the most diagnostic indications for the influence of ambient percolation flux/liquid-phase mobility are temperatures measured during the heat-up period and relative humidity measured during the cool-down period.

For safety reasons, gas-phase pressures will not be allowed to build up in the HD. Calculations were conducted that represent a pressure relief device in the thermal bulkhead and compared with calculations that allowed for no pressure relief. Without pressure relief, the maximum gas-phase pressure buildup in the HD is 0.07 atm, which results in a peak gas-phase pressure buildup of 0.09 atm in the rock adjacent the HD. (Note that the peak gas-phase pressure buildup occurs at the hottest wing-heater location.) With pressure relief in the HD, the gas-phase pressure in the drift remained very close to atmospheric which limited the peak gas-phase pressure buildup to 0.05 atm in the adjacent rock. Limiting the gas-pressure buildup in the HD resulted in a slightly greater dryout zone ($\Delta Z_{\text{dry}} = 17.8$ m versus 17.6 m) and a slightly higher peak springline temperature (266°C versus 264°C). In general, gas-pressure venting in the HD had a negligible effect on temperature buildup and dryout.

5.3.3 Summation of the Pre-test, Thermal-Mechanical-Hydrological Analyses

5.3.3.1 Introduction

The report, *Thermal-Mechanical-Hydrological Analyses for the ESF Heated Drift Test* (Francis et al. 1997b), documents the pre-test TMH response of the HD and surrounding rock induced by the horizontally-emplaced in-drift floor (canister) heaters and wing heaters with a total power output of approximately 210 to 220 kW. The experimental TMH response will be determined by measurements of temperature, moisture content, and displacement on and within the DST block. The analyses performed include TH and TM calculations, with predictions of temperatures and displacements at selected locations in the drift where MPBX will be installed. Input parameters for the calculations were obtained as much as possible from either the DST or the nearby SHT blocks.

TH modeling was performed using a two-dimensional (X-Z), cross-sectional model representing the center of the HD; a two-dimensional (Y-Z), longitudinal model used to characterize edge cooling effects as a result of unheated rock mass at either end of the drift; and a three-dimensional, periodic boundary model used to assess the effects of model dimensionality on the TH model predictions. Predicted temperatures for ESF-HD-MPBX-7, 8, 9, and 10 are presented for the two, three, and four

year heating scenarios with two-year cooling. Temperature predictions are given for both high and low bulk permeability cases. Additionally, temperature and liquid saturation contours are shown for each of the TH models applied in the analyses. Temperature and liquid saturation profiles are given for both high and low permeability rock at six month intervals for the different heating scenarios.

5.3.3.2 Results

The two-dimensional and three-dimensional TH models were used to predict temperatures and liquid saturations in the DST block for MPBX locations at the approximate midpoint along the HD centerline. The MPBX locations were chosen because the anchors include a thermocouple for simultaneous measurement of temperature and displacement. Temperature predictions were determined from the two-dimensional (X-Z) TH cross-section model. This TH model domain roughly corresponds to the centerline of the DST where negligible edge cooling effects are expected. The longitudinal (Y-Z) model considers increasing edge cooling effects away from the center of the DST. Other results include temperature and liquid saturation contours for each model domain at six month intervals including the 96°C and 200°C isotherms.

Temperature predictions are shown for borehole numbers 154 through 157. Boreholes 154 and 155 are drilled into the top of the drift at orientations of 30° from vertical. Collars are located at the drift wall. These boreholes house ESF-HD-MPBX-7 and 8. Because of model symmetry, the temperatures predicted for the MPBX-7 and -8 are identical. Borehole 156 is 15-m long and located vertically upward from the top of the drift crown, it houses ESF-HD-MPBX-9. Borehole 157 is 15-m long and located vertically downward from the top of the concrete invert, it houses ESF-HD-MPBX-10. Anchors are located 1, 2, 4, and 15 m from the collar. The anchors are designated 1, 2, 3, and 4, with anchor 1 being the closest to the collar. Predicted temperatures are shown at collar and anchor locations in each borehole as indicated above.

Full power (continuous) heating cycles of two, three, or four years were coupled with two years of monitored cooling. The TH results from low and high bulk permeability cases are shown to indicate the potential range of temperatures at selected borehole locations (midpoint of the HD). It is noted that the knowledge gained from the SHT would indicate that both the low and high bulk permeability cases tend to underpredict the measured temperature results particularly for early times and near field conditions (Francis et al. 1997b). The result that measured temperatures tend to be higher than predicted temperatures, may be driven by typical TH modeling assumptions including isotropy of the fluid conductivity of the host rock, the conceptual model used to describe the mechanism of heat and fluid flow, and the homogeneity of the surrounding host rock. The following results are described for the effective continuum model with isotropic and homogeneous rock properties.

The predicted temperatures at the collar locations were the highest of all other borehole locations. Results from the low bulk permeability case indicate a maximum drift wall temperature of approximately 260°C, 300°C, and 330°C, respectively for two, three, and four year continuous full power heating at the collar of ESF-HD-MPBX-7. Predictions from the higher bulk permeability case at this (collar) location were approximately 10°C less than the lower bulk permeability case. In general, the low bulk permeability temperature predictions were greater than the high bulk permeability temperature predictions. At very early times, however, a slight increase in the convection heat transfer aids in the transport of energy away from the heat source towards the rock

wall. The higher bulk permeability rock will result in a slightly greater temperature as heat is convected more readily from the canister heater to the drift wall. This process occurs while the medium is below the boiling point and the drying front is just beginning to move away from the drift wall. At further locations along the borehole (i.e., anchors 1 through 4), convection effects become more pronounced in the higher bulk permeability simulations as is evident by the prolonged constant temperature regions (96°C) and the inflection points in the temperature predictions of both bulk permeability cases. At the furthest point along the MPBX in the borehole, anchor 4, convective heat transfer results in a slight increase in the predicted temperatures of the high bulk permeability cases when compared to the low bulk permeability cases.

The same general trends are observed in the temperature predictions for ESF-HD-MPBX-9 and -10. Convection heat transfer influences the temperature predictions with increasing distance from the collar at later times, particularly for the higher bulk permeability cases. It is noted that the predicted temperature at the collar of ESF-HD-MPBX-10 is slightly greater than the collar predictions at the other locations because of the proximity of this specific collar location to the canister heaters.

Contour plots of predicted temperatures and liquid saturations have been prepared at six month intervals for each of the TH models used to analyze the HD block. The Y-Z longitudinal model results illustrate the impact of edge cooling while the X-Z model results provide TH predictions at the center of the HD experiment. The three-dimensional X-Y-Z model results are shown only for the low bulk permeability case with a two-year heating and cooling cycle.

The heating results for the low bulk permeability case are shown for each of the heating cycles. It is noted that identical times later in the simulation are not repeated for the longer heating cycles (three- and four-year heating). For example, consider the case with three-year heating, two-year cooling, the displayed results begin at 30 months since the early heating times (6 - 24 months) are already displayed in the previous case (two-year heating, two-year cooling). The four-year heating cycle results are shown for the higher permeability case.

Displacements in the host rock during the heating and cooling phases of the DST at selected MPBX anchor locations were predicted. Results from scenarios of four-year heating; and two-year heating, two-year cooling have been documented. The three-dimensional temperature fields used as input to the TM calculations were obtained from the TH calculations. The predicted displacements are from the following locations: ESF-HD-MPBX-7, -9, and -10, located at the approximate midpoint of the HD; ESF-HD-MPBX-1, which runs horizontally along the length of the HD approximately 7 m south of the center line; and SDM-MPBX-2, located in the sequential mining borehole which is at the same Y-coordinate as the borehole 154 through 157 (roughly the midpoint of the HD). All the predictions are of displacement of the host rock at each anchor location relative to its corresponding collar.

The sensitivity of the predictions to different input parameters including rock mass elastic modulus, rock mass thermal expansion, and bulk permeability has been considered in the TM calculations in the following manner:

- A base case with a rock mass elastic modulus ($E=36.8$ GPa) and thermal expansion values ($\alpha=7.47-51.47$ $\mu\text{m}/\text{m}\cdot^\circ\text{C}$ as a function of temperature), both based on intact rock measurements, and a low bulk permeability ($K_b=2.16\times 10^{-15}$ m^2)
- An in situ elastic modulus case ($E=10$ GPa) based on Goodman jack measurements from the SHT block
- An in situ thermal expansion case ($\alpha=5.27$ $\mu\text{m}/\text{m}\cdot^\circ\text{C}$) based on SHT displacement and temperature data
- The high bulk permeability case ($K_b=6.35\times 10^{-12}$ m^2) for which a different set of temperature predictions were input to the TM calculations.

The base case calculations were run for both the two-year heating, two-year cooling; and four-year heating scenarios. The other three cases were run to simulate the four-year heating scenario to provide comparisons with the base case.

In summarizing the TM results, displacement predictions in the host rock during the heating and cooling phases of the DST at selected MPBX anchor locations indicated a maximum extension of about 15 mm. Expectedly, displacement magnitudes were strongly influenced by the thermal expansion coefficients considered. Also, predictions for the sequential drift mine-by test indicate that their measurements may be used as an indicator of rock mass elastic modulus because of the difference in the predicted behavior using an intact rock value of 36.8 GPa and a representative Goodman jack value of 10 GPa (SNL 1997). The range of bulk permeability values measured in the DST block was not shown to be a strong factor in the TM behavior, including the thermally-induced displacements.

5.3.4 Summation of the Pre-test, Thermal-Chemical Analyses

5.3.4.1 Introduction

The report, *Thermal-Chemical Analyses of the Drift Scale Heater Test: Mineralogical and Geochemical Characteristics* (Glassley 1997), represents the baseline pre-test calculations of the TC behavior in the DST. A boiling front and region of condensate formation will migrate outward from the heated region. Condensate will form along fractures and be imbibed into the rock, in regions where full saturation has not been achieved, or will migrate along fracture surfaces. In the latter case, water will dissolve pre-existing mineral phases that line fracture surfaces, potentially reaching saturation in a number of potential secondary mineral phases. If saturation occurs, precipitation of those phases may occur, provided kinetic barriers to nucleation do not inhibit the mineral growth process. This report describes the first suite of simulations conducted to determine the time-dependent chemical and mineralogical changes expected to develop during the course of the heating phase of the DST. The purpose of these simulations was to provide a first prediction of the chemical

and mineralogical changes that may be measured at the locations of the chemical boreholes (see Table 3-1 for locations).

The temperature distribution and vertical and horizontal components of the velocity field were obtained from TH simulations (Buscheck et al. 1997) for the plane where the chemical boreholes (69, 70, 71, 72 and 73) are located. This calculated data is for times of 1, 2, 3, and 4 years after heater activation. This approach of taking sequential time slices through the flow field was used because current reactive transport simulators that account for non-ideal solute and solvent behavior, and realistic dissolution and precipitation kinetics, generally do not update thermal and flow fields automatically. Code enhancements to address this shortcoming are planned.

The data were fit to a regular mesh of 1 m by 1 m grid blocks. Vertical boundaries of the mesh were located at the access drift (approximately 28 m from the drift center), and at the approximate outer edge of the outer wing heaters. This geometry provided coverage of those regions intersected by the chemistry boreholes.

Initial scoping simulations demonstrated that changes in mineralogy did not occur in regions with temperatures below 40°C. In addition, for conditions above boiling, existing reactive transport codes have limited capabilities to model fluid-rock interaction. Hence, domains were selected above (Zone 1) and below (Zone 2) the heated region where temperatures were between 40°C and 100°C, and the simulations were conducted for the flux fields within these regions.

The code used in the simulations was GIMRT (Steefel and Yabusaki 1995), which allows direct monitoring of changes in porosity, solution composition, and dissolution or precipitation of mineral phases, as a function of temperature; pressure; fluid flux; input solution chemistry; reaction kinetics; and system geometry.

5.3.4.2 Results

Initial simulations indicated that no perceptible changes in mineralogy would occur during the first four years for those regions where the temperature did not exceed 40°C. In regions where temperatures exceed 100°C, mineralogical changes will be dominated by either mineralogical dehydration or vapor-phase alteration of existing mineral phases. Hence, the simulations conducted here considered those regions where temperatures remained between 40°C and 100°C. In the simulations, it was assumed that the coexisting gas phase was buffered to a CO₂ pressure of 0.01 bars, consistent with results obtained from the SHT.

The results demonstrate that large variations in water chemistry should be anticipated in which concentrations of individual cations vary by several orders of magnitude within each zone. This strong compositional zoning of the waters reflects the effect that flow path length has on reaction progress. Those regions farther along the flow path reach saturation in a variety of secondary minerals.

Secondary mineral development is complex, and depends on spatial locations, relative to the drift and wing heaters, and time. The saturation state of the waters varies, but indicates that precipitation

of secondary minerals should be expected above and below the drifts. The extent of precipitation is time-dependent, but will be greatest above the drift.

Counteracting the effects of mineral precipitation is mineral dissolution. Mineral dissolution exhibits complex behavior, and is consistently greatest in the immediate vicinity of the boiling front.

During cool down, reversal of the mineralogical sequence development during heating is anticipated. However, nucleation effects and changes in flow pathways and velocities will lead to inhomogeneous development of secondary phases during this period.

5.4 POST-TEST ANALYSES

As discussed in Section 5.1 and shown in Figure 5-2, the mid/post-test analyses will be conducted in an iterative, semi-annual manner for the duration of the DST. This approach is intended to steadily increase confidence in the predictive capability of the selected process models. Discussion of the post-test analyses will be deferred to future reports documenting the updated analyses and their agreement with corresponding measured responses.

INTENTIONALLY LEFT BLANK

6. MEASURING SYSTEMS

The measurement systems described below are designed to monitor the coupled TMHC processes in the DST. Section 3 (Table 3-1 and Figures 3-1 and 3-2) describes specific locations of the boreholes and instruments for conducting these measurements.

The plan for measuring systems is based on several factors, including lessons learned from previous heater experiments (DOE 1995) and the professional experience and formal education of the ESF Thermal Test Team. A necessary component of the measuring system is the development of numerous boreholes that account for less than 0.1 percent of the total volume of the local rock mass. Also, most boreholes will be either sealed or plugged. Consequently, the presence of the boreholes is not anticipated to adversely affect the measurements of the TMHC behavior.

6.1 BASES FOR DEVELOPMENT

6.1.1 Background for Scientific Rationale/Engineering Judgement

The geometry and objectives for the DST phase of the ESF Thermal Test, as well as the locations, density of instrumentation, and types of instrumentation, were largely determined during a two-day workshop held in late February 1996. Assembled for this meeting were the Principal Investigators (PIs) from Lawrence Berkeley National Laboratory, Lawrence Livermore National Laboratory, and Sandia National Laboratories, who have both academic training and experience in fielding in situ thermal tests. These PIs were supported by other scientists from their home laboratories, as well as scientists and engineers from other M&O teammates. Collectively, the ESF Thermal Test Team has many years of thermal testing experience and has participated in the G-Tunnel tests conducted by Lawrence Livermore National Laboratory and Sandia National Laboratories, the Spent Fuel Test at the Climax Mine, the Waste Isolation Pilot Plant tests in Carlsbad, New Mexico, and the Avery Island tests in Louisiana. In addition, this group of scientists and engineers has studied and visited similar thermal testing conducted in other countries, including Canada (Underground Research Laboratory), Sweden (Stripa), and Germany (Asse Mine). They have also planned, constructed, and operated other complementary thermal or site characterization experiments in the laboratory and the field, as well as conducting analytical and numerical modeling of in situ experiments and natural analogs such as geothermal fields.

The lessons learned in previous tests are part of the experience base of these individuals. Examples of explicit lessons learned are types of epoxy grout to avoid, the importance of instrument density, the importance of measuring parameters on both sides of a plane of engineering symmetry, and the need to anticipate problems in the harsh thermal environment. Implicit lessons learned are more subtle, but equally important: a scientific and engineering intuition about test geometry and performance which is based on experience, training, and modeling. Recent experiences by these individuals in ESF characterization, Large Block Test planning and construction, Waste Isolation Pilot Plant testing, and laboratory testing ensured that their experience base is germane and timely.

In summary, the bases for sources of inputs consist of formal inputs such as those obtained from published literature that are duly referenced. For instance, parameter input such as is needed in the scoping analyses is obtained from the *Reference Information Base* (YMP 1996). Inputs that

are less definitive, such as the layout of the boreholes for the instrumentation, are based on scientific rationale or engineering judgment. This type or source of input is based largely on professional experience and formal education of the members of the ESF Thermal Test Team and peripheral advisory groups or personnel.

6.1.2 Background for Thermal Tests

The test consolidation exercises in FY 1994 and FY 1995 had the goal of reducing the construction time and the cost of the thermal experiments. Previously, multiple tests were planned with some including multiple drifts and instrumentation access from surrounding observation drifts, including drifts at elevations above and below the heated region. The result of these exercises was a reduction in the number of tests to only a few.

The initial test, the ESF Thermal Test, was determined to be a single drift test, with access for instrumentation only from the HD and construction accesses. This was necessary for both cost and schedule reasons; a multiple drift test with observation drifts at multiple elevations would require a much longer period to construct and would be much more expensive. It was determined that much of the relevant coupled processes could be addressed in a single drift test, if horizontal wing heaters were added to simulate heat from adjacent drifts (Buscheck and Nitao 1995). The wing heaters have an additional advantage; they cause the region of flat isotherms to be closer to the heated region, shortening the test duration.

The instrumentation for the SHT is comprised primarily of thermal and mechanical sensors. Hydrological and chemical instruments are being used primarily as means to evaluate their ability to perform adequately in the DST.

The SHT is attempting to create a radial temperature gradient. Temperature sensors and MPBXs were installed parallel to the heater, at various radii, to take advantage of the radial gradient. Because the temperature profile will move outward in time, these instruments will gather data at multiple temperatures as the experiment progresses.

Instruments were installed in each side of the SHT block; the instruments provide the capability to measure the temperature gradient itself, looking for heterogeneity effects. The boreholes are also used to gather deformation data across the temperature gradient, as will be the case for many of the measurements in the DST. Thus, this portion of the SHT provides an early test of the ability to match experimental data with computer simulations for more complex situations.

In planning for the DST, it was determined that the geometry would support some additional aspects that would generate data without compromising the major objective of obtaining coupled process data. A plate loading alcove was added to measure TM behavior in heated and ambient temperature rock. The geometry selected supported installation of instrumentation from one drift to monitor the initial response of rock in the other drift to its excavation (SDMT). Stand-alone permeability, stress, and strain measurement areas were also included to expand the database for ambient conditions.

The ESF Thermal Test Team determined that the DST could be better conducted if it was preceded by a smaller test, for three reasons. First, the small test could use a simple geometry that would support TM analysis; this would provide the rock mass property data needed to interpret the results of the more geometrically complex DST. Second, the small test would be an opportunity to field the array of diagnostic equipment needed in the larger test; this would work out the bugs in an environment that was not critical to the success of the overall project. Finally, the small test would be an opportunity to assemble the multi-organization team and to exercise it, again in a non-critical environment. The small initial phase of the ESF Thermal Test was named the SHT because of its simple heating geometry.

The selection of instrumentation for the DST began with a major constraint: the geometry of the test restricted access for instrument installation to be from the HD, from near that drift's collar, and from a nearby parallel drift. This constraint was generated from the test consolidation exercises, which were driven by cost and schedule constraints (DOE 1995).

6.1.3 Sensor Reliability

The reliability of the various types of sensors was an important consideration during the planning of the DST. Past thermal tests provide an excellent resource to evaluate sensor performance. Previous heater tests provided similar conditions and applications in which sensors needed to be installed in a rock mass that was subjected to harsh thermal environments over an extended period. As shown in Table 6-1, thermal sensors tend to be the most reliable, whereas stressmeters are the least reliable. Mechanical sensors such as the borehole deformation gage and extensometers tend to be dependable. Information about chemical and hydrological sensors is more sparse since most of these previous heater tests were designed for TM observations. The findings in this comparative assessment parallel the strategy for deployment of sensors in the DST. For example, an abundance of thermal sensors (approximately 3,000) will be installed but stressmeters will not be used in the DST.

6.1.4 Temperature Measurements

Temperature was recognized as the parameter most easily measured in the DST (Buscheck and Nitao 1995). Temperature sensors are small, inexpensive, and can be collocated with other types of instruments. Furthermore, coupled processes such as activation of convection loops and phase change leave a distinct temperature signature. Although temperature sensors on the drift wall, on the in-drift (floor) heaters, and in the wing heater boreholes serve a useful purpose by establishing the geometry of the heat source and assessing the importance of thermal radiation and convection within the HD, it is the temperature sensors in the heated rock itself that will measure coupled TMHC processes.

To readily compare the field measurements and the model predictions, temperature measurements in vertical planes are useful. Measurements of the variability in temperature among vertical planes perpendicular to the HD longitudinal axis can characterize the extent of the natural system's heterogeneity on a meter to tens of meters scale, as well as measure end effects. Location of the approximately 3,000 thermal sensors are identified in Table 3-1. Variation of temperature within

Table 6-1. Sensor Performance of Other In Situ Heater Tests*

| Heater Test | Sensor Performance |
|---|---|
| G-Tunnel Underground Facility - Nevada (Small-Diameter Experiments) | Basic instrumentation functioned well |
| G-Tunnel Underground Facility - Nevada (Heated Block Experiment) | Heater and thermal sensors functioned well; Flatjacks failed |
| G-Tunnel Underground Facility - Nevada (TH Field Test) | T-C Psychrometers were inconsistent; calibration problems with high frequency electromagnetic tomography |
| Climax - Spent Fuel Test - Nevada | Thermal sensors were reliable; 100% of original vibrating wire stressmeters failed; problems with extensometers |
| Waste Isolation Pilot Plant - New Mexico (Room A) | 14% remote thermal failure, >70% stress sensor failure |
| Waste Isolation Pilot Plant - New Mexico (Room B) | 36% remote sensor failure, >70% stress sensor failure |
| Underground Research Laboratory - Canada (Buffer Container Experiment) | Approximate sensor failure for all 3 URL tests: <ul style="list-style-type: none"> • Pneumatic piezometers - 13% • Thermal needles - 90% • Psychrometer - 16% • Thermocouples - 2% • Pressure transducers - 15% • Pressure cells - 27% • Pneumatic pressure cells - 0% |
| Underground Research Laboratory - Canada (Heated Failure Tests) | |
| Underground Research Laboratory - Canada (Thermal Hydraulic Experiment) | |
| Basalt Waste Isolation Project - Washington (Test-1) | Problems with 32% of extensometers, 72% of vibrating wire stressmeters, and 15% of borehole deformation gages |
| Basalt Waste Isolation Project - Washington (Test-2) | Problems with 22% of vibrating wire stressmeters and 25% of borehole deformation gages |
| Stripa Underground Test Facility - Sweden (3 Experiments) | Problems with 17% of vibrating wire stressmeters, 73% of borehole deformation gages, and 13% of thermocouples |
| Avery Island Heater Test - Louisiana (Site A) | Problems with many vibrating wire stressmeters; thermocouples and extensometers worked well |
| * Note: Electrical heaters performed favorably in most of these heater tests (Climax test not considered) | |

these planes provides information on the temporal evolution of the temperature field, including signatures of phase change, convection, and enhanced diffusion. The four horizontal and vertical boreholes serve double duty, as they are also members of the horizontal and vertical planes that include the drift axis. The other boreholes allow access to heated regions above and below the drift, but laterally removed from it. Several other planes perpendicular to the drift axis are accessed from the parallel observation drift. Because these boreholes are much longer (because of the drift separation), they generally must serve multiple functions (such as ERT, neutron logging, MPBX, humidity, or chemistry), as well as temperature measurement. Instrument density in these planes is greater on the near side of the HD than on the far side; nevertheless, their temperature sensors provide valuable augmentation of those emplaced from the HD.

The regions above and below the drift are expected to have roughly horizontal isotherms (for homogenous rock) due to the influence of the wing heaters. These regions (which are several meters above and below the drift) are analogous, within only a few years, to regions that are generated some tens of meters above and below parallel HD in a high thermal load repository after a few decades of heating. Thus, the series of parallel horizontal planes defined by the sensors in these boreholes above and below the drift will identify rock heterogeneity, if it exists. In addition, the temperature field (distance between isotherms) and the temporal evolution at a given location are sensitive to several parameters including thermal conductivity, saturation, phase change, convection, enhanced vapor diffusion, and heterogeneities.

The spacing of temperature sensors along a given borehole is an engineering tradeoff. Too many sensors will require a larger borehole to accommodate wiring and can preclude use of the borehole for other instruments. Too few sensors may not capture the phenomena of interest. Also, there is a point of diminishing return on sensor density because the test seeks to identify phenomena that occur on a scale of one meter to tens of meters. A compromise among these factors is a spacing of 30 cm or more between temperature sensors. The spacing between boreholes is much larger because of the constraints on drilling accuracy, time, and expense.

The above discussion of temperature sensors focuses on the vertical planes perpendicular to the drift axis. As mentioned above, these sensors also contribute to other vertical planes. These other planes are augmented with additional temperature sensors from other boreholes. A series of short boreholes will be drilled about 10 m into the crown and floor of the drift, thus the axial vertical plane will be augmented. The sensors in these boreholes also contribute to the series of parallel horizontal planes, but only in the region directly above and below the drift. To provide more spatial definition in these planes in the direction of the drift axis, two long temperature boreholes will be drilled from the connecting drift. These boreholes will be a few meters above the roof crown and equally offset from either side of the drift centerline.

With some exceptions, including the temperature sensors installed from the observation drift, the temperature sensors in this experiment are designed to measure both sides of the three planes of symmetry of the experiment. This is considered important since a key lesson of the Climax Spent Fuel Test was that observation in symmetric locations (with respect to the engineered features) is a powerful method of detecting heterogeneities in the natural features.

6.1.5 Mechanical Measurements

Heating induces thermal expansion in unconfined rock because of the positive coefficient of thermal expansion. Since the heated rock is surrounded by in situ rock at ambient temperature, the expansion is constrained, generating stress in the rock that is superposed on the existing lithostatic stress. Mechanical stress is difficult to measure in situ in real time. Thus, the mechanical measurements of the deformation of the rock in response to the changing stress, will be made using mechanical MPBXs. Also, stresses in the concrete-in-place ground support system will be determined from strain gage measurements. Computer simulations will be used to calculate the deformation for comparison to instrument readings.

The layout of the MPBXs follows the logic for the temperature sensors (see Table 3-1 and Figures 1-3 and 3-1). The emphasis of instrumentation above the drift will concentrate measurements where deformation from heating and gravity are expected to be in the same direction, giving the strongest signals. In addition to the MPBXs installed into the heated region from the HD and the observation drift, two long MPBX boreholes will be drilled from the connecting drift, a few meters beyond each rib of the HD, at an elevation about a meter higher than the drift crown. These boreholes will allow measurement of axial extension of the heated rock, as well as using the plane of symmetry as means to identify the effects of heterogeneity.

Two other MPBXs will be installed in the Plate Heating Test niche, one on the heated and one on the ambient temperature side of the flatjacks. In addition, two ambient temperature MPBXs will be installed at the junction of the connecting drift and HD (one upward and one away from the HD); these instruments will provide ambient data useful for interpretation of the heated data. Two similar MPBXs will be installed at the junction of the observation and connecting drifts. In both cases, the vertical MPBX borehole was also used as a means to measure the amount of non-lithophysal rock above the HD to ensure proper vertical location of the HD.

6.1.6 Hydrological Measurements

Direct measurement of water content of the rock is more difficult than measuring temperature. Three methods are being incorporated in the DST: neutron logging, ERT, and GPR. Direct measurement of air humidity in sealed boreholes will be conducted with electrical impedance. Because of expense and reliability, these measurement locations will be much less dense than temperature measurement locations.

Neutron logging can be done to measure volume-averaged saturation at locations along boreholes accessible by personnel. In practice, the test geometry greatly limits this technique. Neutron logging boreholes are being installed from the observation drift in two planes. Consideration was given to additional boreholes drilled from the connecting drift, but these boreholes were eliminated in an engineering tradeoff that added temperature boreholes in the roof and floor of the drift. It was concluded that this tradeoff was warranted because of the greater density of measurements afforded by the temperature boreholes and the reduced risk. Long longitudinal neutron logging boreholes would be difficult to drill straight enough for the instrument, and a radioactive source stuck in a heated borehole is undesirable. In addition, these long boreholes pose significant risk of physical interference with rockbolt boreholes and other instrument boreholes. Also, they would need to be drilled in an inclined fashion to reach regions of interest, thus losing the symmetry advantage.

The second method of measuring saturation is ERT. This method will be employed extensively, from seven planes perpendicular to the drift axis (five installed from the HD and two installed from the observation drift). Interaction between segments of these planes will allow characterization of the rock saturation on a volumetric basis. This diagnostic technique is anticipated to be sensitive to metallic rockbolts and fractures in the rock; thus, interpretation of the data is not straightforward. However, rockbolts and fractures are stationary in time and space while the saturation distribution is expected to evolve with time; thus, this measurement technique can detect saturation provided the proper precautions are taken. It is anticipated that the ERT experience obtained in the DST will be useful in the design of a performance confirmation instrumentation network for the repository.

The third method of estimating water content changes in the rock mass is by high resolution, cross-hole radar profiling data. The sensitivity of radar measurements to even very slight changes in water saturation suggests the data collection methodology is suitable. GPR will be applied in a cross-hole/tomographic sense in the neutron logging boreholes.

6.1.7 Chemical Measurements

Measurement of the chemical evolution of water and minerals requires the ability to take samples during the test. Two planes will be instrumented using boreholes drilled from the observation drift. Each plane will include five boreholes, three above the HD and two below it. The locations of these boreholes, and the instruments within them, are based on the predictions of condensation conditions.

6.2 THERMAL

The three-dimensional spatial distribution and temporal variation of temperature, thermal conductivity, and thermal diffusivity in the local rock mass (for both the SHT and DST) will be determined.

6.2.1 Temperatures

The range of temperatures to be measured depends on location of the measurement and the duration of heating. The greatest range in temperature will be encountered in the vicinity of the heat sources (i.e., drift wing heaters). In these regions, the range of temperature to be measured will be from ambient to about 350°C. The temperature range will be more clearly defined, especially in the DST, when scoping model calculations are more mature. To properly cover the expected range of temperature, sensors with the capability of measuring temperatures to at least 350°C will be used. Calibrations of the RTDs and thermocouples will be conducted to ensure proper measurement of temperature for the range of temperature and thermal gradients anticipated in the SHT and the DST.

In the ESF Thermal Test, the spatial distribution of the relative changes in temperature is more important than the absolute temperature itself. The precision of the temperature measurement is required to be approximately 1°C. The accuracy of the temperature measurement is required to be approximately 2°C. Accuracy is a measure of conformity to a standard; whereas precision is a measure of exactness. For example, a measurement of temperature may be quite precise in that it can be replicated within a small tolerance, but these measurements could be considered inaccurate if the temperature sensor was not calibrated properly. The spatial density of sensors along an instrument borehole will be higher in regions where greater thermal gradients are expected. The spatial density will also be higher in regions where transition between dryout and condensation is expected to develop during the tests. Measured temperatures will also be used to determine thermal compensation requirements for other instrumentation.

RTDs, high temperature thermistors, and thermocouples can be used to measure temperature. These types of sensors are commercially available, can cover the expected temperature range, and are reliable for long-term monitoring. Thermocouples and RTDs will be used for temperature measurements within the rock mass for the DST. Thermocouples and thermistors will also be used in the DST, determination of temperature compensation on other instrumentation and for temperature

measurements on the rock surface and in the ambient air. The thermocouples used for the rock mass will be Type-K (chromel-alumel, nickel-chromium, and nickel-aluminum) encased in a stainless steel sheath creating a thermocouple probe. The thermocouple probes will be grouted into the boreholes. Individual Type-K thermocouples will be attached to the rock surface, the insulation, and placed in the ambient air in the DST. Type-K thermocouples were selected because of their wide temperature range and linearity. For the DST, many of the mechanical measurements will include thermal compensation. These temperature measurements will typically be made with Type-K thermocouples and thermistors. However, the type of temperature-measuring device to be used will be determined after additional instrumentation design.

The method of installing RTD temperature sensors in a borehole will be similar to that described by Lin et al. (1991). Temperature sensors will be bundled together with pre-determined spacing between sensor tips (Figure 6-1). High temperature sealant will be used to seal the space between sensors within a bundle so that the bundle will not become a pathway for fluid during the test. The measuring tip of each sensor will be slightly bent away from the bundle so that the effect of the bundle itself on the temperature measurement will be minimized. Centralizers will be installed at several locations along the bundle to keep the bundle near the center of the borehole. After the bundle is positioned in the borehole, cement grout, or any borehole sealant deemed appropriate by the scientist in charge, will be pumped into the borehole to seal the annular space between the bundle and the borehole wall. The grouting will be done in two stages to minimize the invasion of grout into fractures. In the first stage, the borehole is swiped with grout to seal the surface and prevent grout from entering fractures when the borehole is grouted. In the second stage, the instrument string is placed in the borehole and the borehole is filled with grout. In this method of installation, the sensors cannot be removed for recalibration.

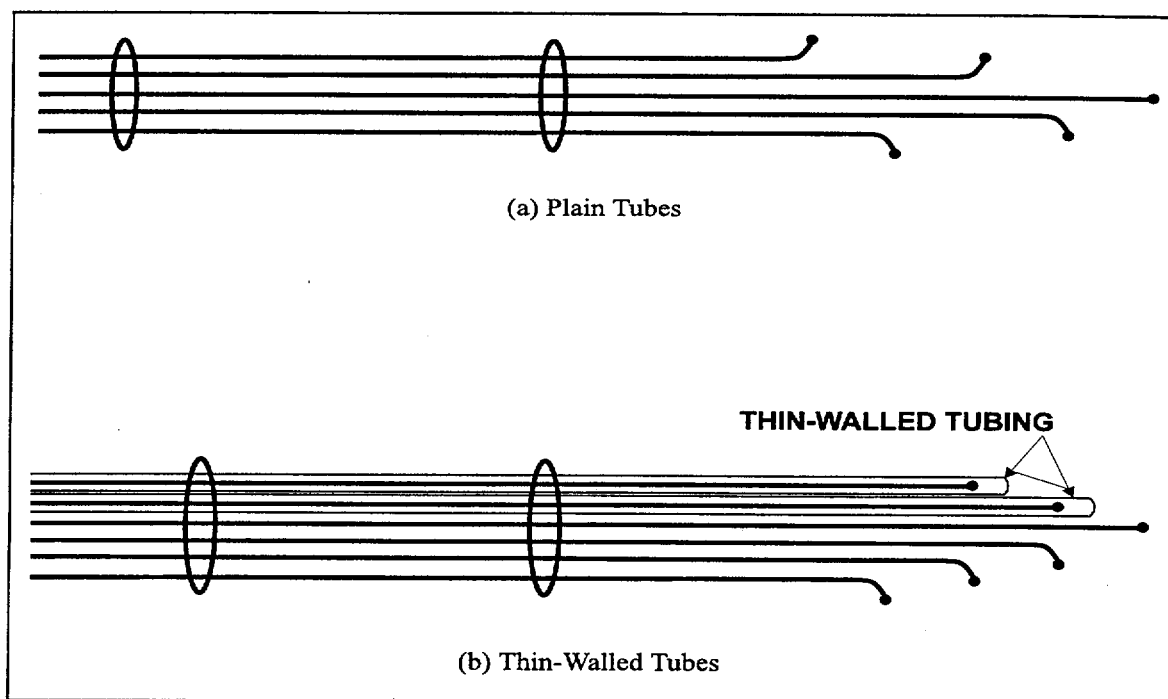


Figure 6-1. Temperature Sensors in Plain and Thin Walled Tubes

Another method of installing RTD temperature sensors is to install a bundle of thin-wall small diameter tubes in a borehole, seal the annular space with grout, and insert one sensor in each tube (Figure 6-1). This method allows replacement of malfunctioning sensors and removal of sensors from the borehole for real-time calibration during the test.

Thermocouple probes are easily installed in one step. The probe is inserted and grouted using a grout tube attached to the probe. The boreholes for the temperature measurement will be about 7.5 to 10-cm in diameter. The boreholes do not have to be straight, as long as the sensor bundle or probe can be installed and grout/sealant can be pumped into them. However, the as-built locations need to be determined within 1 to 2 cm. Fracture distribution within each borehole will also be determined. This information will be needed for the analysis of the temperature data. The boreholes will be arranged to ensure three-dimensional measurement of the thermal field.

6.2.2 Thermal Conductivity and Thermal Diffusivity

Determination of thermal properties is needed for test design and data interpretation. Some of the Tptpmn thermal properties, such as thermal expansion coefficients, thermal conductivity, and heat capacity, have been determined in the laboratory on small samples. Rock mass in situ thermal properties are needed for understanding the coupled TMHC processes. Specifically, in situ thermal conductivity and diffusivity are needed to determine the effect of fractures on thermal conduction.

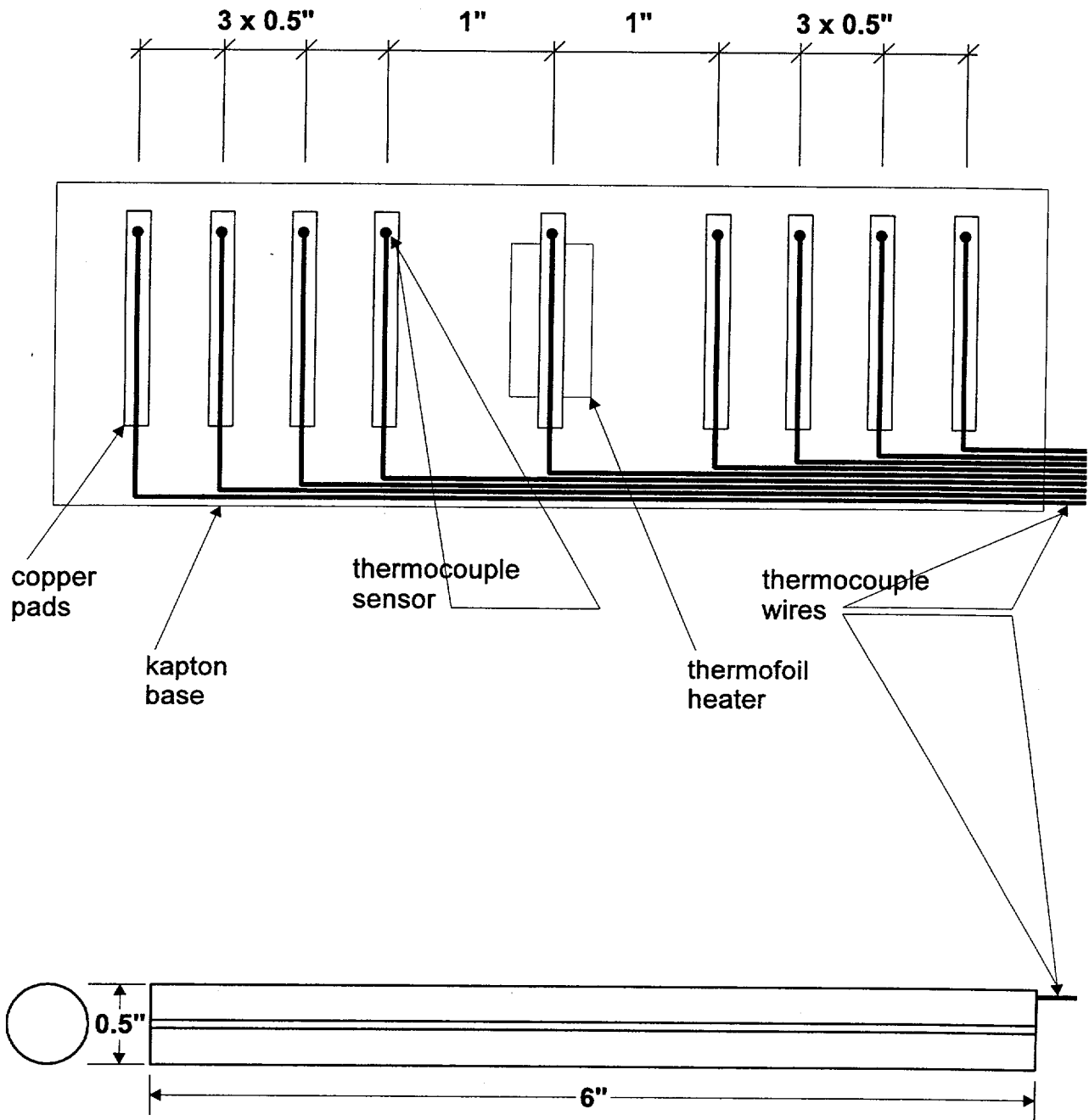
A thermal probe was developed at the University of Nevada, Reno, to determine in situ thermal conductivity and thermal diffusivity. The probe is called rapid estimation of thermal conductivity (**k**) and thermal diffusivity (α) or REKA. REKA is a self-contained probe consisting of a heat source and 16 temperature sensors. During measurements, a small amount of heat, about 2 watts, is transferred to the rock and temperature differences are measured. The accuracy of the measured thermal conductivity and diffusivity is estimated to be about 5 percent. The REKA probe assumes the rock will behave in a homogenous, isotropic manner, which may not be the case. Nonetheless, its application is valid since more sophisticated measurement devices do not exist. Also, any error introduced during the interpretation of the data attributed to the presence of nonhomogeneous and anisotropic conditions is considered acceptable.

When assembled, a REKA probe is a rigid cylinder of approximately 0.5 cm in diameter and about 60 cm in length. The REKA probe can be grouted in a borehole of approximately 1.2 cm in diameter (Figure 6-2). The borehole has to be sufficiently straight to allow probe insertion.

6.3 MECHANICAL

TM behavior of the potential repository host rock must be understood for several functions. Repository design and preclosure worker safety analyses require TM data for determining the emplacement drift stability and the performance of the ground support system. The stability of the HD and performance of the ground support system need to be investigated because they affect the preclosure performance and retrievability of the waste packages in a potential repository. For these purposes both stress and displacement in the rock mass surrounding the HD will be monitored during the test (before, during, and after the heating). More attention will be paid to the displacement in the

FOIL LAYOUT VIEW



FORMED TUBULAR PROBE

Figure 6-2. Sketch of REKA Probe

entire rock mass. In addition, in the DST, the mechanical properties of the rock mass will be determined by using a plate loading method in a narrow niche, which will be constructed outside of the heated region. The rock mass will be stressed by the flatjacks and its deformation will be measured by displacement measurement devices such as extensometers.

Repository design, waste package design, and postclosure performance assessment require information about the near field environment, in which the TM behaviors can affect drift stability and near field hydrology. The mechanical measurements to be made in the ESF Thermal Test for these objectives include displacement, stress, and acoustic properties. These are discussed below in separate sections.

6.3.1 Displacement Measurement

Extensometers will be used to measure the displacement in the rock mass. The expected range of displacement will be from zero to several mm. The accuracy required for the purpose of studying rock mass stability is about 0.1 mm, which is also the accuracy that can be achieved by standard MPBXs. These instruments will be installed in boreholes and on the drift walls. Available MPBXs include rod, wire, and optical extensometers. The mechanical displacement measuring devices (the first two types of extensometers) have been used extensively in geotechnical applications. The effects of temperature on thermal expansion of the instruments (i.e., extension rods) must be determined. The extensometer boreholes need to be sufficiently straight for proper installation of the MPBXs.

6.3.2 Coupled Thermal-Mechanical Measurement

The contribution of TM behavior to the coupled TMHC processes is mainly through the thermal expansions that occur as the rock mass is heated. This results in a change in porosity and permeability of the rock mass from fracture aperture changes. Porosity and permeability changes can also be caused by thermal fracturing in the matrix and relative displacements in fractures. Two types of measurements will be conducted to monitor the change in porosity and permeability: displacement measurement in boreholes, focusing on the displacement of fractures, and acoustic emission and velocity measurements. The displacement measurement in boreholes is similar to that described in Subsection 6.3.1, except that more attention will be paid to monitoring the displacement across fractures and in the matrix separately. The instruments to be used and the borehole requirements will be the same as in Subsection 6.3.1. The anchors of the extensometers will be located according to the location and orientation of fractures in each borehole. Also, bulk rock mass displacements can be correlated to bulk porosity and permeability changes in a broad manner.

6.3.3 Modulus Measurement

The measuring systems for the plate loading test conducted in conjunction with the DST include flatjacks, hydraulic pump and pressure manifold, pressure transducers, thermocouples, MPBXs, wire extensometers, and blanket heaters. The plate loading test consists of a double-acting setup in which two flatjacks apply identical loads to both the ambient and thermally perturbed walls of the plate loading niche. The pressure in the flatjacks is controlled using a pressure manifold that ensures identical pressure in each of the flatjacks, and pressure is monitored using pressure transducers. The

displacement of the rock mass under both sides of the loading system is monitored using short (2- to 3-m long) MPBXs installed in boreholes drilled parallel to the loading direction. A wire extensometer monitors the deformation of the reaction frame within the plate loading niche. A blanket heater is applied on the thermally perturbed side of the niche to provide a uniform temperature gradient there. Temperatures on the surface and within the rock mass are monitored using thermocouples. Typically, plate loading tests are conducted by cycling the load over a prescribed range and monitoring the displacement and flatjack pressure histories.

6.3.4 Acoustic Emissions/Seismic Imaging Measurements

Previous work at Stripa and the Climax mine (Majer et al. 1981, Majer and McEvilly 1984) indicated that thermal-induced stresses cause acoustic emission activity. The acoustic emission is a volumetric measure of the stress distribution and rock quality and can augment other deformation measuring techniques. Both the temporal and spatial distribution of the activity will be measured, analyzed, and located. In addition, acoustic emission activity serves as point sources to provide a means to measure the change in seismic wave propagation characteristics (P- and S-wave velocity and amplitude variations) as functions of time. A three-dimensional image of the wave propagation characteristics will be developed from the results of the passive imaging and from utilizing active sources. The three-dimensional image will be used to infer rate, location, and amount of induced fracturing, and stress relief on pre-existing fractures versus new fractures. An array of 16 accelerometers will be emplaced around the HD in 16 of the RTD boreholes (138, 139, 140, 142, 143, 144, 159, 160, 161, 163, 164, 165, 171, 172, 174, 175). Active piezoelectric sources will be placed in boreholes 139, 143, 160, and 164. These sources will be activated routinely (anticipated to be once a day) to monitor rock property changes as heating progresses. The frequency range monitored will be 100 Hz to 15,000 Hz. The sensitivity of the array was based on experience obtained from the Stripa and Climax heater tests.

The measuring system for the Acoustic Emission/Seismic imaging measurements consists of high temperature industrial accelerometers for passive monitoring and piezoelectric transducers for active monitoring. The sensors are commercially available. A model rated by manufacturer to operate up to 150°C is deemed adequate based on the locations of the sensors and pre-test simulations of the DST giving the anticipated temperatures after four years of heating.

6.4 HYDROLOGICAL

Spatial distribution and temporal variation of hydrological properties in the rock mass will be determined during the tests. Three parameters related to the hydrological properties in the rock mass will be determined; they are gas/air pressure, relative humidity, and liquid water saturation. These measurements are described in the following sections.

6.4.1 Gas/Air Pressure

Gas/air pressure will be measured both in sealed boreholes and in alcoves/drifts/tunnels. In a sealed borehole, the gas/air pressure will be measured using a gas pressure transducer (see Figure 6-3). Barometric transducers will be used to measure the atmospheric pressure in alcoves, drifts, and tunnels. The range of gas pressure to be expected is from about 0.05 MPa to about 0.5 MPa. This

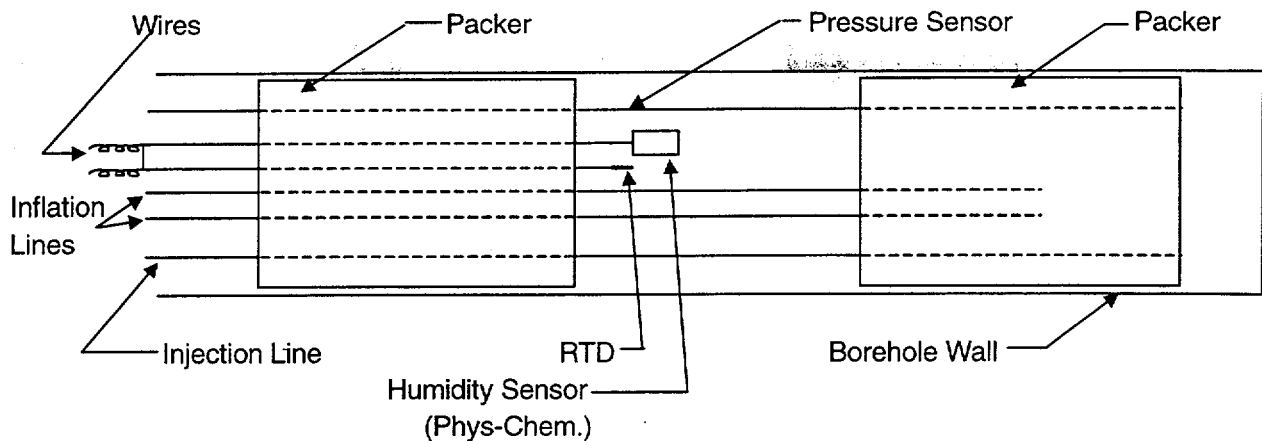


Figure 6-3. Schematic of a Packer System with Humidity Sensors and Pressure Transducers

estimate is based on the results obtained in the G-Tunnel test (Lin 1991). A more definitive range of pressure may be determined when detailed scoping model calculations are conducted. The precision of the pressure measurement should be about 1 percent of the measured pressure. The gas pressure will be measured at strategic locations so that the effect of pressure gradient on the moisture movement can be determined. Those locations include the dryout region, the condensation region, and the transient region between them. Scoping model calculations will be conducted to determine those locations with respect to the heaters. Several measurement points will be established for each strategic location, to allow for uncertainty in the model calculations.

There are several methods for measuring the gas pressure in a rock mass. Each of these methods involves using a pressure transducer. The method selected for the DST installation involves sealing a pressure line in a borehole with its open end located at a measuring point, and connecting a pressure transducer at the other end of the pressure line. This method requires only ambient gas pressure transducers that have long-term reliability. This method also requires verification that the pressure measured at one end of a pressure line is the same as at the other end especially when the temperature at the measurement location (the open-end of the pressure line) is different from that where the pressure transducer is located. However, there is no reason to doubt the gas pressure within a pressure line, with an inner diameter of approximately 3 mm, will reach an equilibrium in the typically slow responses of a rock mass to the thermal disturbance from an in situ thermal test. Finally, this method will be designed properly to avoid complications including those stemming from moisture accumulation.

The boreholes to be used for the gas pressure measurement will be from 7.5 to 10 cm in diameter. The borehole is required to be sufficiently straight so that a packer assembly, which is usually a few meters in length, can be installed. The gas pressure measurement can share a borehole with other measurements, such as humidity, which is described in Subsection 6.4.2.

6.4.2 Humidity

Relative humidity is an important parameter to measure during thermal testing because it is an indicator of rock saturation. In a sealed airspace in contact with a rock mass, the moisture potential of the rock mass will come into equilibrium with the moisture potential of the air, as described by the Kelvin Equation:

$$\mu = \rho RT/M \ln(\text{RH})$$

where

| | | |
|--------|---|--|
| μ | = | moisture potential, Pa |
| ρ | = | density of the fluid, gm m ⁻³ |
| R | = | the universal gas constant, 8.3145 Pa m ³ mol ⁻¹ K ⁻¹ |
| T | = | temperature, K |
| M | = | gm molar weight of the fluid, gm mol ⁻¹ |
| RH | = | relative humidity. |

This equation indicates that the relative humidity is the ratio of the partial pressure of water vapor in the rock pores and the saturated vapor pressure of the bulk liquid. The measurement of a reduction of water vapor partial pressure is important because it indicates drying of the rock mass.

The humidity sensors (humicaps) used in the SHT are commercially available and measure changes in electrical capacitance due to humidity. However, the capacitance design does not give a strong enough signal when the borehole length is beyond 10 m. The hydrology boreholes in the DST are 40 m long; therefore, an alternative design measuring impedance has been developed. Relative humidity sensors in the DST have been developed based on the commercially available Phys-Chem Scientific EMD-2000 Micro Relative Humidity Sensor (see Figure 6-3). The Phys-Chem humidity sensor changes electrical properties due to water vapor absorption on a polyelectrolyte, which has been deposited over interdigitated gold terminals on an alumina substrate. The sensor impedance changes over five orders of magnitude from 0 to 100 percent relative humidity. For installation in the DST hydrology boreholes (Figure 6-3), the Phys-Chem humidity sensor is mounted in a Teflon enclosure at the end of each pneumatic packer. Each sensor terminal is connected to an RG-178 shielded coaxial cable which runs to drive electronics located near the collar of each borehole. The shields are allowed to float downhole and are grounded at the electronic circuit board. The Phys-Chem humidity sensor is operated at approximately 2,500 Hz with a ± 5 volt drive signal. The circuit output is an analog signal which varies from 0 to 3 Volts.

The Phys-Chem humidity sensor and its drive electronics are calibrated using standard salt solutions for ambient temperature calibration. Calibration at an elevated temperature is performed within a controlled environmental chamber. To maintain known psychrometric conditions within the environmental chamber, streams of water and air are injected at controlled temperatures. Air flow is controlled using mass flow controllers prior to heating the air, and the water flow is controlled using a high precision piston pump. PID controllers ensure the temperature stability of the gas mixture entering the test chamber.

6.4.3 Liquid Water Saturation

Spatial distribution and temporal variation of liquid water saturation level in the rock mass will be determined to monitor the dehydration-rehydration processes caused by the heat in the thermal tests. The liquid water saturation level will be determined in two modes: line measurement along a borehole using neutron logging, and two-dimensional sectional and three-dimensional volumetric imaging. Two- or three-dimensional imaging is accomplished using ERT which measures the variation of the electric properties of rock. Figure 6-4 shows a diagram of neutron logging in a borehole. The locations of these measurements will be determined by scoping model calculations so that the results will be most effective in understanding the dryout and condensation processes.

The precision of determining moisture content using neutron logging is estimated to be approximately 5 percent in water saturation level for both ambient and elevated (100°C) temperature. Currently, calibration of neutron logging is in progress to further verify that 5 percent precision can be obtained for temperatures ranging from ambient to 100°C.

Based on the calibration curves (determined in the laboratory) of electrical resistivity as a function of water saturation, the correlation of water saturation level to electrical resistivity has about 1 percent precision in saturation level when the saturation level is below 40 percent. For saturation levels greater than 40 percent, the precision degrades to about 10 to 20 percent. The ERT precision is about 10 to 20 percent. Therefore, the precision of determining water saturation level using ERT is about 10 to 20 percent when the saturation level is below 40 percent, and 20 to 30 percent when the saturation level is greater than 40 percent. The application of ERT precision to field measurements is not well understood. This problem is mostly resolved with multiplicity of measurement devices which include ERT, GPR, and neutron logging.

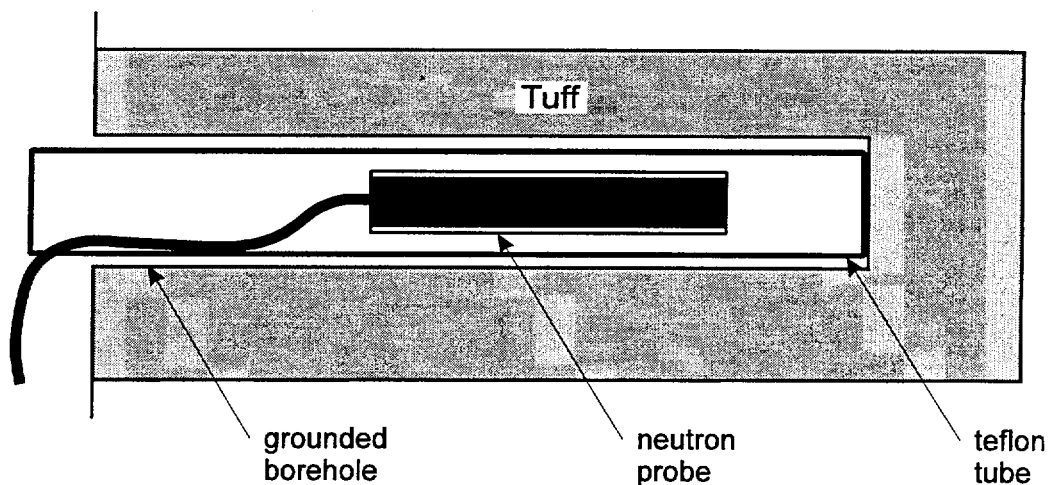


Figure 6-4. Neutron Measurement Boreholes

Figure 6-5 shows the configuration of the ERT boreholes and the measurement techniques. The ERT was used in a low, electrically conductive rock (Tptpmn) for the first time in the SHT. Because of the low conductivity, specially engineered techniques are required in the installation of the electrodes. ERT is sensitive to electrically conductive objects in contact with the rock mass to be imaged. The data reduction techniques for ERT are advanced but their applicability to the unsaturated Topopah Spring tuff requires verification. The boreholes to be used for ERT will be similar to those for other measurements, such as temperature and humidity. The boreholes are 7.5 to 10 cm in diameter.

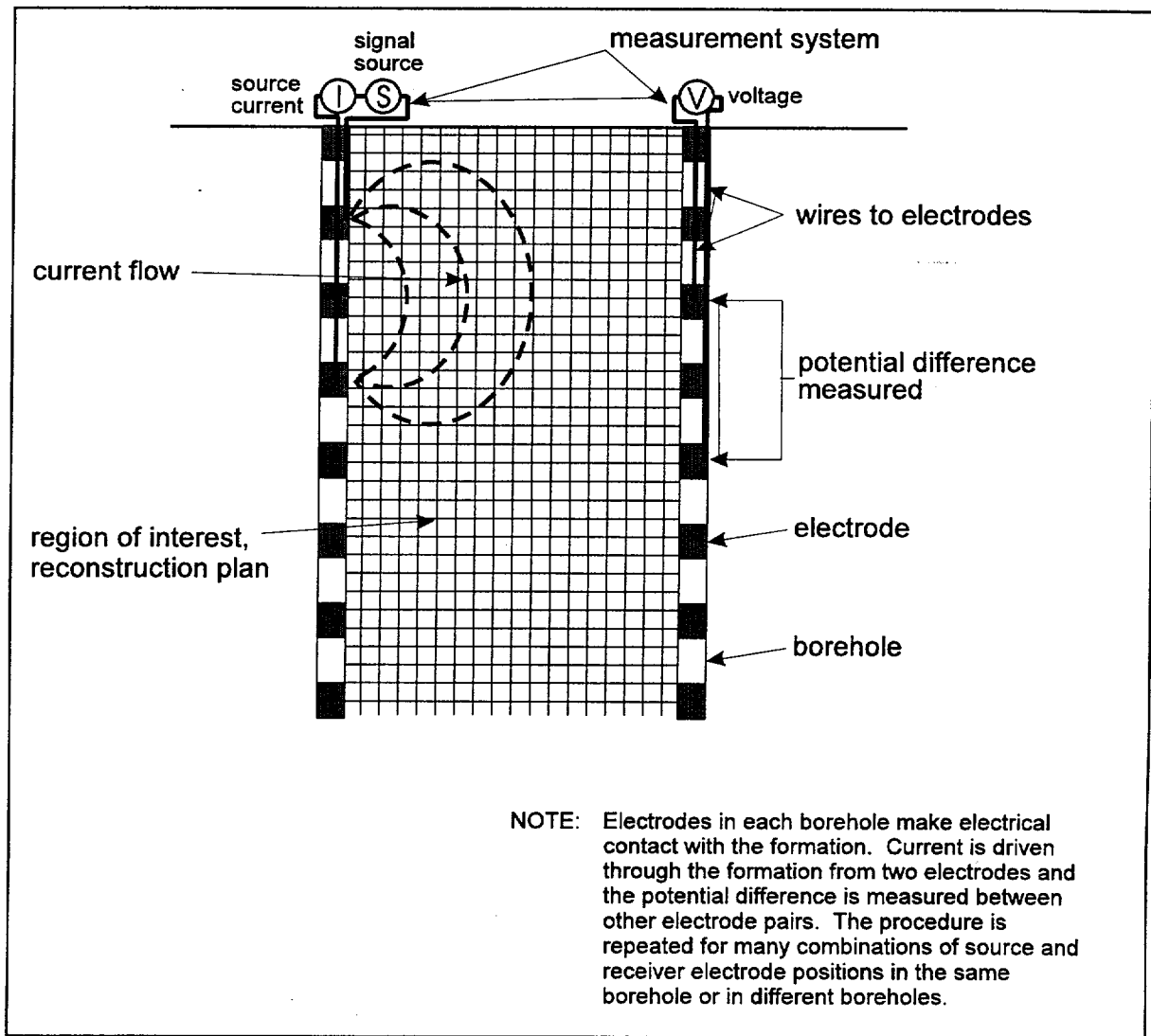


Figure 6-5. Schematic Diagram Showing Data Collection Approach for ERT Measurements

Although neutron logging is a well established and reliable method of moisture measurement in the field, it is well known that the depth of measurement in neutron logging is limited to a few inches from the borehole wall. Another method which provides greater depth of measurement is GPR. However, GPR is an indirect measurement that requires calibration of the measured dielectric parameter to moisture content and temperature. Downhole GPR measurements, in which the receiving antenna is run into the borehole and the transmitting antenna is moved along the surface, have been conducted successfully in sites located in Idaho. Antennae suitable for use in neutron boreholes are available.

For the DST, radar will be applied in a cross-borehole/tomographic sense across the heated region to derive temporal changes in the dielectric properties of the rock. This information will be used to infer the temporal and spatial saturation changes as heating progresses relative to the location of fractures. The method involves placing radar transmitter in one borehole and a receiver in another to record the time and amplitude of the radar signals at various positions along the boreholes. The boreholes were selected to image an entire cross-section of the heated region across two different planes intersecting the HD (Boreholes 47 through 51 and 64 through 68).

Measurements will be made periodically during the heating phase. Both 100 MHZ and 200 MHZ will be used to optimize the resolution and depth of penetration. The frequency selection was based on prototype tests in the SHTs. Laboratory measurements of temperature and moisture content will be performed on several different cores to calibrate the thermal and moisture effects on the dielectric constant.

The radar data will be acquired using the Sensors and Software pulse EKKO GPR system equipped with prototype 100 (or 200) MHZ center frequency borehole antennas. This system consists of six basic components; namely, a pair of identical antennas (one for transmitting, and one for receiving), a transmitter electronics unit, a receiver electronics unit, a control console, and a personal computer acting as a recording system and data storage unit.

In summary, the measurement of moisture content throughout the heated rock mass, including the dryout zone, is complex; consequently, various techniques will be used including ERT, neutron logging, and GPR. The combination of the usage of a wide variety of measuring techniques and the density of devices to be installed in the local rock mass provides extra confidence that the measured moisture content will be representative to the extent practical.

6.5 CHEMICAL

The water chemistry in the near-field environment will play an important role in the performance of waste package materials and the transport of radionuclides through the altered zone of a repository. The water chemistry will be affected by the rock-water interaction, caused by TH processes, and by introduced materials such as cement grout, ground support materials, and waste package materials. Chemical measurements, which will determine the effect of rock-water interaction and introduced materials in the near-field environment, are described in this section.

6.5.1 Rock-Water Interaction

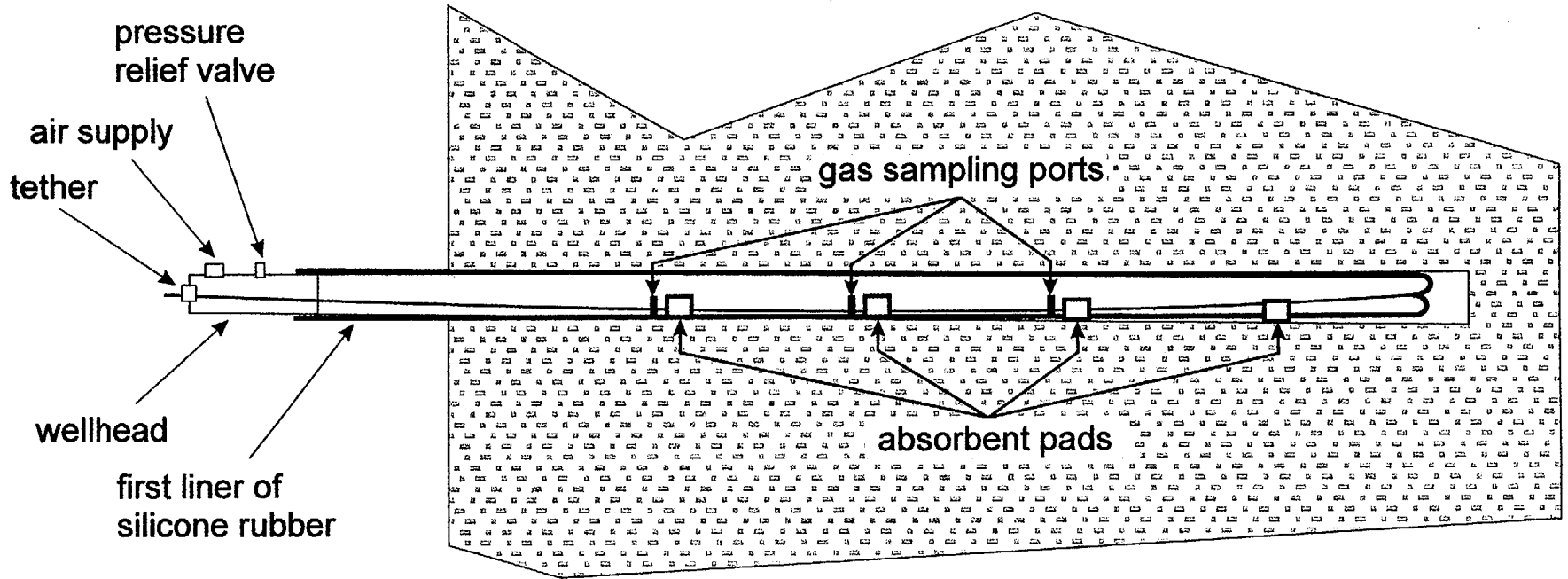
The host rock for the potential nuclear waste repository at Yucca Mountain is partially saturated with water. However, when heat from radioactive waste is introduced into the rock mass, the original in situ pore water will be mobilized by some or all of the following processes: evaporation/boiling, flow along thermal/gas pressure gradients, binary diffusion, and buoyant gas phase convection. Moisture mobilization will mobilize the pore water from the high temperature region near heat sources to regions away from the heat sources. Some of the mobilized (or other in situ) water may return to the heated region by gravity (from above) or capillary forces (from any direction). Rock-water interaction is likely to be intensified in regions where the saturation level is increased due to the moisture movement. The rock-water interaction will be further enhanced as the temperature in the water and rock mass is elevated. This rock-water interaction may affect the hydrological properties of the rock mass, as observed in the laboratory by Lin et al. (1995). The rock-water interaction will also change the chemistry of the pore water.

Pore water and gas will be measured in situ at several locations as functions of time in the DST. Chemical and isotopic data will be generated from laboratory analyses of water periodically collected from several locations in the DST block. The Science Engineering Associates Membrane In Situ Sampling Technique (SEAMIST) liner, using high temperature membrane material, will be used to seal the boreholes. Pore-fluid sampling devices (absorbent pads) will be installed on the SEAMIST system (ten per borehole) which is shown in Figure 6-6. The wet absorbent pad will be removed from the borehole to recover water. This process of fluid sampling should not change the hydrology and water chemistry significantly. In addition, gas sampling ports will be located at three pad locations. This will allow sampling of gas and analysis of gas-phased composition and rate of gas generation for the major gas-phase species (i.e., O_2 , CO_2 , and CH_4). Finally, water and gas sampling will also be conducted periodically in packer intervals of hydrology holes (if and when water is found) and analyzed in the laboratory. In addition to fluid sampling in the SEAMIST system, water and gas can also be collected from different zones isolated by high temperature packers in the twelve hydrology holes targeted for air-permeability testing.

6.5.2 Waste Package Materials

The performance of waste package materials will be tested by two means. Coupons of candidate waste package materials will be placed at strategic locations such as hot/dry locations near heaters and warm/wet regions in the condensation zones. Up to 192 coupons of candidate waste package materials may be mounted on either side of packers in the 12 hydrology boreholes to evaluate corrosion potential of the material in various environments without any instrumentation, and placed at various TH zones, such as dryout zone and condensate zone. The coupons will be tested before and after the DST to evaluate their corrosion potential.

A candidate corrosion allowance waste package material (or similar materials) was used to construct the floor heater to be emplaced in the HD of the DST. This will provide a full-scale in situ test of the performance of the materials. The floor heater, as described in Section 8, will be examined before and after the thermal test for corrosion. It is likely that some of the materials (floor heaters and coupons) will corrode slightly.



m:\data\123\wagrey_1.cdr, 7/10/97

Figure 6-6. SEAMIST System for Chemical Sensors and Sampling

6.5.3 Introduced Materials

Introduced materials include all artificial and natural materials introduced into the ESF during the construction and testing phases. The reaction of the introduced materials may have significant effects on the chemistry of the near-field environment. The introduced materials include, but are not limited to, grout materials, ground-support materials, testing equipment/instrumentation, and exhaust of diesel fuel used in powering equipment. The introduced materials to be tested in the DST are those most likely to remain in the test region during the entire test duration. Passive testing methods, such as visual observations with the HD camera, will be used to observe the introduced materials. Samples of the introduced materials will be examined in the laboratory before and after the tests. Samples of the rocks adjacent to the introduced materials will also be tested in the laboratory and observed in the field before and after the tests.

6.6 MISCELLANEOUS

6.6.1 Moisture Introduced/Extracted During Drilling

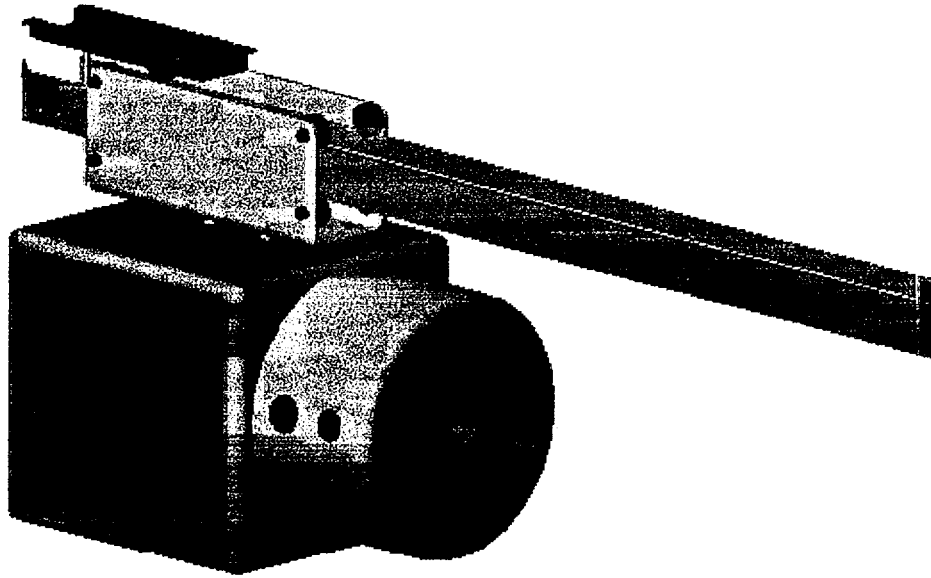
Water was used in the drilling of boreholes in the ESF Thermal Test. Drillers measured and recorded the amount of water used in drilling each borehole. It is standard practice to keep logs of water used during drilling which provides for an accounting of the net water loss. Although moisture introduced during the drilling of boreholes will be measured, it is not a major concern because the moisture content of the local rock mass will be measured immediately prior to heater turn-on. These baseline measurements will come from the last array of planned neutron logging, ERT, and GPR devices (see Subsection 6.4.3). Furthermore, it is estimated that a total loss of drilling fluid into the rock mass, which is highly unlikely, would increase the moisture content by less than 3 percent (Datta 1996a).

6.6.2 Ventilation

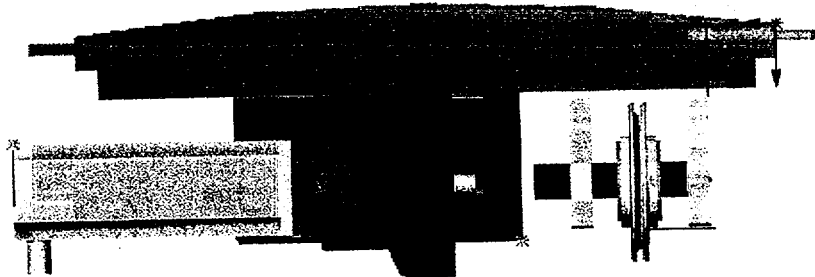
The ESF construction group will monitor the ventilation system in the ESF Thermal Test area. The flow rate will be metered and the relative humidity measured (humidity sensor) in both the inlet air and exhaust air in the ventilation system will be measured and recorded.

6.6.3 Visual (Video Camera) and Remote Observations

A window will be installed in the thermal bulkhead of the HD. Visual observation of the HD will be made through that window. In addition, a remotely controlled camera (see Figure 6-7) will be capable of entering the HD so that pictures, both infrared and visible light, can be recorded. The camera system will be housed in an approximate 60-cm cubic structure and consist of two video cameras and an infrared camera. One of the video cameras will be mounted in the front of the camera system with a fixed focal length. The other video camera and the infrared camera will have zoom lenses and will be mounted on a swivel. The camera system will operate along an aluminum



(a) Remote Unit with Track



(b) Remote Unit with Track

Figure 6-7. Remote Controlled Camera Designed for the Heated Drift

tract fixed to the roof of the HD. The camera system will be capable of operating in a 300°C environment for up to 45 minutes. Insulation and dry-ice coolant will provide thermal protection. The camera system will be operated remotely. Repairs are anticipated to be easy since the camera system will be stored outside the HD when not in use. The camera system will be operated as needed to ensure proper observation of thermal and visual images within the HD.

6.6.4 Vapor/Air Flow in the Heated Drift

It is not considered necessary for the HD to be sealed gas-tight, but measurement of the relative humidity and total air pressure in the HD will benefit model calculations. Humidity sensors will be used to monitor the relative humidity at the elevated temperature environment in the HD. High temperature gas pressure transducers will be used to measure the total air pressure in sealed boreholes. Pressure transducers, humidity sensors, and RTDs will also be located in three distinct locations in the HD. In addition, the relative humidity and air flow rate from the drift through the bulkhead pressure relief system will be measured using instruments similar to those used in the ventilation system.

6.6.5 Video Logs of Boreholes

Before the start of the DST, it is anticipated that all but 10 of the 147 boreholes in the DST will be logged with video. These videos provide both qualitative and quantitative evaluations of fracture characteristics in the DST block. This fracture information can be combined with air-permeability testing (see Section 4.1.2.3) and fracture mapping of the drift surface (see Section 4.1.2.2) to develop a more complete understanding of fracture and permeability conditions in the DST block.

Boreholes were videoed based on Los Alamos National Laboratories procedure LANL-EES-13-DP-613, RO. The entire system consists of the downhole video camera system, monitor, and VCR. The TV/VCR was first configured to record, and then the camera was inserted into the borehole. The camera was paused as needed. The video tape was viewed to ensure visibility and adequacy. The process was repeated if the video information was inadequate. Any unusable entries or video runs were identified as inadequate. The following information was recorded in the scientific notebook: borehole identifier, date, M&TE serial numbers if applicable, the location of the zero datum point, traceability between the notebook and the video, depth correction measurements if applicable, and total depth.

7. CONSTRUCTION

Construction requirements for the DST pertain largely to drift and alcove excavation; drilling, coring, and instrumentation of boreholes; and procurement and installation of the various ground support systems to be tested. Figure 3-1 shows the plan view of the DST including the observation and connecting drifts. Ground support, mainly rockbolts and welded wire mesh, for the DST facility is as stringent as that used in the ESF main drift and was based on rock quality estimates. In the DST, ground support is installed to test a cast-in-place concrete support system for repository emplacement drifts (CRWMS M&O 1996e).

The issue regarding the introduction of water during the drilling of boreholes for heaters and instrumentation has been addressed in a technical letter memorandum (Datta 1996a). Basically, conservative calculations indicate that the moisture content of the local rock mass will not increase more than 3 percent. Given this minimal perturbation and the provision to measure the moisture content of the local rock mass immediately prior to heater turn on, the use of water as a drilling fluid is not anticipated to affect the performance of the DST.

For ESF Testing Activities, the Construction Management Organization will provide a management interface between the Test Coordination Office (TCO) and ESF Constructor. The TCO will coordinate testing field activities with the Construction Management Organization which will ensure that all testing related support required of the ESF Constructor is provided.

The ESF Constructor will provide underground and surface labor, materials, and equipment to conduct scientific test operations in the Thermal Testing Facility and on the ESF pad as requested by the ESF Thermal Test Team and coordinated by the TCO. Scientific test operations include:

- Drilling activities
- Survey of borehole collar locations and orientation
- Grouting support
- Constructing a concrete liner test section
- Constructing a concrete invert
- Constructing two DCS/test equipment rooms
- Hanging cable tray
- Producing alcove survey as-constructed records
- Producing concrete and grout as-constructed records
- Providing appropriate ESF electrical power and communication for testing usage
- Providing appropriate surface facilities for equipment storage and checkout
- Transportation of equipment inside the ESF.

The ESF Constructor has the responsibility for ensuring a safe working site and the safety of all underground and ESF pad personnel.

7.1 OBSERVATION DRIFTS

The observation, connecting, and heated drifts (see Figure 3-1) were excavated with an alpine miner and/or drill and blasting. Conservative estimates have shown that the effects of drill and blasting

in the ESF Thermal Test Facility will not adversely impact the ESF Thermal Test (Datta 1996b and Lee 1997). Width and height are approximately 5 m for the constructed drifts. Primary construction activities include:

- Breakout from the main drift
- Excavation
- Geologic and Rock Mass Quality mapping
- Sampling
- Niches for DCS and Plate Loading Test.

7.2 DRIFT SCALE TEST

Figure 3-1 and Table 3-1 provides an overview of the plans and geometries for DST construction including the drifts and boreholes. Drilling of the instrumentation boreholes and the wing heater boreholes were started soon after the HD was mined. Boreholes were constructed by wet drilling because it is less expensive than dry drilling and more conducive to a highly active work environment such as exists during construction of the DST facility. Also, any additional moisture added to the rock mass from wet drilling will be included in the baseline (pre-test) measurements of moisture content. Coring provides samples for characterization of the test region and ensures better alignment. Most of the boreholes have a nominal 7.5 or 10 cm diameter. All activities generated from the FWP for the DST are subject to determination of importance evaluations.

The types of DST boreholes are shown schematically in Figure 1-3 and listed in Table 1-3 and below:

- Thermal
- Mechanical
- Hydrological
- Chemical.

All boreholes are cleaned to be free of debris so that instruments can be installed properly. Borehole imaging techniques are being used to record the fractures before instrument installation. If practical, boreholes were sealed after drilling. The sealing methods chosen depended on the function of each borehole. All boreholes are surveyed after their construction so that the location of instruments in them is accurately determined.

The bundles of temperature sensors installed in the temperature boreholes are somewhat flexible. Therefore, the temperature boreholes did not have to be as straight as the mechanical boreholes, but need to be straight enough that enough annular space would be left for grouting the entire length of the bundle. The mechanical MPBX boreholes needed to be straight enough so that the MPBX assembly, which is likely to be a rigid cylinder several meters long, would be properly installed.

The neutron tool is a rigid cylinder 30 to 60 cm in length. The neutron boreholes needed to be straight enough for the neutron tool to move freely within. Teflon tubes were installed in the neutron boreholes as liners. Although the teflon tubes are flexible, the boreholes needed to be straight enough so that annular space would be left for grouting the entire length of the liner to the rock. The

REKA probes are rigid cylinders about 1 to 2 m in length. The boreholes for the probe were constructed such that the probe could be installed and still leave enough annular space for grout/sealant along the entire length of the probe.

The SEAMISTs to be installed in the chemical boreholes are flexible so the boreholes do not have to be very straight. The wall in the chemical boreholes must be fairly smooth for sealing purposes. The packers installed in the hydrologic boreholes are rigid cylinders several meters long.

7.3 ANCILLARY ESF THERMAL TEST ACTIVITIES

Construction of ancillary ESF Thermal Test features includes the SDMT, Plate Loading Test alcove, site characterization boreholes, and the HD bulkhead. The performance criteria for SDMT boreholes drilled from the observation drift are listed below.

- Three boreholes were cored at a decline from horizontal, nominally 7.5-cm (3.0 in.) diameter and nominally 26.0-m (85.3 ft) long from the observation drift toward the HD, to allow for the installation of instrumentation to measure pre-test and post-test rock mass convergence, convergence rate, and displacement.
- Convergence pins were installed in the HD as excavation proceeded to allow for the measurement of roof-to-floor and wall-to-wall convergence.

The geometry of the Plate Loading Test alcove is a small, rectangular niche from the connecting drift, with geometry as follows: 6-m long, 3-m high, and 2-m wide. The Plate Loading Test is well located because the large forces (1 to 3 million pounds) imposed on the rock mass are not likely to affect the integrity of the rock because of the nearly three-dimensional confinement. Regardless of the technique chosen for the excavation of the Plate Loading Test alcove, excavation must be carefully controlled to limit rock damage.

Along the northern end of the connecting drift, site characterization boreholes that include a cluster of three hydrological boreholes nominally 7.5-cm (3.0 in.) diameter and nominally 20.0-m (65.6 ft) long, were drilled at a slight incline from horizontal for the measurement of air permeability, moisture content, water chemistry, and water potential. These three boreholes were cored with air as the drilling fluid.

A thermal bulkhead will be designed by the M&O architect/engineer to provide: safe personnel access to the HD, a partial thermal barrier, and visual observation of the HD during the DST. The bulkhead will be located 13.25 m from the centerline of the connecting drift, and constructed of plate steel, beams and insulation. The bulkhead will be equipped with a personnel access door such that access can be maintained for personnel and equipment prior to heater activation. The bulkhead will also be equipped with a camera passage door, viewports, and a self contained lighting system. Thermocouples, strain gages and flow meters will be located on the bulkhead for measurement of corresponding responses. All cables from the heaters and HD sensors will pass through the bulkhead to the DCS and power monitoring enclosures located in the connecting drift.

INTENTIONALLY LEFT BLANK

8. HEATING SYSTEMS

8.1 INTRODUCTION

Electrical heaters will be placed on the invert of the HD and in horizontal wing-heater boreholes for the DST. Scoping model calculations (see Section 5.2) have been conducted to determine heater specifications such as power output and duration (Buscheck and Nitao 1995, Buscheck et al. 1997, and Birkholzer and Tsang 1997). Criteria for determining the heater specifications include the maximum temperature in the HD, the volume of the rock mass to be heated, and the volume of the rock mass to be dried by heating. In addition to the heaters, the heating system will include a control system, which will control heater output in accordance with predetermined heating/cooling schedules. Even though problems from instantaneous heating did not develop in other thermal tests, the current plan for heater startup may include an incremental increase to full power over a 24-hour period if deemed necessary by the ESF Thermal Test Team. The following discussion describes the wing and floor heaters, heating controls, and heating/cooling plan.

The HD in the DST is nominally 47.5-m long and will house nine floor heaters along the centerline of the HD. Fifty wing heaters are uniformly spaced in 11.5-m boreholes drilled into the two sidewalls of the HD. The total heat output available for the floor and wing heaters will be approximately 68 kW and 143 kW, respectively. In four years of heating, this heater power (discussed in Section 8.2.2) will create a drying zone around the HD extending approximately 10 m into the surrounding rock. The maximum temperature in the drift wall will be kept within 200°C. The heating plan is discussed in Section 8.3. The heaters to be emplaced in the drift and the wing heater boreholes are described in the following sections.

8.2 HEATER DESCRIPTION

Figure 8-1 shows a plan view of the 9 floor heater and 50 wing heater locations. Specific detail of those two types of heaters are provided below.

8.2.1 Floor Canister Heaters

The floor (canister) heaters to be placed in the HD will consist of approximately 1.7-m diameter and 4.6-m long steel canisters housing 30 heaters (Figure 8-2). The heaters are mounted on the inside curved surface of the canisters evenly spaced along the circumference. This arrangement of the heaters is designed to minimize the temperature differential between the top and bottom surfaces of the canister due to convection. The end covers of the canisters have an opening for the passage of the heater lead wires. The canister heaters will be placed with a spacing of 0.6 m in the drift as shown in Figure 8-1.

Each of the thirty heaters in each canister is a multi-zone heater with heat output of 250 watts at 208 volts. This power design for the nine floor (canister) heaters results in a total power output of 68 kW. The heaters have one primary and one back-up heating element wired independently. Each of the thirty heaters can be switched on or off independent of the others; however, the primary and back-up elements in each heater cannot be energized at the same time.

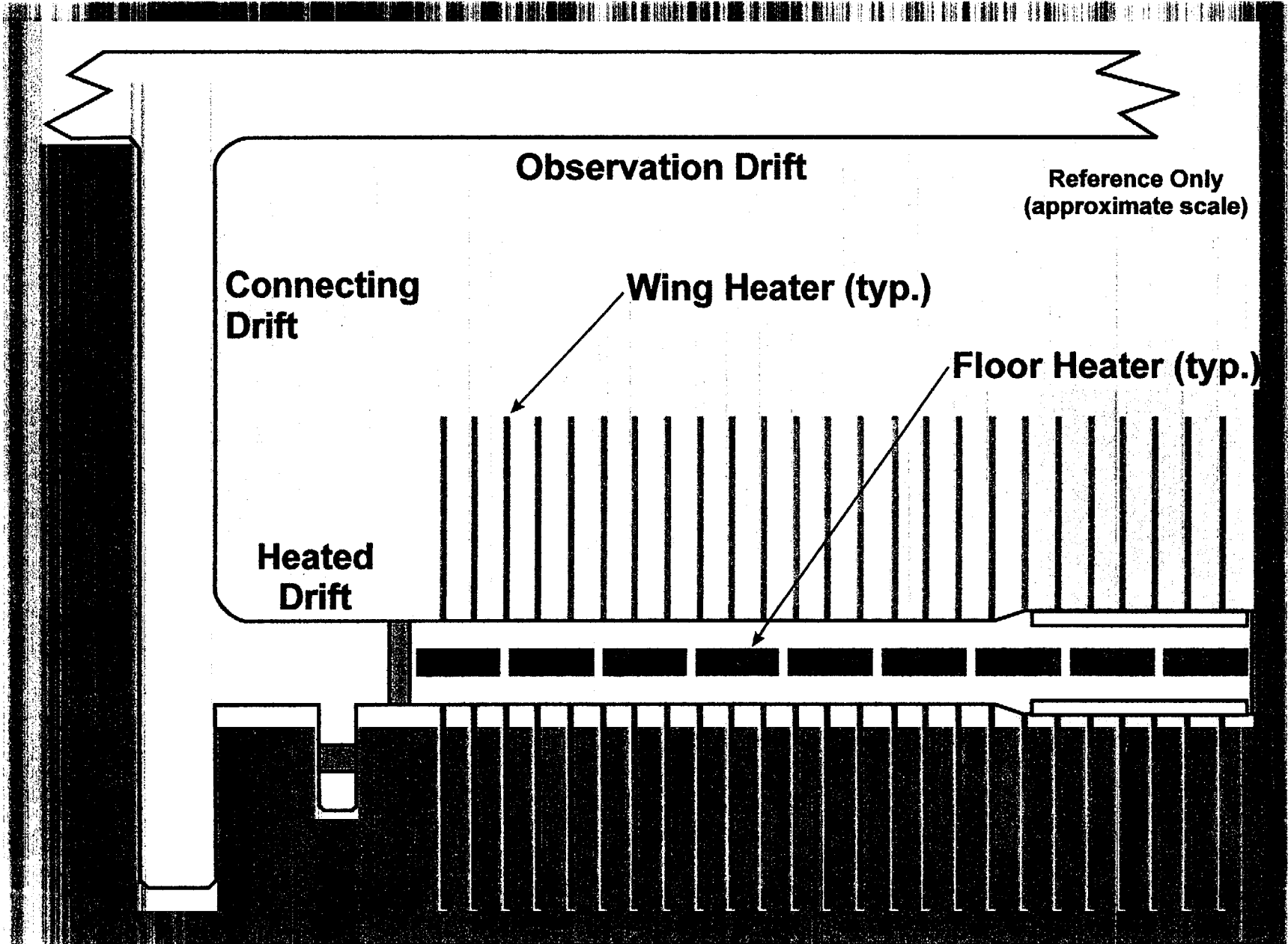
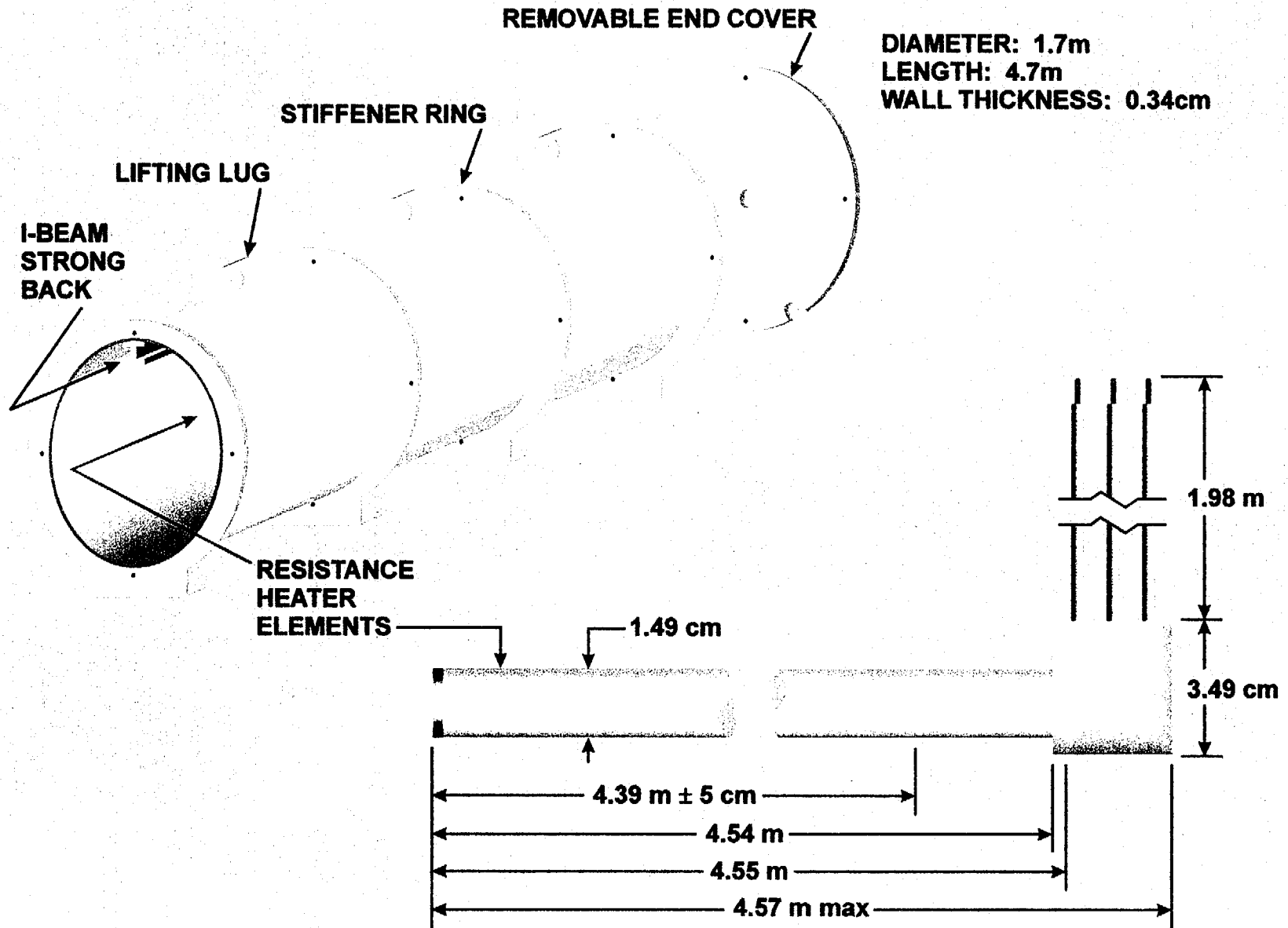


Figure 8-1. Plan View Showing Locations of Floor and Wing Heaters



m:\data\123\wagrev_1.cdr, 7/10/97

Figure 8-2. Floor Heater Design

Experience in the G-Tunnel thermal test (Ramirez et al. 1991) indicates that sealing the electrical terminals and connectors from ambient moisture is essential for prolonging heater life. Potting at the heater end of the lead wires and covering the terminal strips (at the lead wire/power cable connection) with high temperature epoxy are intended to avoid galvanic effects and potential initiation of corrosion.

Thermocouples will be mounted at various locations on the surface of the canisters to monitor the temperature. The measured temperature will be used as indicator of heater performance and may be used to control heater power, to the limits discussed in Section 8.3.

8.2.2 Wing Heaters

A total of fifty wing heaters (twenty-five on either side) will be placed in horizontal boreholes (nominally 11.5-m long) drilled into the sidewalls of the HD at nominally 0.25 m below the springline. The purpose of the wing heaters is to minimize the peak temperature in the rock around the HD while heating a larger volume of rock. Also, the wing heaters give the total heat source a planar appearance.

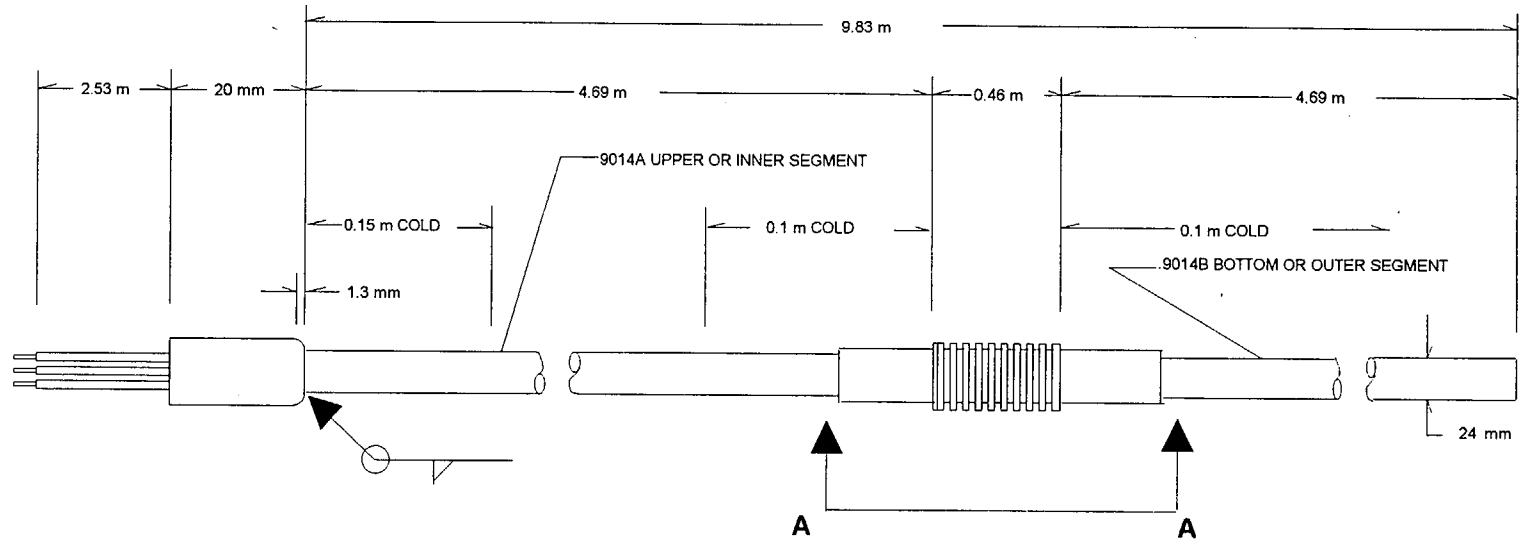
The wing heaters are nominally 10-m long with an inner and outer segment joined together by an accordion-like flexible joint (Figure 8-3). Each segment is a multi-zone heater independent of each other with the heat outputs of the inner and outer segments being 1145 watts and 1719 watts, respectively at 208 volts. Like the heaters of the floor heaters, each wing heater segment will have a primary heating element and back-up element wired independent of each other. Each wing heater segment can be switched on or off independently; however, the primary and back-up elements can not be energized simultaneously.

The wing heaters will have five thermocouples mounted on them, two on each segment and one on the flexible joint, to monitor their performance. As with floor heaters, the connections at one end of the wing heater lead wires will be potted while those at the other end will be covered with high temperature epoxy to avoid galvanic effects.

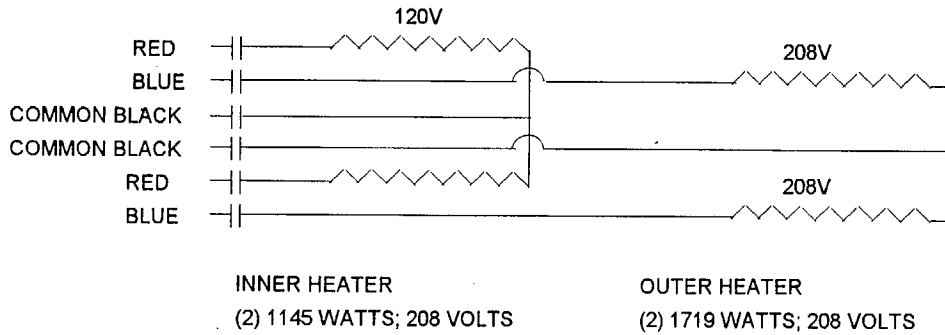
8.2.3 Heater Monitor Panels and Controllers

There will be one monitoring panel for each of the nine canister heaters and one panel each for the twenty-five wing heaters on either side of the HD for a total of eleven panels. The heater monitoring panels are equipped to individually energize each of the 370 heaters, that is, fifty outer wing heaters, fifty inner wing heaters and thirty heaters in each of the nine canisters. However, the primary and back-up heating elements in each heater can not be energized simultaneously. The monitoring panels are also equipped with one current transducer per each heater. The output of the current transducer is fed to the DCS and is used to compute the power output of each heater. The current transducers allow the performance of the heaters to be monitored.

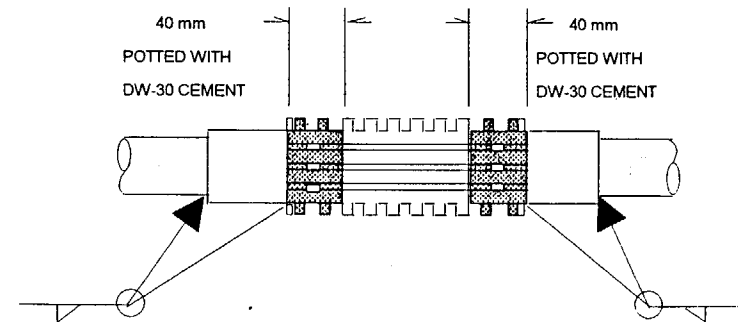
WING HEATER (SPLICED 0.935 MULTICELL)



WIRING DETAIL



VIEW A-A



NOTES:

1. ETCH POTTING CUP WITH 9014, DATECODE AND WATLOW.
2. SLICE BELLOWS OVER (1) SECTION OF MULTICELL BEFORE ADDING LEADS AND POTTING.
3. ALL WELD JOINTS MUST PASS HELIUM LEAK TEST OD 10⁷ CC PER SECOND.
4. WELD WIRE TO INSIDE OF POTTING CUP AND COLOR CODE GREEN.
5. INNER AND OUTER CIRCUITS WITH COMMON LEADS.

BAB000000-01717-4600-00007 REV 01

8-5

December 1997

Figure 8-3. Wing Heater Design

There will be one heater controller between the power supply transformer and the wing heater panel and one between the transformer and the canister heater panels. The heater controllers will allow the output of the wing heaters and canister heaters to be set at 0 to 100 percent of design capacity at any time.

Two Q measurements of the amount of heat applied in the DST will be made and recorded at any time—one for the group of 50 wing heaters and one for the group of 9 floor (canister) heaters.

8.3 HEATING/COOLING PLAN

A workshop was held June 3, 1997 at Lawrence Livermore National Laboratory to refine the heating/cooling plan for the DST. In addition to the ESF Thermal Test Team, it was attended by representatives of the DOE and the U.S. Nuclear Regulatory Commission. Results from parametric analyses of TM, TH, and TC behavior anticipated in the DST were presented and discussed. A consensus of the Yucca Mountain participants was reached on a DST heating/cooling plan with the following features:

- Heating duration (full and/or partial): 4 years
- Cooling (no heating) duration: 4 years
- Initial power output: canisters - 80% (54 kW); wing heaters - 100% (143 kW)
- Maximum, nominal temperature along drift wall: 200°C
- Volume of dryout zone (less than 46% saturation): greater than 10,000 cubic meters
- Temperature along the outer edge of the wing heaters to be slightly greater than comparable drift-wall temperatures
- Sufficient volume of rock, traversed by chemical and hydrological sensors, at 95°C for approximately 3 years
- Heating/cooling schedule will be adjusted, as needed, to ensure DST objectives are satisfied (see Section 2).

(Note: The U.S. Nuclear Regulatory Commission representatives observed and commented. Although they were not part of the consensus, they did not object.) This baseline heating/cooling plan is considered to be realistic based on extensive, parametric analyses and a well-designed heater configuration. Specifically, the heater layout represents a culmination of much planning in terms of heater type, number, distribution, power output, redundancy, and reliability.

9. DATA COLLECTION AND SERVICE SYSTEMS

The DCS specific to the DST will be provided by the Yucca Mountain Site Characterization Project Exploratory Studies Facility Data Collection System Team under the Scientific Program Field Work Package (FWP), *Exploratory Studies Facility Data Collection Systems* (CRWMS M&O 1996b). This FWP provides the controls utilized by the ESF TCO to manage the configuration, procurement, installation, calibration, operation, and maintenance of data collection (acquisition) systems specific to site characterization activities conducted in the ESF. The test-bed being instrumented in the DST consists of about 200,000 cubic meters along a length of about 50 m.

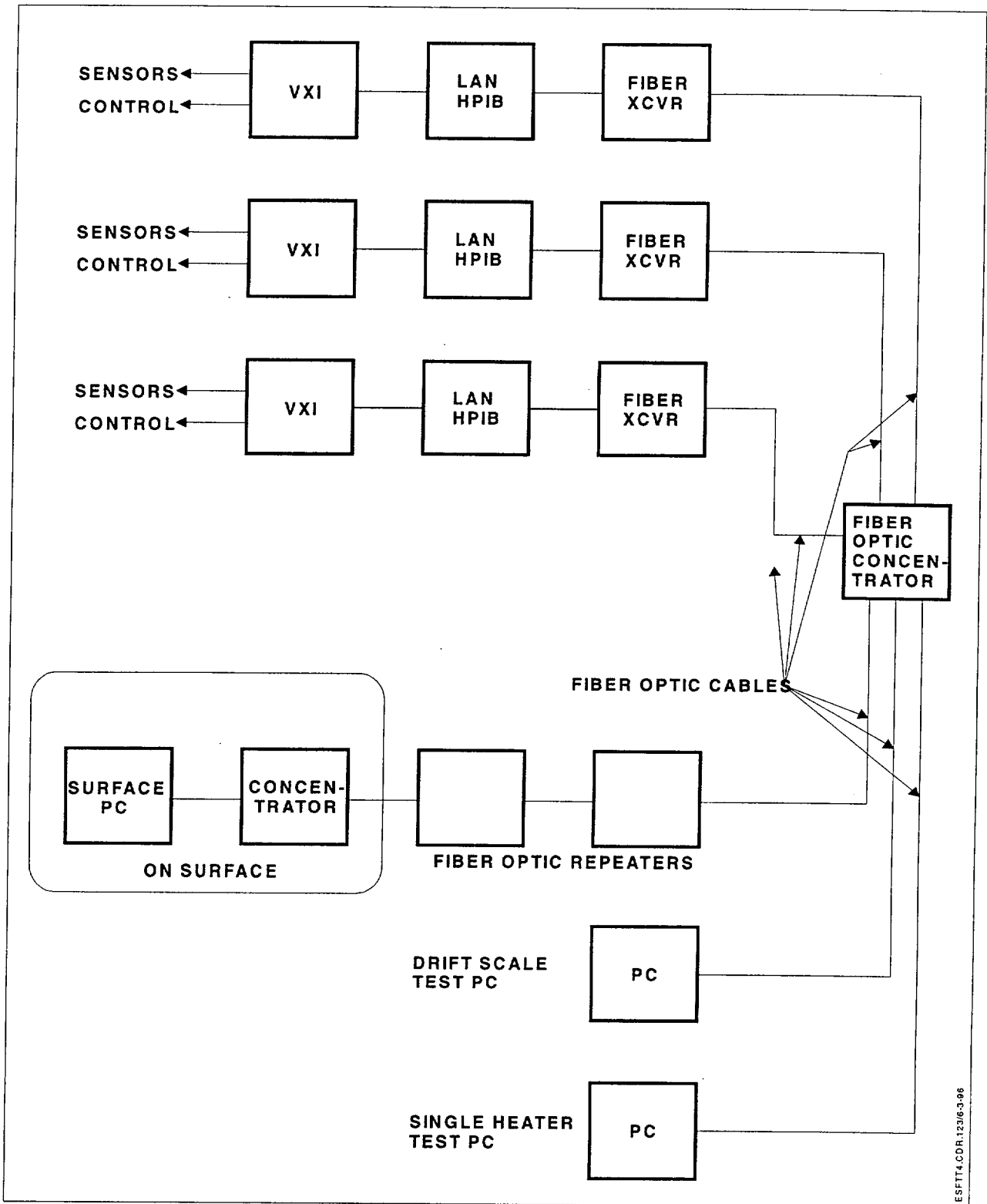
9.1 DATA COLLECTION SYSTEM (INTEGRATED)

9.1.1 General Description

Data collection for the DST will be provided by the DCS. The DCS is shown schematically in Figure 9-1 and is a distributed DCS. This DCS consists of distributed VXI data collection modules such as the Hewlett Packard HP-IB measurement system operating on the VXIbus standard over a copper wire or fiber optic Local Area Network (LAN). The use of the VXIbus standard with an HP-IB measurement system allows for easy test configuration of the data collection channels and rapid integration of system components. The software environment for the VXIbus is HP-VEE, Hewlett-Packard's graphical programming environment. The DCS data collection configuration will be accomplished using HP-VEE with high-level icons representing major test programming tasks such as test instrument channel configurations, data displays, and operator interfaces. The DCS will undergo acceptance testing and calibration as required and controlled by the Scientific Program Field Work Package, *Exploratory Studies Facility Data Collection Systems* (CRWMS M&O 1996b). The DCS configuration, procurement, installation, calibration, operation, and maintenance is conducted by the ESF DCS Team under the direction of the ESF TCO. Geotechnical test instrumentation and the heater assemblies are provided and calibrated by the PIs. Scanning rate of all automated data collection will be at least once per hour. A selected group of sensors may be scanned as frequently as once per 5 seconds during certain periods of active testing.

9.1.2 Location and Layout

The DCS is a distributed DCS with VXI modules operating through LAN gateways located in the observation drift with the main computer placed in an enclosed air conditioned office niche provided by the ESF TCO. The LAN gateways and HP-IB measurement instrumentation will be housed in NEMA 12 enclosures and will be located as near to the test instrumentation as possible to minimize cabling requirements. No DCS equipment is presently planned to be located in the HD due to the hostile thermal environment. Cabletrays will be used to route the many cables from the test instrumentation in the HD and on the test rock mass to the HP-IB measurement system. Power will be provided by transformers located outside of the DST area in order to reduce AC noise problems. A regulated AC power conditioner and an on-line uninterruptible power supply (UPS) will provide power to the HP-IB measurement system, LAN gateways, main computer, and necessary test instrumentation during periods of ESF power failure. No provision is being made to provide UPS



NOTE: All connections shown to the Fiber Optic Concentrator are fiber optic cables.

Figure 9-1. Drift Scale Test Data Collection System (Block Diagram)

back-up power to the test heaters during periods of ESF power failure, but DCS data collection functions will continue for all of the geotechnical test instrumentation. It may be possible to use the ventilation back-up generator on the ESF pad to power the heaters during a prolonged power outage if the ventilation system is turned off and the ESF evacuated of personnel. Such an arrangement is currently being investigated. Contingencies, besides a UPS, for potential problems, exist which include the usage of interchangeable parts, availability of an assortment of spare parts, alarms connected to the computers, and the design of backup channels.

9.1.3 Drift Scale Test Instrumentation Data Collection Channel Requirements - 5620 Channels

Currently, the channel types and numbers for the DST are as identified in Table 9-1; however, these assignments are preliminary and subject to revision as necessary.

Table 9-1. Geotechnical Instrumentation Data Collection Channel Requirements

| Instrument Type | | Number of DCS Channels | Parameter Measured |
|-----------------|------------------------------------|------------------------|-------------------------------------|
| 784 | Thermocouples | 784 | Borehole and Instrument Temperature |
| 1936 | Resistive Temperature Devices | 3872 | Borehole and Instrument Temperature |
| 19 | Multi-point Borehole Extensometers | 110 | Rock Displacement |
| 10 | Cross-Drift Wire Extensometers | 10 | Rock Displacement |
| 19 | Resistive Strain Gages | 76 | Deformation |
| 48 | Humidity Sensors | 48 | Borehole Humidity |
| 48 | Pressure Sensors | 48 | Borehole Pressure |
| 195 | Other Temperature Sensors | 195 | Borehole Temperature |
| 130 | SEAMIST Sensors | 130 | Rock Chemistry |
| 640 | Heater Monitors | 640 | Heater Performance |
| 30 | Miscellaneous Monitoring | 30 | Heater Adjustments |

9.1.4 Hardware Description

Figure 9-2 diagrams the DCS distributed data collection network. The HP E2050A LAN/HP-IB gateway provides a low cost avenue for HP-IB measurement systems operating over the fiber optic LAN. At its most basic level, the gateway communicates instructions and data between the main computer and the VXI measurement hardware that read the test sensors. The main computer does the bulk of the job. The gateway connection is through standard TCP/IP protocols.

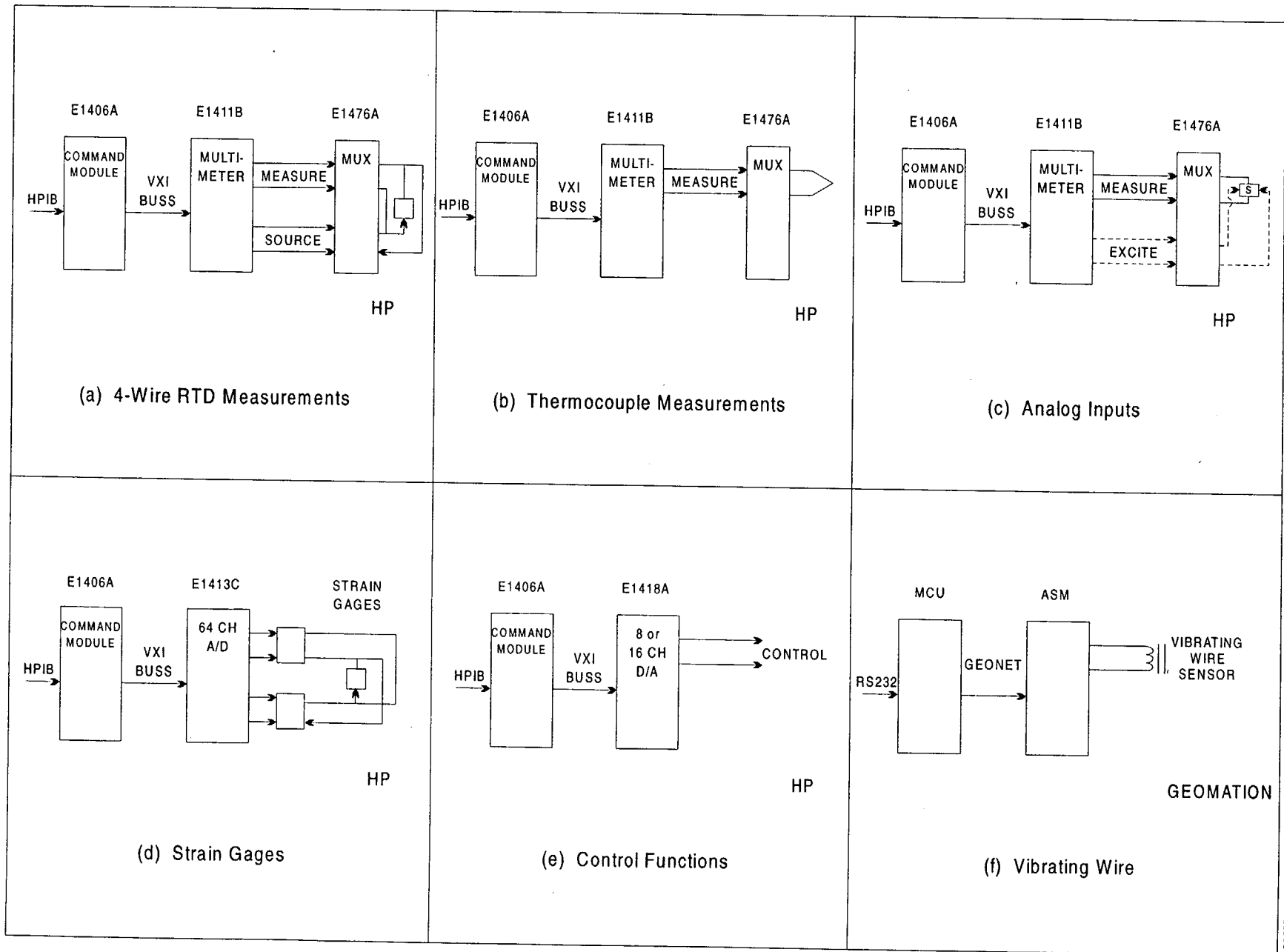


Figure 9-2. Data Collection System Hardware Block Diagram

The gateway produces all the benefits of the LAN remote operation, resource sharing, distributed control, and expanded use of the network. The computer passes messages over the LAN, through the gateway, to the HP E1406A command module which receives the SCPI (Standard Commands for Programmable Instruments) commands (messages), converts these messages into binary, and sends these messages to the HP-IB devices that make the measurement from test sensor. Multiple VXI bus mainframes at data collection points appear as a single VXIbus system with the use of the HP E1482B VXIbus extender that ties them together.

The measurement device blocks of the system are a 5-1/2-digit multimeter, a digital to analog (D/A) converter, and a 64 channel relay multiplexer.

- The HP E1412A 6-1/2-digit multimeter is a low-noise integrating analog to digital (A/D) converter. It is software calibrated and provides for DC voltage, AC voltage, 2 and 4-wire resistance, offset compensated ohms, thermocouple, thermistor, and 3 or 4 wire RTD measurements.
- The HP E1476A, a 64 channel relay multiplexer with dual bank configuration can connect 64 channels of thermocouple, 64 channels of voltage, 32 channels of 4-wire resistance, or 32 channels of current source. It is dynamically reconfigurable.

In Figure 9-2(a), 4-wire RTD Measurements, the command module sends messages to the multimeter and the multiplexer to source and measure the RTD. The measured signal is sent to the computer for conversion into engineering units. In Figure 9-2(b), Thermocouple Measurements, the command module sends messages to the multimeter and the multiplexer to measure the thermocouple. The measured signal is sent to the computer for conversion into engineering units. Thermocouples do not need excitation. In Figure 9-2(c), Analog Inputs, the command module sends messages to the multimeter and the multiplexer to measure and excite (if necessary) the analog sensor. The measured signal is sent to the computer to convert it to engineering units. In Figure 9-2(d), Strain Gages, the command module sends messages to the multiplexer to provide strain gage bridge completion and excitation and measure the signal. The measured signal again is sent to the computer for conversion into engineering units. In Figure 9-2(e), Control Functions, the command module sends messages to the D/A converter to control the heater elements. Feedback for control is through the RTD and thermocouple channels described above. In Figure 9-2(f), Vibrating Wire, the Geomation master control unit measures the vibrating wire signal and converts it to engineering units. The master control unit then sends the data to the NMS, the dedicated computer.

The DCS hardware is designed to collect all data channels once per hour and some subset, maybe 150 channels, in a fifteen minute cycle. The DCS computer will acquire the data from the monitored channels, store the acquired data, and periodically upload the acquired data to the surface computer. Any vibrating wire channels will be acquired with the Geomation equipment and these data will be merged with the DCS computer data in the Data Management Computer in the TCO Office on the ESF pad.

Because of the large number of data points produced daily by the DCS system and the need to monitor the progress and operation of the test from the surface, a fast, reliable LAN, utilizing fiber

optics communications link will be established from the thermal test facility to the surface ESF pad. Such a system will allow ESF TCO field technical personnel on the ESF pad rapid access to the DST DCS and other DCS systems for test monitoring and data transfer purposes with only minimal staff needed. This network may be upgraded to provide high-quality voice (telephone) communication from underground and video monitoring.

9.1.5 Data Management

All data collected from the ESF for site characterization is governed by the FWP, *Exploratory Studies Facility Data Collection Systems* (CRWMS M&O 1996b). Data collection is provided by DCSs, data loggers, or by PI-supplied and installed DCS. A Data Manager will be assigned by the ESF TCO, and will oversee all aspects of ESF data collection in accordance with the ESF DCS FWP. An organizational chart for the ESF DCS activity is shown in Figure 9-3.

The Data Manager establishes how DCS data are obtained by either downloading data to a portable computer, or by proper recording of data in a scientific notebook. The Data Manager shall be notified by the PI of the date, location, and type of data obtained for each data download. The Data Manager and the associated Test Project Engineer are responsible for compiling data collection requirements from PIs. Data collection requirements may include (but are not limited to) defining data monitoring equipment requirements, data sources, and data monitoring schedules. The Data Manager will integrate this information with the governing FWP requirements, and will assign tasks to the Engineering and Technical Support staffs to complete equipment installation. The Data Manager will prepare Field Work Requests for Data Distribution, and instruct the DCS Field Technical Support staff to prepare and distribute data in accordance with written, documented PI instructions. The Data Manager is responsible for tracking all data management activities.

The ESF TCO shall assist the Data Manager by conducting field operations (i.e., equipment installation, installation verification, or data downloading) as directed by the Data Manager.

Primary responsibilities for the Data Manager are as follows:

- Integrate the identification by the PIs of ESF data to be acquired including ventilation data and conduct the necessary interfacing.
- Review all data collection parameter change requests and verify DCS field operations compliance.
- Review, accept, and forward PI data requests to the DCS Field Technical Support staff.
- Review, accept, obtain PI approval, and document the DCS installation.
- Instruct the DCS Field Technical Support staff to acquire data according to identified PI requests.
- Instruct the DCS Field Technical Support staff to distribute data according to PI request.

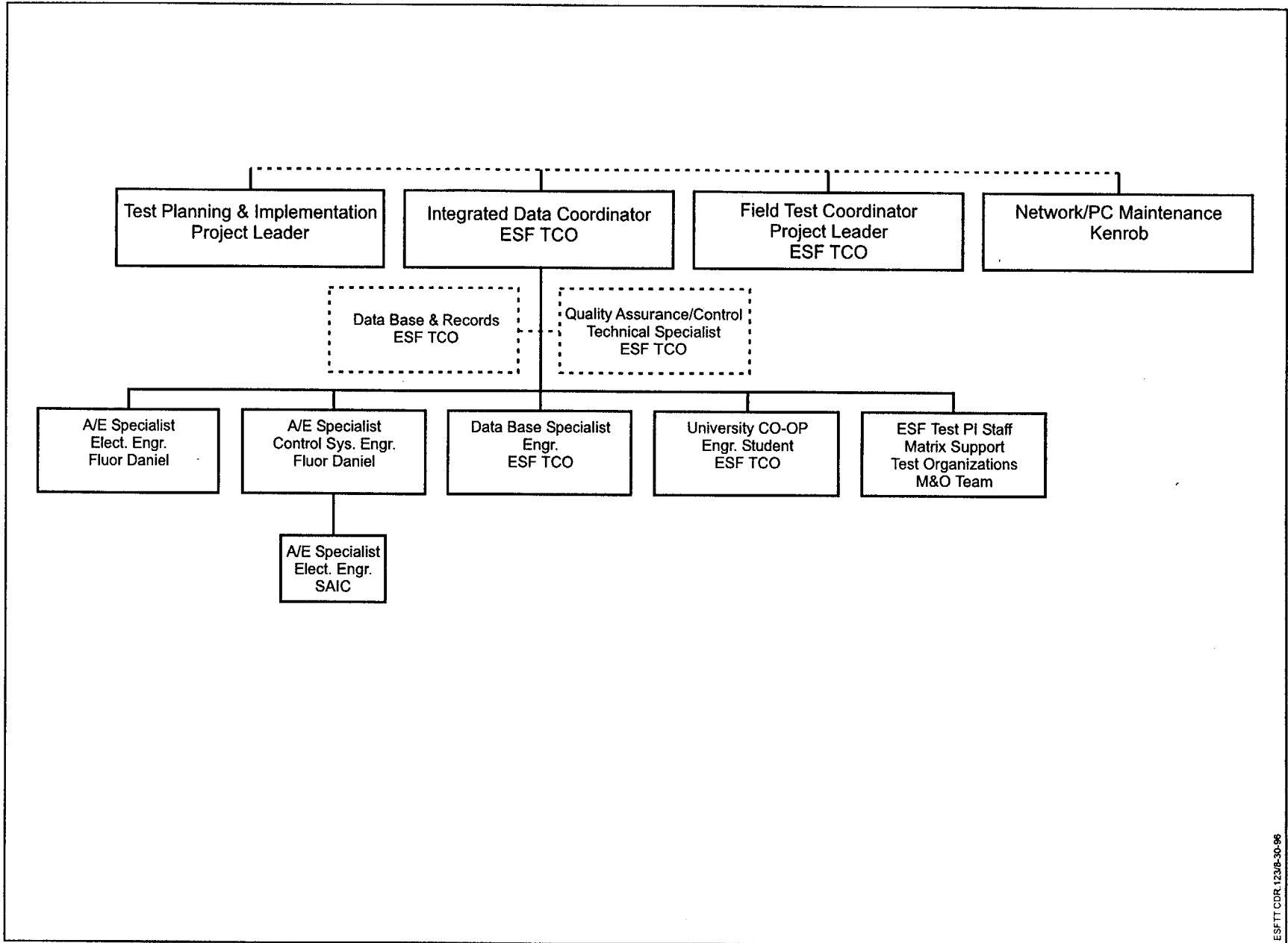


Figure 9-3. Data Collection System Organization Chart

- Document and track the following items:
 - PI data identification and defining parameters
 - PI data requests
 - Data management processes, and
 - Administrative copies of DCS archive data and related information.

- Prepare and distribute reports, including:
 - DCS instrument configuration
 - Data collection information, including dates and locations of sensors read and transfers of data to the PI
 - Calibration records for test instrumentation and DCS equipment
 - DCS equipment maintenance records, including equipment malfunctions and repairs
 - Verification and acceptance of equipment installation.

9.1.6 Data Distribution

The Data Manager will transfer data to the PI organization and/or other organizations as directed by the PI. At present, it is planned to distribute ESF DCS data from the Data Management Computer in the form of compact discs. Data collected and distributed by the DCS are quality assurance data. No DCS data shall be submitted to the Technical Database via the DCS; all submissions to the Technical Database are the responsibility of the PI in accordance with YAP-SIII.3Q, *Processing of Technical Data on the Yucca Mountain Site Characterization Project*. The Data Manager will provide the PI with two copies of the compact discs, to facilitate Technical Data Submission. DCS-acquired data will be distributed only at the direction of the Data Manager, based on PI requests, in accordance with the FWP, *Exploratory Studies Facility Data Collection Systems* (CRWMS M&O 1996b). The Data Manager will initiate data transfers, but may not be part of the physical data transfer process. The Data Manager must approve requests to purge data from DCS on-line storage prior to any DCS test data being erased from on-line storage after data back-up and archival. When possible, without degrading the integrity or security of the data, the Data Manager may permit a PI to access data in an on-line electronic transfer, such as by means of data servers. At present, transfers of data made in this manner are not traceable data, and may be used for monitoring activities only; data transferred through an on-line access will be evaluated in terms of its appropriateness for proper quality assurance accountability. Archive records shall be provided by the Data Manager for submission to the Records System as they are created during the archiving process. In summary, the Data Manager submits records and the PI submits data. These archived records are expected to contain a complete record of all DCS data including (but not limited to) test data collected by the DCS, manually entered data, and all common data. If PI test data is downloaded by the PI, the PI shall notify the Data Manager of the date, location, and type of data downloaded.

9.2 DATA COLLECTION SYSTEMS (NON-INTEGRATED)

Some measurement systems, which independently collect data from the DST block at discrete times, are needed to properly conduct the DST. These measuring systems are self-contained in that they either have computers or readout devices from which data can be recorded electronically or manually. The non-integrated DCSs planned for the DST are listed below:

- REKA (rapid evaluation of thermal conductivity (**k**) and thermal diffusivity (**alpha**))
- Plate loading
- Ground penetrating radar
- Neutron logging
- Electrical resistivity tomography
- Bulkhead vapor pressure
- HD camera
- Acoustic emissions/seismic tomography
- Video borehole logging (pre-test only).

Each of these systems are discussed in Section 6. Topics associated with the integrated DCS such as location and layout, channel requirements, hardware description, and data management are not considered germane in this discussion of non-integrated DCSs. Frequency of measurements will vary with each system from a few hours to a few weeks which is considerably less frequent than the hourly rate planned for the integrated DCS. Nonetheless, this disparity is not considered detrimental to the effectiveness of the non-integrated DCS planned for the DST.

9.3 DATA SERVICE SYSTEM

9.3.1 Background

The following discussion describes the process for handling data after it has been acquired from the DCS. This method, hereafter referred to as the Data Service System (DSS), reflects several discussions and interaction with various organizations within the M&O including the TCO, Scientific Programs Operations, and Technical Data Management. A similar but smaller-scale service with the SHT data has been developed and implemented. This learning or shakedown experience has helped shape the development of the DSS.

Details of the DSS that explain more fully how the DSS complements the existing DCS for the SHT and the planned DCS for the DST, are presented below.

9.3.2 Objectives

The objectives of the DSS are two-fold:

- Provide a standardized and centralized system for handling SHT and DST data after it has been formally collected by the respective DCSs.

- Provide a comprehensive data service that will allow PIs/laboratories to better conduct their scientific evaluations.

Figure 9-4 provides a flowpath of the ESF Thermal Test data. Figure 9-4 also describes the DSS and its relationship with both the data's origin (DCS) and its destination (Technical Data Management/Reference Information Base). Also, this schematic graphically shows how the two objectives are satisfied.

A standardized and centralized DSS provides obvious benefits that will not only be cost-effective but will reduce the likelihood of data misinterpretation. Another aspect of the DSS is that it will warehouse calculated data as well as measured data. This feature will allow technical investigators to evaluate calculated data generated elsewhere, thereby facilitating integrated, interpretive evaluations of all data. For example, all three laboratories are responsible for the TH analyses of the SHT. Historically, each of these investigators will evaluate only the agreement between the measured data and their calculated data. But, as the evaluations of the coupled relationship of the TMHC processes become more in-depth, it will be necessary for the investigators to have ready access to all calculated data.

The QA ramifications of the DSS will be investigated to ensure proper security, traceability, and validity. To date, much of the data has been informally sorted and presented as "draft" material. The transition of preliminary acquired data into fully developed data will occur as the data are collected, serviced, and analyzed (see Figure 9-4). In general, the DSS, like the DCS, is considered an M&O management and administrative service with distinct responsibilities that complement those of the technical investigators.

9.3.3 Features

A brief overview of the DSS features are provided below:

- **Restricted Network**—This feature will allow electronic access by intended end users - namely the ESF Thermal Test Team.
- **Electronic Diagnostics**—This feature will periodically examine the chronological behavior of each sensor. Logic will be developed that will identify anomalous measured responses. Such anomalies will be flagged such that the investigators can determine whether the cause is from a malfunction or natural phenomenon. This feature ensures all data is screened in a consistent, thorough manner before it is evaluated.
- **Data Tracking Numbers**—DTNs will be assigned to expedite the transfer of data within the network of investigators. DTNs will allow data to be transferred electronically rather than by other, slower alternatives such as mailing of compact discs.

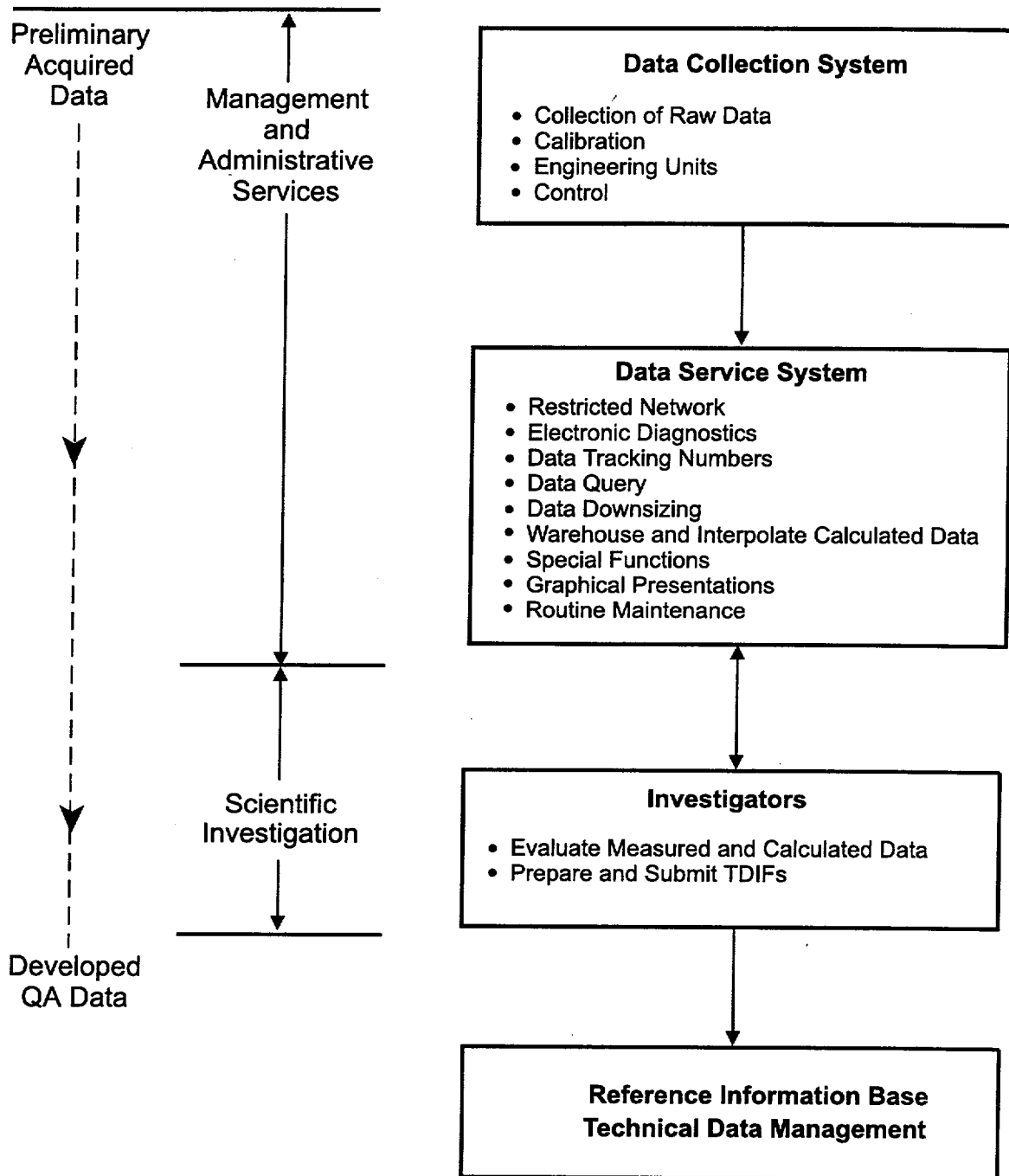


Figure 9-4. Data Flowchart for the ESF Thermal Test

- **Data Query**—This feature will allow queries of the data in a variety of formats. For example, an investigator may chose to examine the temperature from five distinct thermal sensors since the inception of the thermal test. Relational logic will accommodate this request with simple, straightforward query commands.
- **Data Downsizing**—This feature will allow investigators to access a more manageable quantity of data than exists in the master data set established in the DCS. For example, the monthly mass storage for the unzipped SHT data is approximately 50 megabytes. Mass storage problems are likely to be more burdensome when the number of sensors and duration for the DST is considered.
- **Warehouse and Interpolate Calculated Data**—This feature will store calculated data such that all investigators can have ready/electronic access of all data so that they can more thoroughly evaluate the agreement between measured and calculated data. Also, to facilitate the evaluation of the agreement between calculated and measured data, this feature will temporally and spatially interpolate calculated data. This data interpolation will allow one-to-one comparisons of measured and predicted data.
- **Special Functions**—This feature will provide for generic or tailored mathematical evaluation of data. An example of a generic mathematical evaluation would be the ongoing calculation of the average heater power. A tailored example would include a situation where a technical investigator wants to obtain the average heater power for a specific month. It is anticipated that the number of special functions would evolve/increase with time.
- **Graphical Presentations**—This feature is necessary to accommodate the frequent requests from DOE to graphically depict current results from the ESF Thermal Test for presentations to the U.S. Nuclear Regulatory Commission, U.S. Nuclear Waste Technical Review Board, and the public. Preparation of draft graphics for these purposes have been ongoing since the activation of the SHT.
- **Routine Maintenance**—This feature involves the necessary periodic updates to the DSS as data becomes available. It will also include refinements to the DSS to implement improvements as they develop.

10. CONTINGENCY PLANNING

This chapter discusses contingency planning to delineate more clearly the processes needed to resolve unlikely, but conceivable, problems which would impair the performance of the ESF DST. The discussion provides solutions for potential problems, if they occur, which will allow the DST to continue, for the most part, as planned. Given the potential for minor or major complications and the corresponding consequences, was considered prudent to plan, to the extent practical, for their occurrence. Therefore, a comprehensive contingency plan was woven into the DST design to minimize adverse effects of reasonably-possible problems.

10.1 RESERVE HEATING CAPACITY

Proper heating of the DST is fundamentally important to its successful completion. Therefore, a contingency to ensure the proper operation of the heaters has been developed. Although heating problems in the SHT were minimal, the potential for problems with the electrical heaters planned for the DST is far greater because of the longer heating phase and number of heaters.

The 9 floor and 50 wing heaters in the DST have been designed such that they can operate at a reduced capacity during normal operation. Specifically, heating capacity could be increased by changing the voltage from a standard 208 to 240 volts. Reserve heating capacity is recommended for the following reasons:

- A higher percentage of heaters could fail without significantly affecting the overall DST performance.
- The heater power could be increased to compensate for heat transferred into the rock being more effective than predicted.
- The additional expense is estimated to be a minor investment when the potential benefit to the overall success of the DST is considered.
- Replacement of failed heaters during the heating period should be avoided for several reasons including the restricted access, elevated thermal environment, and the potential for adverse impact to the measurement of THC behavior.

The number of mini, multi-zone heaters in a floor heater is 30. Redundant heating in the floor heaters is not as important as in the wing heaters provided the heaters are spaced within 10 centimeters of each other. This observation stems from thermal design analyses which indicate that the radiative mode of heat transfer is highly efficient when the floor heaters are in close proximity (see Figure 8-1). Because of this thermal phenomenon, the single most important contingency for proper performance from the floor heaters is the provision of sufficient reserve heating capacity.

10.2 POWER OUTAGES

The following discussion of power outages is arranged in short-term and long-term scenarios.

10.2.1 Short-Term

Short-term power outages will be kept to a minimum, as discussed in Section 8, but it is quite possible they will occur in the remote setting and harsh, underground environment inherent to the DST. Since power outages should be kept infrequent and short in duration, contingency planning focuses on both reliability and redundancy of the power source.

Power within the ESF can be divided into three categories: conventional, standby, and UPS. Two major circuits feed the ESF and are dedicated to utilities, lights, and the various testing alcoves. Therefore, the DST will share power with other users. At present, standby power for the DST is not considered necessary since most power requirements will come from the heaters. Nonetheless, a backup generator will be available to supply backup power for the DCS and ventilation system. The short interval of time that conventional power would not be available (estimated not to exceed 12 hours based on experience with the SHT during the operations of the TBM) will not affect the DST given the thermal mass and the ability to model outages in the numerical analyses. The other power consideration is the UPS. This contingency will be available to the DCS in terms of backup batteries. The use of batteries will ensure that this minor power requirement is always available such that data collection will not be interrupted.

A reliable conventional power source begins with proper connections, insulation, and installation of the massive amount of local wiring needed for the DST. Even though these precautions, which are part of the original DST design, are taken, it is important to have contingencies for power loss from the main source or an outage elsewhere such as faulty wiring between the surface and the thermal test facility. If the main source of power is lost temporarily, then, as discussed above, an alternate power source may or may not be available to supplement power until the main power source is restored. A power outage of more than 12 hours is unlikely and precautions can be taken to further reduce the likelihood of a power outage greater than 12 hours. If the power outage is from a minor problem, such as faulty local wiring, on-site personnel monitoring the DST will make repairs using readily-available tools and materials, or a redundant heater element will be selected. Repair of faulty wiring within the DST block is not planned. Should that need arise, specific planning will be developed. In summary, power outages may occur, but with the inclusion of minor contingency planning, are not anticipated to affect adversely the operation of the DST.

10.2.2 Long-Term

The following discussion focuses on the ability of DST components to withstand a design-basis earthquake and subsequent long-term power outages. Although the heaters and other equipment for the DST are not subject to seismic design criteria, the following discussion compares the risk of a disruptive seismic event and its impact to the cost and schedule of the DST.

The probability of a seismic event of sufficient magnitude to disrupt the ESF Thermal Testing activities for an extended period is considered small. This assumption is based on preliminary seismic hazard assessments done by the Project and will be supported further by the Probabilistic Seismic Hazard Assessment to be completed in early FY 1998.

The primary issue that must be addressed concerns long-term interruption of heater power. If a disruptive event, such as an earthquake, were to cause power outages, it would not compromise the integrity of the test, based on the assumption that power to the DCS would not be interrupted. This is a reasonable assumption, since the power distribution system is designed to comply with seismic design requirements; in addition, a backup generator will be available prior to heater activation to ensure uninterrupted power to the DCS and the measuring systems. Therefore, the DST would not be compromised for the following reasons:

- Heater power outages of approximately one day would produce a slight perturbation of the temperature distribution in the DST block because of the relatively low thermal conductivity of the rock. Decreases in rock temperature would be monitored using the extensive network of temperature sensors in the surrounding rock. In addition, changes in heater temperature would also be observable through the network of temperature sensors on the floor and wing heaters.
- Heater power outages of approximately one week would cause the rock mass temperature to decrease rock which may influence the measured responses. However, the extensive network of instruments on the heaters and in the surrounding rock would monitor this thermal perturbation.
- In the unlikely event that heater power is interrupted for a month or longer it may be necessary to re-baseline the DST before restarting the heaters. This approach would be established through quantitative analyses taking into account the duration of the power outage and measurements made during the interruption. The re-baselining process may involve several days of data collection at near-ambient temperature. Useful information would be collected and the heating phase of the test would be restarted. Another contingency for an extended heater power outage would be to continue collecting measured data until power could be restored. Subsequent numerical analyses of the DST would simply simulate the temporal fluctuation in power.

10.3 ROCKFALLS

Free falling rock during the construction or operation of the DST is an inherent problem in an underground environment. Standard safety and design precautions are likely to reduce or eliminate rockfalls. It is anticipated that the likelihood of a rockfall creating a problem is less during the construction phase than the operational phase because the time duration is shorter, prevention procedures are more proven, and the thermal environment (ambient temperatures) will be less harsh. Furthermore, rockfalls during the operational period have a greater potential for influencing the proper performance of the ESF Thermal Test. For these reasons, most of the discussion regarding contingencies for rockfalls is focused on the operational period of the DST.

Should a rockfall occur, despite the installation of the rockbolts and mesh or cast-in-place ground support systems, the initial task, excluding those pertaining to safety, will be to assess the extent of damage to the test equipment such as floor heaters, remote sensing devices, measuring devices, and wiring. It is unlikely that the resulting damage will require an immediate response (less than 48 hours) given the redundancy designed into the DST. For example, the large number of heaters and

measuring devices, size of the test drift, reserve heating capacity, and structural integrity and protection of the equipment will help mitigate damage from a rockfall. With the time available, the situation will be evaluated on a case by case basis. This may include evaluation of alternative actions by the ESF Thermal Test Team, numerical simulations of altered test conditions to assess the long-term ramifications on the DST performance, and solicitation of input from other informed and experienced sources either within or outside the Yucca Mountain Site Characterization Project. If problems from the damage still persist, and could ultimately jeopardize the success of the DST, a premature entry into the test area will be considered as a remedy (see Section 10.5).

10.4 REPAIR AND MAINTENANCE STRATEGY

The development of a contingency strategy for conditions where unplanned equipment repair or maintenance becomes necessary is prudent given the DST's harsh thermal environment, multi-year duration, usage of new measuring devices, and importance to the overall program. For example, the SEAMIST measuring system was developed recently and consequently is not as extensively tested for elevated temperatures in excess of 200°C, multi-year durations, and overall harsh environments as other measuring devices such as RTD, thermocouples, and extensometers.

This contingency of premature entry into the DST will not be exercised until all other less complex and less intrusive contingencies have been either evaluated or tried. It is anticipated that the process to cool the drift, effect repairs, and reheat the drift will take less than three days for most repairs. It is anticipated that if the HD is blast cooled with modified ventilation, entry would not require special clothing other than standard personal protective equipment required for the nonheated areas outside of the HD. Generally, a premature entry is intended to quickly resolve those problems which, left alone, would jeopardize the successful completion of the DST. Because of the configuration and time duration, this contingency is not being considered for the SHT.

A premature entry into the isolated DST implies that a doorway would be included in the bulkhead and the HD designed such that it can be readily blast cooled. Based on past analyses (Svalstad and Brandshaug 1983), perturbation of the thermal environment in the rock mass is estimated to be minor and occur within a meter of the drift wall for a blast cooling duration less than three days. Consequently, it is anticipated that perturbation to the THC environment will also be limited to the same thin layer of rock mass surrounding the HD. Also, THC perturbations created by blast cooling can be implemented into numerical simulations of the DST.

Another provision to minimize the impact of a premature entry into the HD will be to reverse the blast cooling process with a blast warming process using reserve heating capacity and/or additional heaters. This provision will accelerate the re-establishment of the THC environment that existed prior to entry. Also, blast warming can be readily simulated in the numerical analyses of the DST. Because of the need to minimize the duration of a premature entry, the emplacement of heaters and measuring devices and the ancillary equipment located in the drift has been simplified to the extent practicable. Therefore, should some faulty component need to be repaired with a premature entry, the repair would be conducted in a straightforward, expeditious manner.

10.5 ADDITIONAL HEATING PERIOD

As mentioned previously, the heating duration for the DST is anticipated to last four years. As this heating duration nears completion, the measured data will be assessed to determine if sufficient heating has occurred. In general, this decision will be based largely on the observation and assessment of hydrological phenomena such as the development of a representative dryout zone. Specific hydrologic criteria to be evaluated prior to the end of the four-year heating duration is cited in a study by Buscheck and Nitao (1995). It is anticipated that an extension of the heating duration will be on a yearly basis such that the planned heating duration for the DST is not substantially exceeded.

10.6 WAREHOUSE SPARE PARTS

Provisions will exist to ensure the availability of spare parts for the DST. This provision is largely limited to those components of the test that are readily accessible. For example, components of a DCS or plate loading tests are readily accessible whereas the heaters and measuring devices located within the HD would not be readily accessible. In addition to the availability of spare parts, test components that are commercially available will be used wherever practical.

10.7 INADEQUATE SENSOR PERFORMANCE

A contingency for inadequate sensor performance is considered necessary because of the duration of the harsh thermal environment projected for the DST. During the planning of the DST, experiences from other thermal tests were considered. Past heater tests that provided insight regarding sensor performance include:

- G-Tunnel Underground Facility (Nevada)
- Climax Spent Fuel Test (Nevada)
- Waste Isolation Pilot Plant (New Mexico)
- Underground Research Laboratory (Canada)
- Basalt Waste Isolation Project (Washington)
- Stripa Underground Test Facility (Sweden)
- Avery Island (Louisiana).

Tables 3-2 and 6-1 provide an overview of these past thermal tests in terms of sensor performance as well as power output, test duration, and processes. In summary, thermal sensors tend to be the most reliable and stress sensors tend to be the least reliable. Sensors for the measurement of displacements, such as borehole deformation gauges and wire extensometers, also have a favorable history. Information on sensors for measurement of hydrological and chemical behavior is more scarce since many of the previous heater test targeted thermal-mechanical response in the local rock mass. In general, hydrological and chemical sensors are anticipated to be perform but with a lower reliability than most thermal and mechanical sensors. (Note: Electrical heaters have performed favorably in the previous applicable heater tests identified in Table 6-1).

The instrumentation design for the DST parallels the finding from the investigation of previous heater tests (see Table 3-1). Thermal sensors are used abundantly throughout the DST block in that they account for more than 80 percent of the DST sensors. Conversely, stressmeters are limited to mostly the comparatively more reliable pressure transducers which account for less than 2 percent of the DST sensors.

Another issue regarding sensor performance is post-test calibration. Some sensors will be extracted after the completion of the DST such that they can be calibrated. This precaution will ensure better sensor performance. Conversely, because of the inherent nature of the DST, some sensors will remain permanently installed in the DST block. In these cases, post-test calibration will not be possible.

11. SCHEDULE

11.1 PURPOSE AND SCOPE

The purpose of this section is to summarize the scheduling and sequencing of the activities that make up the DST. As part of the planning, an *ESF Thermal Test Operating Plan* has been developed and submitted as a separate document (CRWMS M&O 1996d). The operating plan will be actively used to manage and track the activities associated with the DST and will be updated, as needed, to reflect progress and changes in the planned activities.

The Operating Plan is a detailed schedule of activities or events along with an explanation of how the events are sequenced to best accomplish the end results. The Operating Plan provides:

- An integrated schedule for planning, construction, test implementation, data analysis, and reporting
- A logical sequencing of events to ensure that activities conducted in parallel do not interfere with each other, the steps in each activity are done efficiently and in the proper order, and important activities have not been overlooked
- A means to manage the resources available over given periods of time and to track progress toward the major milestones of the test program.

The summary schedule for the DST is provided in Figure 11-1. A more detailed schedule for each phase of the test has been discussed in the report entitled *ESF Thermal Test Operating Plan* (CRWMS M&O 1996d). Also, revisions to the schedule presented in this previous report will be documented in a future report. The summary schedule is divided into five main segments:

- Development & Installation
- Conduct Test
- Reporting
- Analyses
- Characterization.

The summary schedule shows the logical time phasing of the activities. A brief explanation of the activities and the sequencing needed to meet schedule and cost objectives is provided below.

11.2 PLANNING

The planning for the DST is somewhat more extensive than previous ESF testing in that the complete test design document is being produced for Project-wide review. It is important that both the testing community and the users of the data be familiar and comfortable with the test plan. The tests must clearly satisfy the needs of repository design and performance assessment as outlined in Section 1. The information in this planning report, along with some additional detail provided by the PIs, will feed ongoing development of the Test Planning Package. The FWP (a replacement for

Drift Scale Test: Summary Schedule (Calendar Years)

| DESCRIPTION | Start | Finish | Total Days | 95 | 96 | 97 | 98 | 99 | 00 | 01 | 02 | 03 | 04 | 05 | 06 | 07 | 08 |
|--|----------------|----------------|--------------|----|----|----|----|----|----|----|----|----|----|----|----|----|----|
| | | | | | | | | | | | | | | | | | |
| Drift-Scale Test | 10/1/96 | 9/30/06 | 3652d | | | | | | | | | | | | | | |
| Development & Installation | 10/1/96 | 12/8/97 | 434d | | | | | | | | | | | | | | |
| In Drift Heater Procurement | 10/2/96 | 4/25/97 | 206d | | | | | | | | | | | | | | |
| Instrument & Equip. Procurement | 10/1/96 | 7/14/97 | 287d | | | | | | | | | | | | | | |
| Drill Boreholes in Access Drift | 12/10/96 | 4/7/97 | 119d | | | | | | | | | | | | | | |
| Drill Boreholes & Install Instruments | 2/12/97 | 8/19/97 | 189d | | | | | | | | | | | | | | |
| Preparedness Assessment | 10/27/97 | 12/3/97 | 38d | | | | | | | | | | | | | | |
| Heaters Turned On | 12/8/97 | 12/8/97 | 0d | | | | | | | | | | | | | | |
| Conduct Test | 10/1/96 | 12/9/05 | 3357d | | | | | | | | | | | | | | |
| Ambient Characterization | 10/1/96 | 8/4/97 | 308d | | | | | | | | | | | | | | |
| Submit Ambient Characterization Report | 8/4/97 | 8/4/97 | 0d | | | | | | | | | | | | | | |
| Heat-Up Stage | 12/8/97 | 12/9/01 | 1463d | | | | | | | | | | | | | | |
| Conduct Plate Load Test | 10/1/98 | 12/23/98 | 84d | | | | | | | | | | | | | | |
| Cool-Down Stage | 12/10/01 | 12/9/05 | 1461d | | | | | | | | | | | | | | |
| Reporting | 9/1/97 | 8/26/02 | 1821d | | | | | | | | | | | | | | |
| Prepare As-Built Report | 9/1/97 | 1/28/98 | 150d | | | | | | | | | | | | | | |
| As-Built Report | 2/28/98 | 2/28/98 | 0d | | | | | | | | | | | | | | |
| Prepare Final Heating Data Report | 12/7/01 | 8/26/02 | 263d | | | | | | | | | | | | | | |
| Submit Final Data Heating Report | 8/26/02 | 8/26/02 | 0d | | | | | | | | | | | | | | |
| Analyses | 10/1/96 | 9/30/06 | 3652d | | | | | | | | | | | | | | |
| Pre and Post-Test SDM Analyses | 10/1/96 | 9/1/97 | 336d | | | | | | | | | | | | | | |
| Pre-Test Heated Drift Analyses | 10/1/96 | 7/15/97 | 288d | | | | | | | | | | | | | | |
| Submit Pre-Test Heated Drift Analyses Report | 7/16/97 | 7/16/97 | 0d | | | | | | | | | | | | | | |
| Analysis vs Data Assessments | 12/8/97 | 9/30/06 | 3219d | | | | | | | | | | | | | | |
| Final Post-Test Analyses | 8/26/05 | 8/26/06 | 366d | | | | | | | | | | | | | | |
| Submit Final Post-Test Analyses Report | 8/26/06 | 8/26/06 | 0d | | | | | | | | | | | | | | |
| Characterization | 10/1/96 | 8/26/06 | 3617d | | | | | | | | | | | | | | |
| Pre-Test Characterization Report | 10/1/96 | 8/4/97 | 308d | | | | | | | | | | | | | | |
| Submit Pre-Test Characterization Report | 8/4/97 | 8/4/97 | 0d | | | | | | | | | | | | | | |
| Post-Test Characterization | 12/9/05 | 8/26/06 | 261d | | | | | | | | | | | | | | |
| Submit Post-Test Characterization Report | 8/26/06 | 8/26/06 | 0d | | | | | | | | | | | | | | |

Figure 11-1. Summary Schedule (Calendar Years) for Drift Scale Test

the Test Planning Package which is not shown on schedule) is developed by the TCO according to current procedures to direct implementation of the work in the field. These packages are phased to accommodate the planning schedule and the construction schedule.

11.3 FACILITY CONSTRUCTION

Construction of the HD stopped temporarily to install instrumentation for the SDMT in the pillar between the observation drift and the HD. This instrumentation was installed before the HD was constructed. After the instrumentation for the SDMT was installed, the HD was excavated. During construction, normal construction monitoring activities were also conducted. In general, construction activities have remained within the schedule.

11.4 DRIFT SCALE TEST

The initial phase of instrumentation installation for the DST occurred during construction because the instrumentation is needed for the SDMT. Following construction, the remainder of the instrumentation boreholes were drilled, both in the HD and in the connecting and observation drifts. Because the design specifies a substantial number of boreholes to be drilled, the installation time for this test is significant and is the single most important schedule activity. The drilling time was estimated based on availability of two crews on two shifts per day. Procurement of the in-drift heaters began in late FY 1996 with procurement of the instrumentation beginning in early FY 1997, such that it was available for installation upon completion of the HD. The wing heaters are similar to the heater used in the SHT test, thereby taking advantage of the design work done earlier for that test. A preparedness assessment is planned before the heaters are activated to ensure that:

- Quality assurance procedures are in place and are being followed.
- All test planning prerequisites have been met.
- Proper environmental, safety, and health operational and safety procedures are complete including but not limited to the hazard controls listed in the Thermal Test Safety Assessment Review.

The heating period of the DST is currently planned for approximately four years. This duration is subject to change pending an assessment of the initial results. A monitored cooling period about as long as the heating period will follow. At the conclusion of cooling, representative samples will be collected for laboratory testing. Laboratory test results on post-test samples will be compared to results on samples taken before the test to analyze chemical and hydrological property changes resulting from the heating.

Reporting of DST results will be in two phases (see Figure 11-1 for completion dates). The first report will include a detailed description of the test preparation and installation (as-builts). Included in this report will be characterization information collected as the facility was constructed. This would include data such as rock quality (Q) estimates, initial permeability, and descriptions of joint orientation and filling. The second report will be a final data summary including both heating and cooling periods. These reports will provide the data in a reasonable time frame for prompt project

access. In accordance with procedure YAP-SIII.3Q, interim data transmittals using Technical Data Information Forms to the project data base are also planned at least quarterly during the test. Analysis of the data will occur on an ongoing basis and will be reported separately. Also, pre-test and post-test characterization reports will be prepared prior to and after the DST, respectively.

The test analysis is also divided into three parts (see Section 5). The first is a test design basis analysis that compiles the predicted test results based on current modeling capability. This is an important step for model evaluation. Prior to the initiation of the DST, a comprehensive analysis will occur to establish baseline predictions of the THC behavior. During the test, data will be compared periodically to the predicted behavior. These comparisons will be the basis for mid-test corrections in the test procedure, if needed. For example, if the rock is not heating as fast as predicted, the heater power could be adjusted so that the test will achieve the temperature ranges needed to meet data specifications. The second major analysis will follow the heating period and provide detailed comparisons of predictions and measurements. Also, rock mass properties including the coefficient of thermal expansion, thermal conductivity, rock mass modulus permeability, diffusion coefficient, and mineral/water composition will be determined. The final report will include analysis of the cooling period and a more complete analysis of the entire test.

Laboratory testing will accompany the in situ tests. These tests are primarily intended to characterize the rock before and after the DST. The results will be used for development of rock properties for modeling purposes and evaluation of the coupled THC processes.

12. QUALITY ASSURANCE

12.1 PURPOSE AND SCOPE

The purpose of this section is to outline the QA methodology and controls to be applied to the DST. Several organizations exist which support the DST, each operating under the same QA program, but with different procedures. Therefore, care has been taken to establish an overall QA methodology that supports the ESF Thermal Test Team and is compatible with teammate organization differences in procedural implementation. Where interfaces exist, clear communication has been established. The QA plan for the DST is described below in two main parts: a planning phase and an implementation period. During the planning period, the flow-down of requirements has been established and maintained, and plans are being developed, reviewed, and controlled for the implementation phase. The implementation phase will result in the development of the DST, the procurement and installation of the instrumentation, and the initiation and operation of the DST. These two phases overlap somewhat in that the planning goes through several iterations of refinement, while in parallel, partial implementation of the test may be ongoing such as facility construction and procurement, and installation of instrumentation.

12.2 PLANNING

The process for test planning is shown in Figure 12-1. In this figure, the flow-down of requirements and process steps are shown in rectangular boxes. The QA elements or procedures associated with each process element are shown in octagonal boxes. The flow-down for site characterization testing starts with the SCP (DOE 1988) which specifies several study plans. The principal study plans associated with the DST are those associated with SCP Section 8.3.1.15.1 and the waste package design in SCP Section 8.3.4.2.4. In the SCP, a preliminary estimate of user needs from repository design, performance assessment, and licensing was developed. Also, preliminary test configurations, designed to acquire appropriate data and test certain concepts, were documented. Subsequently, test concepts have been further defined in study plans.

In 1995, a major change in project direction dictated that a single set of consolidated tests be developed to replace the SCP test suite. The result of this project change is documented in the *In Situ Thermal Testing Program Strategy* (DOE 1995) and an updated version of this report which is currently being reviewed by DOE. The consolidation effort examined in detail new and modified design and performance assessment requirements to ensure compliance with current needs. The activity described in the DST plan are based on these concepts with some additional modifications. The DST plan is maturing in phases into a detailed test plan that will form the basis for the test design and the project test planning documents that will direct the work. Because of the iterative nature of the test design process and the tight schedule for test development, certain pieces of the test plan needed by the ESF designers and others will be provided through the TCO using their procedures for transmitting test design input and test related information. The TCO will also develop an FWP, and other necessary planning and implementation documents in accordance with project procedures.

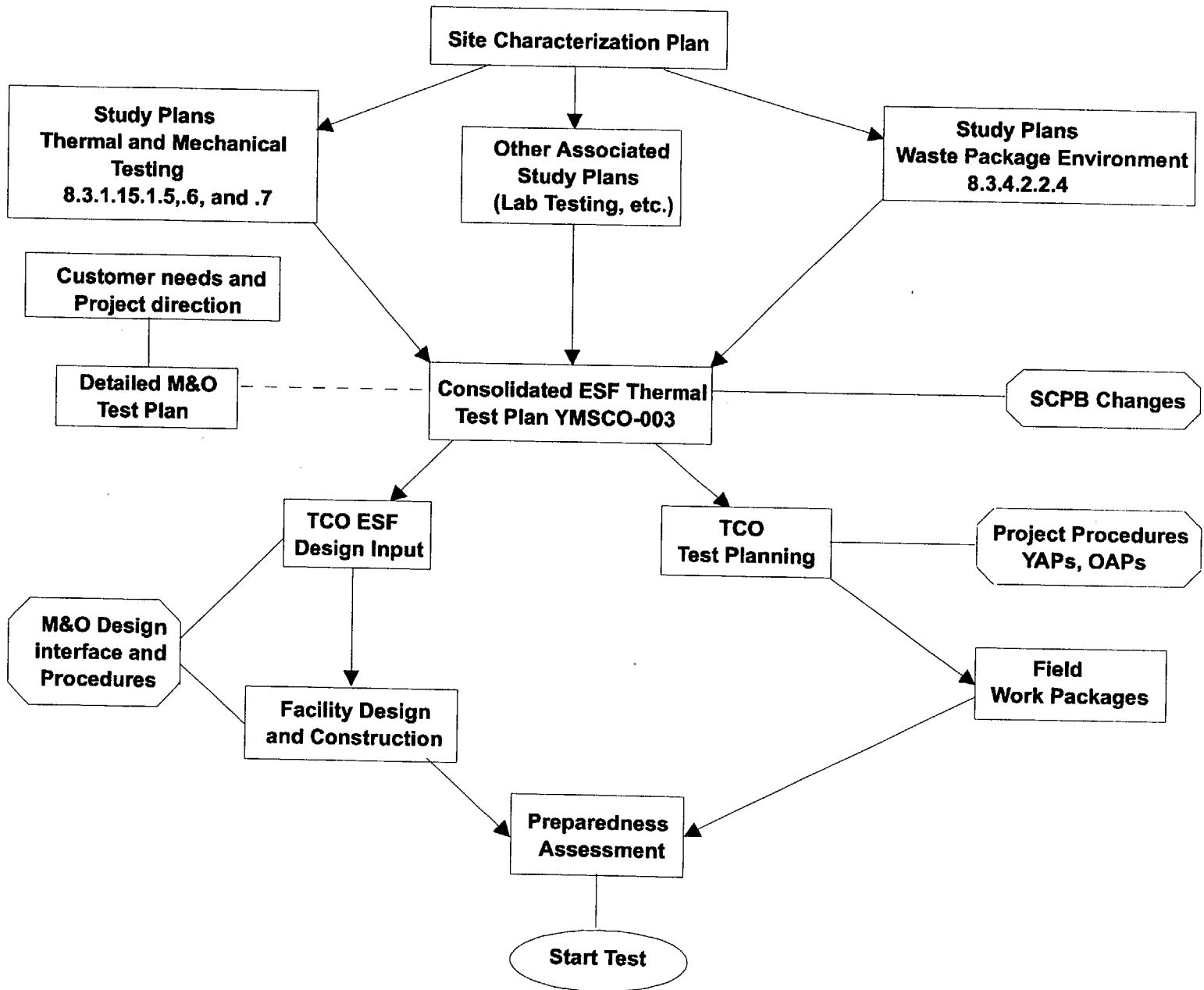


Figure 12-1. Test Planning Process and Controls

Interfaces associated with the field implementation of the ESF Thermal Test are:

- ESF Thermal Test Team/ESF TCO
- ESF TCO/ESF Designer
- ESF TCO/ESF Constructor-Operator.

The FWP is the document for the formal control of these interfaces. The interfaces associated with the conceptual planning and development of the ESF Thermal Test are:

- ESF Thermal Test Team/Repository Designer
- ESF Thermal Test Team/Waste Package Designer
- ESF Thermal Test Team/Performance Assessor.

Formal control of these interfaces will be addressed in the work-specific implementing documents.

In the planning process, the PI interface is primarily through the development of the FWP. In developing this information and providing it to the TCO and documenting it in the FWP, each PI is expected to use the appropriate procedures that are part of their organization's QA system.

Because there are two main parts to the ESF Thermal Test, the SHT and DST, planning has been at different stages for each thermal test. After the detailed test plans and work packages for the DST are completed and approved, the facility is readied, and the test equipment and instrumentation installed; the test will be ready to start. At this juncture, at the direction of M&O management, a preparedness assessment will be conducted.

12.2.1 Analyses and Software

Several sets of analyses will be performed to plan for various elements of the DST, to predict the coupled-process behavior of the rock during the tests, and to interpret data resulting from the tests. Most of these analyses will use scientific/engineering software with complex models of rock-mass behavior. There are three general phases of analysis for each test effort; each has a different degree of QA control applied.

The first phase is for test planning. In this phase, preliminary calculations are performed to estimate temperature, stress, moisture, and chemical distributions in the rock over time that result from the emplaced heat source. Parametric studies are used to optimize the test geometry and thermal loading to produce measurable effects, and to estimate parameter ranges for instrumentation selection and placement. These analyses will employ scientific/engineering software that are entered into configuration management and identified in the analysis reports, but additional controls are not required because of the preliminary nature of the work and its application.

After the test area has been characterized to get site-specific information for analysis input, pre-test predictive analyses are conducted. These are more formally documented analyses that include actual (as built) test geometry and site specific material properties. The analyses predict the behavior of the rock as the experiment is conducted. The results of these analyses are used to assist in controlling the experiment and initial data interpretation by comparisons of data with predictions,

and to form a basis for model validation exercises. QA controls on the analyses and on the software used will be implemented in accordance with the approved QA procedures of the organizations conducting the work.

Finally, after the test is completed (or at strategic points during the test), post-test analyses will be conducted. These analyses are generally used to better interpret the data by using the models to try to match test data. A secondary use is to advance model validation. Because of the exploratory nature of some of the analyses, QA controls will vary depending on the specific application. Model validation runs will be done with all QA controls in place so that the results can be used later in the licensing process. Data interpretation analyses will use qualified software, but other controls may be relaxed, depending on the type of analysis.

12.2.2 Preparedness Assessment

Management plans to conduct a review of the state of the test preparedness to assure that all actions and prerequisites needed to successfully conduct the DST have been accomplished. Several Yucca Mountain Site Characterization Office and teammate organization procedures are available to guide these assessments. Management may select a procedure or portions of procedures commensurate with the complexity of the DST. Management has appointed a review team of qualified individuals who are independent of the DST. They will develop a checklist of the conditions to be satisfied before starting each test. General conditions to be checked may include such items as QA and technical procedures, data system readiness, environmental health and safety procedures, personnel training, system safety, and test plans. After all conditions are found acceptable, heating will be initiated.

12.3 TEST IMPLEMENTATION AND DOCUMENTATION

Figure 12-2 illustrates the process for conducting the test. As in Figure 12-1, the rectangular boxes indicate process steps and the octagonal boxes represent applied QA controls. The data collection will be performed by the PIs using a central Data Acquisition System. For the most part, the QA controls applied are those of the PI organization related to data collection, handling, review, and submittal. There are two specific areas where process and interfaces are quite important. These areas, calibration and data management, are discussed briefly below.

This is a conceptual planning and overview document, and all inputs used in this report are conservatively considered to be unqualified. However, neither observations from this report nor inputs, as cited in the report, will be used to develop the actual thermal tests. The testing activities themselves will be developed under the QA program requirements of procedure YAP-5.7Q, *Testing Field Work Packages*, and the inputs, used in support of the test development activities, will also be controlled per the requirements of YAP-5.7Q. Should information or inputs from this report be used in any other implementation, development, or analysis document which is subject to the Quality Assurance Requirements and Description (DOE 1997) requirements, this information/input is required to be controlled as TBV in accordance with the appropriate procedures.

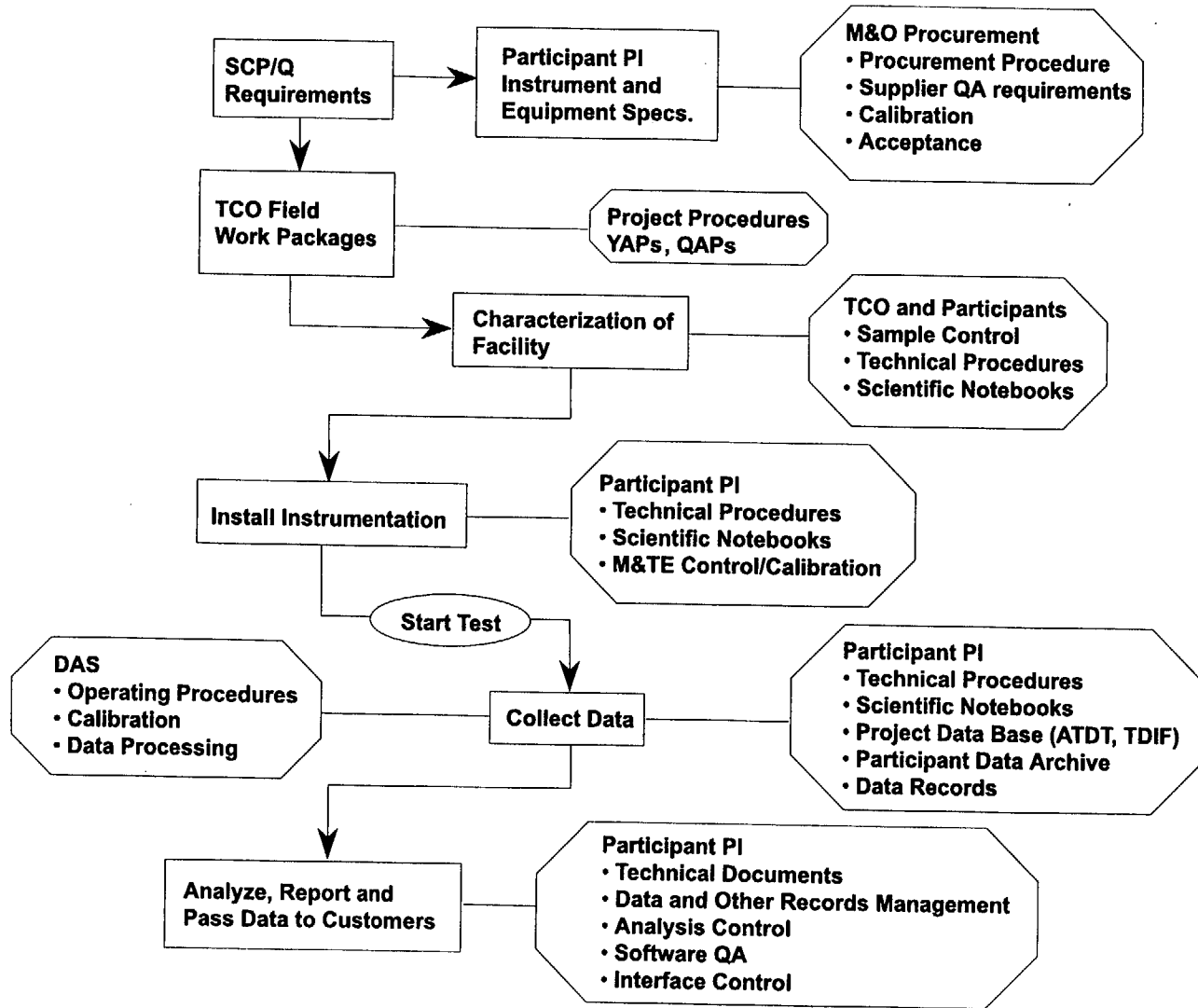
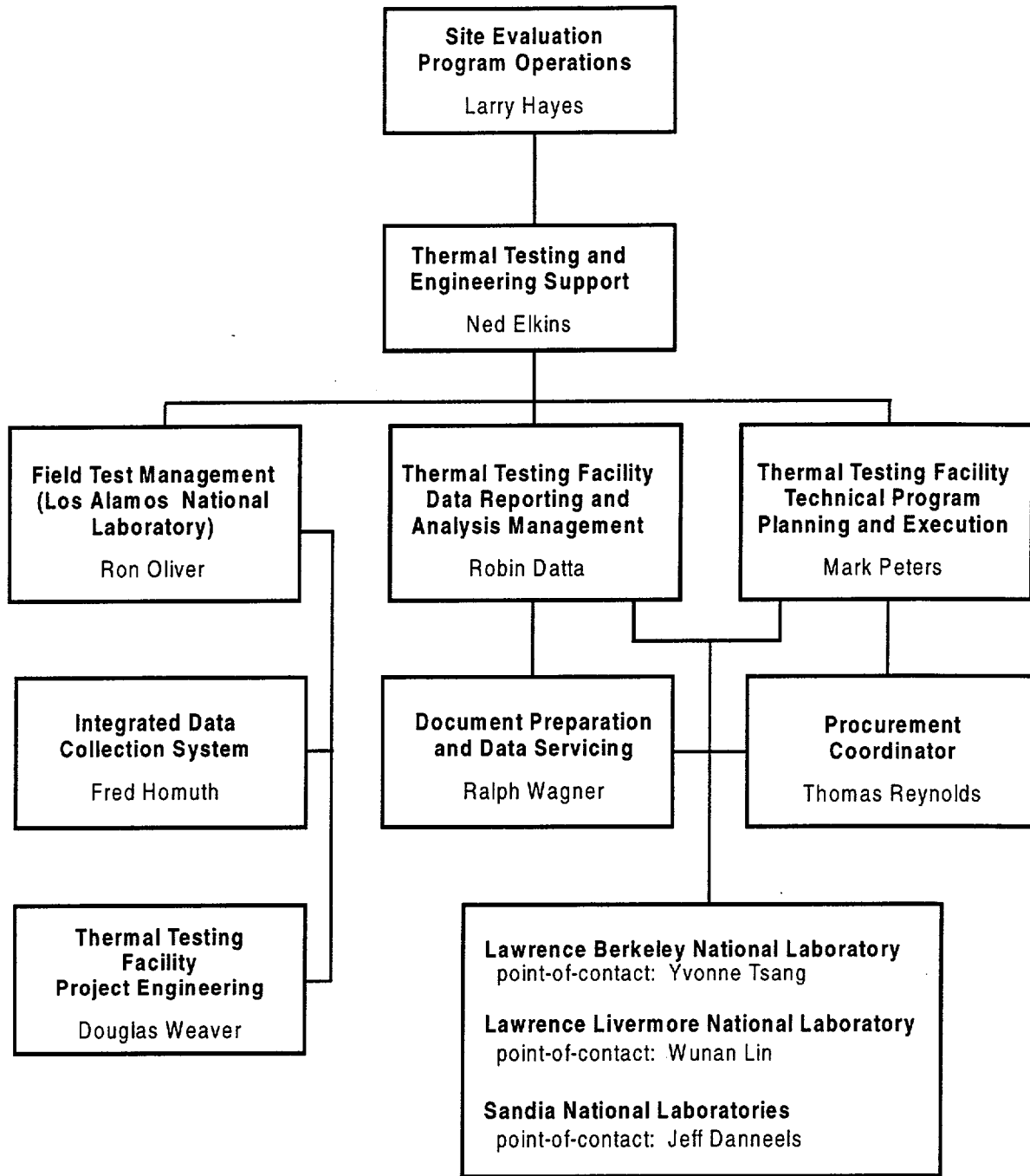


Figure 12-2. Drift Scale Test Implementation

12.4 ORGANIZATIONAL STRUCTURE OF THE ESF THERMAL TEST TEAM

Figure 12-3 shows the organizational structure of the ESF Thermal Test Team. In many ways, this grouping of the four laboratories, other M&O teammates, and outside consultants is a microcosm of the entire M&O structure. Basically, the ESF Thermal Test Team consists of management, technical investigators, and field management. An estimated 50 personnel contribute, directly or indirectly, to the development, construction, and evaluation of the ESF Thermal Test in which a large component is the DST. The ESF Thermal Test Team has evolved from approximately 10 personnel two years ago to its present size.

Since this report was prepared for overview and planning purposes only, formal discussion of conclusions and recommendations were not applicable and therefore not included.



TPM /BAB00000-01717-4600-00007

Figure 12-3. Organizational Structure of the ESF Thermal Test Team

INTENTIONALLY LEFT BLANK

13. REFERENCES

- Barton, N; Lien, R.; and Lunde, J. 1974. "Engineering Classification of Rock Masses for the Design of Tunnel Support." *Rock Mechanics*. Vol. 6, No. 4.
- Berge, P.A. 1996a. *Monthly Report, Engineered Barrier System Field Test Task, Yucca Mountain Site Characterization Project, April 1996*. Livermore, California. Lawrence Livermore National Laboratory.
- Bieniawski, Z.T. 1974. "Geomechanics Classification of Rock Masses and Its Application in Tunneling." *Proceedings of the Third International Congress on Rock Mechanics*. Vol. IIA. Denver, Colorado. Lisbon, Portugal: International Society for Rock Mechanics.
- Birkholzer, J.T. and Tsang, Y.W. 1997. *Pretest Analysis of the Thermal-Hydrological Conditions of the ESF Drift Scale Test*. Berkeley, California: Lawrence Berkeley National Laboratory.
- Blair, S. C.; Berge, P. A.; and Wang, H. F. 1996. *Geomechanical Analysis of the Large Block Test*. UCRL-ID-122898. Livermore, California: Lawrence Livermore National Laboratory.
- Buscheck, T.A. and Nitao, J.J. 1995. *Thermal-Hydrological Analysis of Large Scale Thermal Tests in the Exploratory Studies Facility at Yucca Mountain*. UCRL-ID-121791. Livermore, California: Lawrence Livermore National Laboratory.
- Buscheck, T.A.; Shaffer, R.J.; Nitao, J.J. 1997. *Pretest Thermal-Hydrological Analysis of the Drift-Scale Test at Yucca Mountain*. Livermore, California: Lawrence Livermore National Laboratory.
- CRWMS [Civilian Radioactive Waste Management System] M&O [Management and Operating Contractor] 1995a. *Repository Design Data Needs*. BC0000000-01717-5705-00012 REV 00. Las Vegas, Nevada: Author.
- CRWMS M&O 1995b. *FY 1996 Annual Project Implementation Plan*. B00000000-01717-4600-00051. Las Vegas, Nevada: Author.
- CRWMS M&O 1996a. *Test Design, Plans and Layout Report for the ESF Thermal Test*. BAB000000-01717-4600-00025. Las Vegas, Nevada: Author.
- CRWMS M&O 1996b. *Exploratory Studies Facility Data Collection Systems*. Field Work Package FWP-ESF-96-001, Rev. 0. Las Vegas, Nevada: Author.
- CRWMS M&O 1996d. *ESF Thermal Test Operating Plan*. BAB000000-01717-4600-00026. Las Vegas, Nevada: Author.
- CRWMS M&O 1996e. *Heated Drift Cast-in-Place Concrete Lining Test Configuration Requirements Analysis*. Las Vegas, Nevada: Author.
- CRWMS M&O 1997a. *Single Heater Test Interim Report*. BABEAF000-01717-6900-00001, REV 1. Las Vegas, Nevada: Author.
- CRWMS M&O 1997b. *Ambient Characterization of the Drift Scale Test Block*. BADD00000-01717-5705-00001, REV 00. Las Vegas, Nevada: Author.

- Datta, R. 1996a. Letter Report. *Use of Water in the Thermal Testing Facility*. LV.D.RND.06/96-041. U.S. Department of Energy, Civilian Radioactive Waste Management System, Management and Operating Contractor.
- Datta, R. 1996b. Letter Report. *Drill and Blast Excavation of the Thermal Testing Facility*. LV.SPO.RND.7/96/446. July 18, 1996. Las Vegas, Nevada: U.S. Department of Energy, Civilian Radioactive Waste Management System, Management and Operating Contractor.
- DOE (U.S. Department of Energy) 1988. *Site Characterization Plan, Yucca Mountain Site, Nevada Research and Development Area, Nevada*. DOE/RW-0199. Las Vegas, Nevada: Author.
- DOE 1994. *Civilian Radioactive Waste Management Program Plan*. DOE/RW-0458. Washington, D.C.: Author.
- DOE 1995. *In Situ Thermal Testing Program Strategy*. DOE/YMSCO-003. Las Vegas, Nevada: Author.
- DOE 1997. *Quality Assurance Requirements and Description*. DOE/RW-0333P. Las Vegas, Nevada: Author.
- Francis, N.D.; Sobolik, S.R.; Ho, C.K.; Eaton, R. R.; Preece, D. 1997a. *Pre-Experiment Thermal-Hydrological-Mechanical Analyses for the ESF Heated Drift Test*. SLTR97-0002. Albuquerque, New Mexico: Sandia National Laboratories Nuclear Waste Management Center.
- Francis, N.D.; Sobolik, S.R.; Ballard, S 1997b. "Thermal-Hydrologic-Mechanical Analyses of the In Situ Single Heater Test, Yucca Mountain, Nevada." *Sixth Symposium on Multiphase Transport in Porous Media*. ASME International Mechanical Engineering Congress and Exposition.
- Glassley, W. E. 1997. *Thermo-Chemical Analyses of the Drift Scale Heater Test: Mineralogical and Geochemical Characteristics*. Level 4 Milestone SP9320M4. Livermore, California: Lawrence Livermore National Laboratory.
- Lee, M.Y. 1997. *Blast Vibration Monitoring in the Thermal Test Facility/Connecting Drift and Heated Drift*. SP32IM4. Albuquerque, New Mexico: Sandia National Laboratories.
- Lin, W. 1991. "Pressure Measurements." Final Report. *Prototype Engineered Barrier System Field Test (PEBSFT)*. UCRL-ID-106159, Chapter 6, pp. 76-81, Ramirez, A. ed. Livermore, California: Lawrence Livermore National Laboratory.
- Lin, W.; Roberts, J. J.; Glassley, W.; and Ruddle, D. 1995. *The Effect of Rock-water Interaction on Permeability*. UCRL-JC-119574. Livermore, California: Lawrence Livermore National Laboratory.
- Majer, E.L. and McEvelly, T. 1984. *Acoustic Emission and Wave Propagation Monitoring at the Spent-Fuel Test—Climax*. LBL-17546. Berkeley, California: Lawrence Berkeley National Laboratory.
- Majer, E.L.; McEvelly, T.; and King, M.S. 1981. "Monitoring an Underground Repository with Modern Seismological Methods." *International Journal of Rock Mechanics and Mining Sciences & Geomechanics Abstracts*, Vol 18, pp. 517-527. Oxford, New York: Pergamon.

- Nitao, J.J. 1989. *V-TOUGH—An Enhanced Version of the TOUGH Code for the Thermal and Hydrologic Simulation of Large-Scale Problems in Nuclear Waste Isolation*. UCID-21954. Livermore, California: Lawrence Livermore National Laboratory.
- Nitao, J.J. 1993. "The NUFT Code for Modeling Nonisothermal, Multiphase, Multicomponent Flow and Transport in Porous Media." *EOS Supplement* 74(3), 31. 1.0. Washington, D.C.: American Geophysical Union.
- Nitao, J.J. 1995. *Reference Manual for the NUFT Flow and Transport Code, Version 1.0*. UCRL-IC-113520. Livermore, California: Lawrence Livermore National Laboratory.
- Pruess, K. 1987. *TOUGH User's Guide*. Nuclear Regulatory Commission Report NUREG/CR-4645. Lawrence Berkeley Laboratory Report LBL-20700. Berkeley, California: Lawrence Berkeley National Laboratory.
- Pruess, K. 1991. *TOUGH2—A General Purpose Simulator for Multiphase Fluid and Heat Flow*. LBL-29400. Berkeley, California: Lawrence Berkeley National Laboratory.
- Pruess, K.; Simmons, A.; Wu, Y.S.; and Moridis, G.J. 1996. *TOUGH2 Software Qualification*. Lawrence Berkeley Laboratory Report LBL-38383, UC-814. Berkeley, California: Lawrence Berkeley Laboratory Report
- Ramirez, A.L.; Buscheck, R.; Carlson, R.; Daily, W.; Lee, K.; Lin, W.; Mao, N-h.; Ramirez, A.; Ueng, T-S.; Wang, H.; and Watwood, D. 1991. *Prototype Engineered Barrier System Field Test (PEBSFT) Final Report*. UCRL-ID-106159. Livermore, California: Lawrence Livermore National Laboratory.
- SNL 1994. *Excavation Investigations: Study Plan 8.3.1.15.1.5*. Albuquerque, New Mexico: Sandia National Laboratories.
- Steeffel, C. D. and Yabusali, S. B. 1995. *OS3DIGIMRT Software for Modeling Multi Component-Multi Dimensional Reactive Transport, User's Manual and Programmer's Source Guide*. Richland, Washington: Battelle Memorial Institute.
- Stock, J. M., Healy, J. H., and Hickman, S. H. 1984. *Report on Televiwer Log and Stress Measurements in Core Hole USW G-2, Nevada Test Site, October-November, 1982*. U.S. Geological Survey Open File Report 84-172. Menlo Park, California.
- Svalstad, D.K. and Brandshaug, T. 1983. *Forced Ventilation Analysis of a Commercial High-Level Nuclear Waste Repository in Tuff*. Topical Report RSI-0175. SAND81-7206. Albuquerque, New Mexico: Sandia National Laboratories.
- Tsang, Y.W.; Wang, J.; Freifeld, B.; Cook, P.; Suarez-Rivera, R.; and Tokunaga, T. 1996. *Letter Report on Hydrological Characterization of the Single Heater Test Area in the ESF*. Milestone Report OS327322D1, DTN: LB960500834244.001. Berkeley, California: Lawrence Berkeley National Laboratory.
- Wu, Y.-S.; Ahlers, C.F.; Fraser, P.; Simmons, A.; and Pruess, K. 1996. *Software Qualification Selected TOUGH2 Modules*. Lawrence Berkeley Laboratory Report LBL-39490, UC-800. Berkeley, California: Lawrence Berkeley National Laboratory.

YMP 1996. *Reference Information Base*. YMP/93-02. Las Vegas, Nevada: Yucca Mountain Site Characterization Office.

Zimmerman, R. M., and Finley, R. E. 1987. *Summary of Geomechanical Measurements Taken in and Around the G-Tunnel Underground Facility, NTS*. SAND86-1015. Albuquerque, New Mexico: Sandia National Laboratories.

6/2/97

Los Alamos

NATIONAL LABORATORY

*Earth and Environmental Sciences Division
EES-13 — Nuclear Waste Management R&D
Mail Stop J521, Los Alamos, New Mexico 87545
Phone (505) 667-9768, Fax (505) 667-1934*

THIS IS A YMP
MILESTONE

NO.
SP321BM4

June 2, 1997

EES-13-06-97-1559

Larry Hayes
TRW Environmental Safety Systems, Inc.
Management and Operating Contractor
Mail Station 423
1180 Town Center Drive
Las Vegas, NV 89134

ATTENTION: T. A. Grant

Request for approval of Milestone SP321BM4, "Mineralogic Variation in Drill Holes USW NRG-6, 7/7a, SD-7, 9, 12, and UZ#14," (Delivery Mineralogical Analysis of Cuttings and Core Report) by S. J. Chipera

Dear Mr. Hayes:

In compliance with YAP-30.12, milestone SP321BM4, "Mineralogic Variation in Drill Holes USW NRG-6, 7/7a SD-7, 9, 12, and UZ#14," (Delivery Mineralogical Analysis of Cuttings and Core Report) by S. J. Chipera is enclosed for programmatic review.

This paper documents work done under WBS 1.2.3.2.1; does not fulfill a Level II milestone requirement; and has undergone technical and policy review.

In compliance with YAP-SIII.3Q, the DTN number for this record package is LADV8313 21AQ97.001. In compliance with AP 5.1Q, revision 3, I have attached a YAR form.

Sincerely,



Gilles Y. Bussod

GYB/SHK/ni

- Enclosures:
1. Paper (5 copies)
 2. Review sheets
 3. YAR

Cy w/enc. 1
P. P. Bell, M&O/TRW, Vienna, VA
P. Dixon, M&O/LANL, Las Vegas, NV
A. L. Thompson, EES-13/LV, MS J902
K. A. West, EES-13, MS J521

Cy w/enc. 1, 2, 3
S. J. Chipera, EES-1, MS D469
S. H. Klein, EES-13, MS J521
J. E. Young, LATA, MS J521
EES-13 File, MS J521

DRAFT DISCLAIMER

This contractor document was prepared for the U.S. Department of Energy (DOE), but has not undergone programmatic, policy, or publication review, and is provided for information only. The document provides preliminary information that may change based on new information or analysis, and is not intended for publication or wide distribution; it is a lower level contractor document that may or may not directly contribute to a published DOE report. Although this document has undergone technical reviews at the contractor organization, it has not undergone a DOE policy review. Therefore, the views and opinions of authors expressed do not necessarily state or reflect those of the DOE. However, in the interest of the rapid transfer of information, we are providing this document for your information.